The SCATTERING of ELECTRONIC EXCITATIONS in SUPERCONDUCTORS

Dissertation submitted by

DAVID ALISTAIR TINDALL

for the degree of Doctor of Philosophy

Emmanuel College,

University of Cambridge.

1971

Declaration

I hereby declare that this dissertation is not substantially the same as any that I have submitted for a degree or diploma or other qualification at any other University. I further state that no part of my dissertation has already or is being concurrently submitted for any such degree, diploma or other qualification.

I further declare that this dissertation is my own work, except where the work of others is referred to specifically in the text.

D. A. Tindall

D.A.Tindall,
Emmanuel College,
Cambridge.

March 1971

Acknowledgements

This thesis is the outcome of work carried out in the Royal Society Mond Laboratory between October 1967 and November 1970, under the supervision of Dr. J.R.Waldram. I have benefited greatly by discussions with members of the Laboratory especially my colleagues engaged in Sluggery: Eric Rumbo and Mike Wade on practical matters, and John Shepherd and John Tomlinson for their help with superconductivity theory. Neither can I forget the many practical and theoretical suggestions made by Prof. A.B.Pippard; outstandingly in connection with the boundary resistance problem.

All members of the Mond workshop have been engaged in some aspect of the apparatus; for this and their always-ready advice on technical matters I owe a great debt of gratitude. Frank Sadler made many a valuable suggestion, especially in the design stage, and the construction of the main part of the cryostat was very ably undertaken by Mick Ford (with accident damage very skilfully repaired by David Swainston). A characteristically excellent job of the rotating structure was made by Paul Booth, who also cheerfully assisted with the tedious task of winding the coils. Because of the rapidly changing attitude to the handling of Helium in the Lab., this may be the last thesis to acknowledge the supply of Helium. In my case the cryostat was filled by Paul on the first 22 of 52 occasions, sometimes at considerable inconvenience to himself. I also acknowledge Charles Walker for

the cheerful supply of thousands of litres of Nitrogen.

I am indebted to Terry Brown and John Pratt of the Crystal Growing Unit for assistance with the preparation of the specimens.

These acknowledgements would not be complete without a reference to the MagLab boys: Doug and Keith for innumerable useful things.

For financial assistance I am indebted to the Science Research Council for a Studentship, to Emmanuel College for a Bachelor Scholarship and to the Cavendish Laboratory.

D. A. Tindall

D. A. Tindall,
Royal Society Mond Laboratory,
Cambridge.

CONTENTS

SUMMARY OF SYMBOLS USED IN THE TEXT

a^N, a^S	N and S domain thicknesses
a	$a^N + a^S$
E	Electric field
e	Electronic charge
f	Occupation probability
f_o, f_o'	Fermi function and its derivative
g, g_1, g_2, g_3, g_4, g_1^S, g_1^N, g_2^S, g_2^N	Departure of occupation probability from equilibrium
$\bar{g}$	Average of g around the fermi surface
H	Applied magnetic field
H_c	Critical magnetic field
H_o	H_c evaluated at 0° K
H_{th}	Threshold field for onset of resistance
h	Height of potential step; H/H_c
I	Integral in the boundary resistance theory
I_s, I_c, I_o, I_H, I_b, I_{so}	Electric current
J	Current density; $\int j \, d\varepsilon$
j, j^S, j^N	Excitation current $(g_1 + g_2)$
$\underline{k}$, $\delta\underline{k}_\perp$	Wave vector
ℓ_o, ℓ_o^S, ℓ_o^N	Total mean free path : $1/\ell_o = 1/\ell_1 + 1/\ell_2$
ℓ_1, ℓ_1^S, ℓ_1^N	Elastic mean free path
ℓ_2, ℓ_2^S, ℓ_2^N	Inelastic mean free path

Q	$\int q \, d\varepsilon$
q	Excitation charge density $(g_1 - g_2)$
R	Reflection coefficient(Andreev)
R, R_1, R_E, R_J	Resistance
R_o	Specimen resistance at H_c
RR	Resistance ratio : $R(293^oK)/R(4.2^oK)$
T	Temperature
T_c	Superconducting transition temperature
t	T/T_c
$V, V', V_1, V_1', \Delta V, \Delta V'$	Potential difference
V_s	Weston standard cell e.m.f.
V_n	Noise voltage referred to the Slug circuit
v_f	Fermi velocity
x_B	Position of the potential step
x_ε	Excitation reflection point
α	$2R/(1 - R)$, interface reflection parameter
Δ, Δ_∞	Bulk energy gap parameter of S
Δ_o	Value of Δ at 0^oK
δ	Δ/Δ_o
η	Fraction of N material, a^N/a
Θ	Field angle with respect to specimen side-arms
Λ	$(\lambda/\ell_o)\ \mathrm{Tanh}(a/2\lambda)$
λ, λ^S, λ^N	Diffusion length
ξ	Coherence length

Q	$\int q \, d\varepsilon$
q	Excitation charge density $(g_1 - g_2)$
R	Reflection coefficient(Andreev)
R, R_1, R_E, R_J	Resistance
R_o	Specimen resistance at H_c
RR	Resistance ratio : $R(293^oK)/R(4.2^oK)$
T	Temperature
T_c	Superconducting transition temperature
t	T/T_c
$V, V', V_1, V_1', \Delta V, \Delta V'$	Potential difference
V_s	Weston standard cell e.m.f.
V_n	Noise voltage referred to the Slug circuit
v_f	Fermi velocity
x_B	Position of the potential step
x_ε	Excitation reflection point
a	$2R/(1 - R)$, interface reflection parameter
Δ, Δ_∞	Bulk energy gap parameter of S
Δ_o	Value of Δ at 0^oK
δ	Δ/Δ_o
η	Fraction of N material, a^N/a
Θ	Field angle with respect to specimen side-arms
Λ	(λ/ℓ_o) Tanh$(a/2\lambda)$
λ, λ^S, λ^N	Diffusion length
ξ	Coherence length

ρ	Ratio of two resistors (p. 26); Resistivity
τ, τ_1, τ_2	Relaxation times corresponding to ℓ, ℓ_1, ℓ_2
ω_c	Cyclotron angular frequency
ε	Excitation energy

Chapter 1

INTRODUCTION

The title of this thesis,"The Scattering of Electronic Excitations in Superconductors", is a very broad one and part of the purpose of this introduction is to set out the particular aspect of the field which is examined here.

Over the years there has been much interest in the properties of the Superconducting-normal(S-N) interfaces in a type I superconductor in the intermediate state.* In particular the discovery of the anomalous rise of thermal resistance(Mendelssohn & Olsen,1950) and its subsequent interpretation by Andreev(1964) in terms of quasi-particle reflection at the S-N boundaries have given an insight into the effects of the boundaries on the electrons. However, when the present experiments were commenced(it is convenient to defer discussion of the recently published results of Landau(1970) until later), measurements of the electrical resistance in the intermediate state had always been made far from the transition temperature, T_c, of the superconductor, and revealed nothing in excess of a linear variation between zero and the full

---

* As many books(especially Shoenberg,1952) give good summaries of the structure and basic properties of the intermediate state, a general review will not be given here.

normal state resistance, R_o, just following the variation of the fraction of normal material present. This was also accounted for by Andreev(1966), in the regime $T \ll T_c$, and the significance of this result is examined in Chapter 4.

Many investigators found resistance variations below the linear (see Shoenberg,1952) but this appears to be due to inadequate care in setting up the structure as Walton(1965) showed that the resistance was always a linear function of field provided that "fully saturated conditions"(i.e. a suitable field rotation and current burst between measurements) were employed. His findings were broadly confirmed in the present experiments, although there were detailed differences observed. However Walton did not make measurements above 0.8 T_c(3 K in the tin samples used) where the measuring current,which he had to use in order to get the necessary accuracy with conventional potentiometers, approached 1% of the critical. As the temperature approaches T_c the current must be reduced if the structure is not to be modified by its passage. This necessitates an improved voltage measuring technique and fortunately quantum interference devices based on the Josephson Effect have rapidly become commonplace in cryogenic laboratories for the measurement of voltages down to the femtovolt level. The Slug (Clarke,1966),which is a particularly simple example, was used in the present experiments. This has ample sensitivity and in practice the detection limit is set by field instabilities and cryostat

vibrations. It was possible to reduce these to give a noise level of typically 5 pV in a 200 Gauss field, nearly three orders of magnitude better than the sensitivity of conventional galvanometers.

Since measurements had not previously been made in the vicinity of T_c, where thermal excitation is important, this regime was clearly of considerable interest and its study forms the backbone of this thesis. The investigations revealed that there was a rise above the linear, which increased roughly exponentially as T_c was approached from below. This additional resistance was appreciable only above the temperature($\approx 0.8\ T_c$) where the BCS energy gap $\Delta \sim kT$ (and, ironically, just where Walton's measurements stopped!). This was regarded immediately as a strong indication that the excitations with energies in excess of Δ were responsible and this idea is developed in quantitative terms in Chapter 4.

A few words of explanation about Chapter 4 are called for at this point as it is the only part of this thesis which is not almost entirely original. When the additional resistance in the intermediate state was first discovered, a theory(originated by Prof.Pippard) was being developed to account for the observations made by my colleague J.G.Shepherd on a related system(S-N-S sandwiches near to the transition temperature of the S material). It was realised that it would be very satisfactory if a single theory could explain both sets of measurements and rough calculations soon showed that this was quite possible. The details were worked

out jointly and a paper(Pippard et al.,1971) was prepared for publication. Parts a, c and d of Chapter 4 bear a strong resemblance to sections 1(introduction) and 4(theoretical model of an S-N interface) of that paper. The detailed analysis of the intermediate state case (sections 4.b, e & f) is however my own, and differs substantially from the(more general) approach adopted in the paper, which quotes the results.

A subsidiary investigation was made of the behaviour of an unsymmetrical specimen(one in which the crystal axes formed a large angle with the specimen axis) as previous work had almost certainly been exclusively on symmetrical specimens. The high temperature behaviour of this specimen showed great similarity to that of symmetrical specimens but there were differences at low temperatures. In this regime, for certain angles of the applied field, the specimen resistance rose above the linear variation(no other specimen did this) although in a different way to the boundary resistance. Some attempt has been made to explain this phenomenon but a fuller investigation is really required.

A number of other properties of the specimens(magnetoresistance, temperature dependence etc.) were also investigated, both for their own sakes and in order to estimate certain quantities(such as inelastic mean free path) required for the interpretation of the boundary resistance measurements.

Chapter 5 is essentially a description of the experimental results

including discussion of the means used to set up the intermediate state structure and the behaviour of the unsymmetrical specimen(SnIII). The main discussion of the results at temperatures near to the transition(boundary resistance) is however deferred until Chapter 6.

In an attempt to provide easy reference all of the numbered Figures have been bound at the back of the thesis, as they are referred to from a number of different points in the text. However the Tables and Plates are to be found near to the appropriate text as this consideration does not apply.

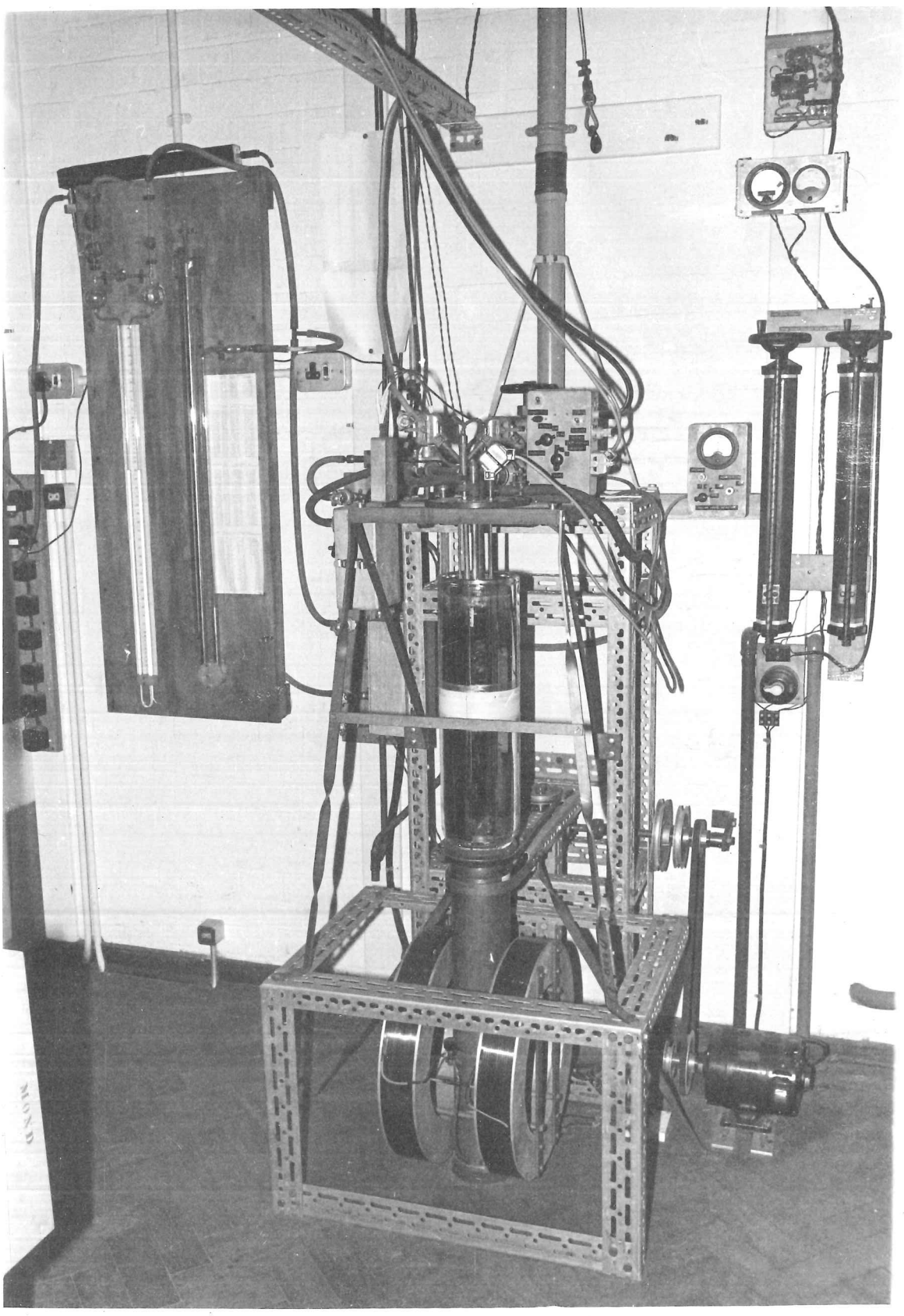

PLATE I

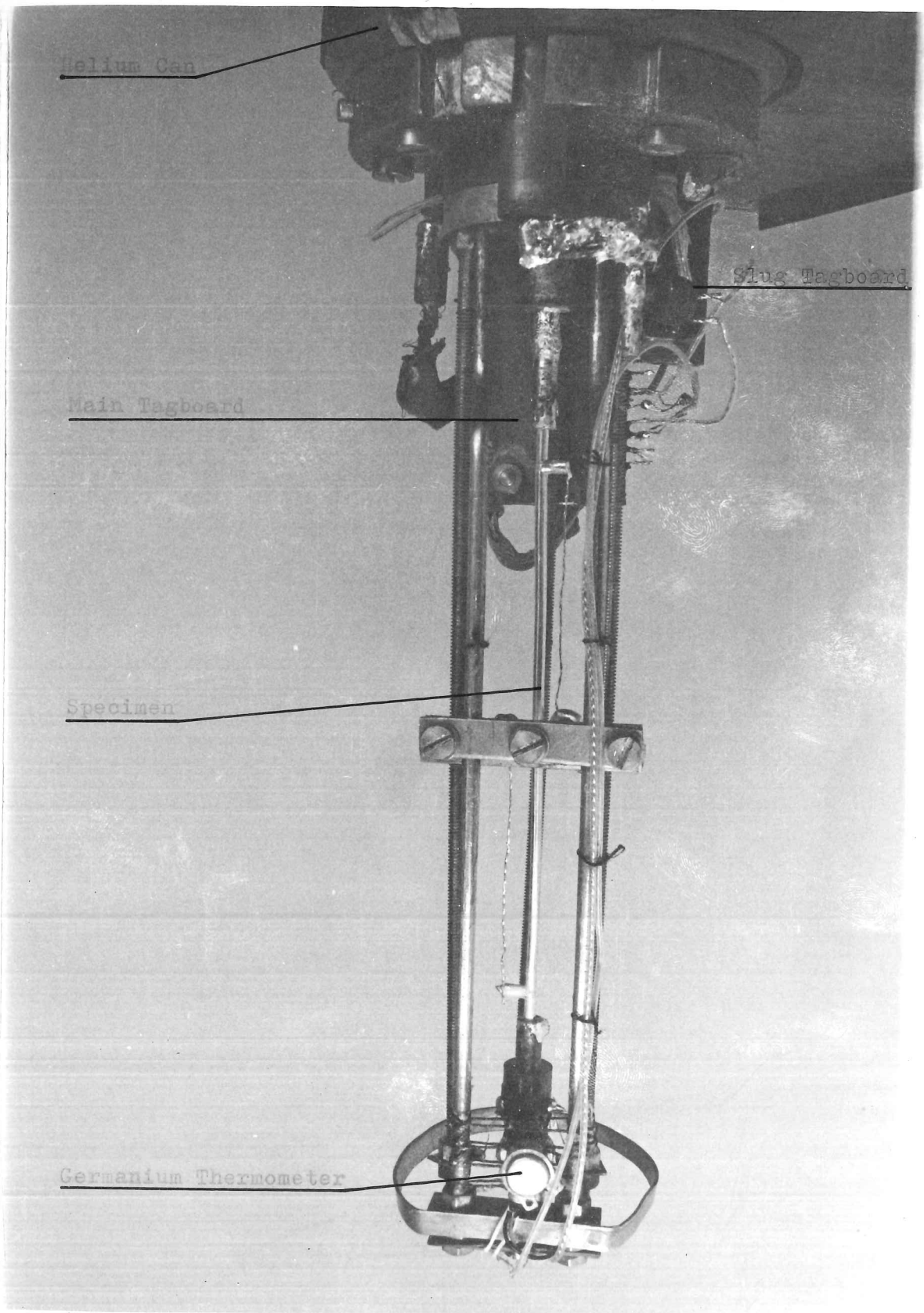
Helium Can
Slug Tagboard
Main Tagboard
Specimen
Germanium Thermometer

PLATE II

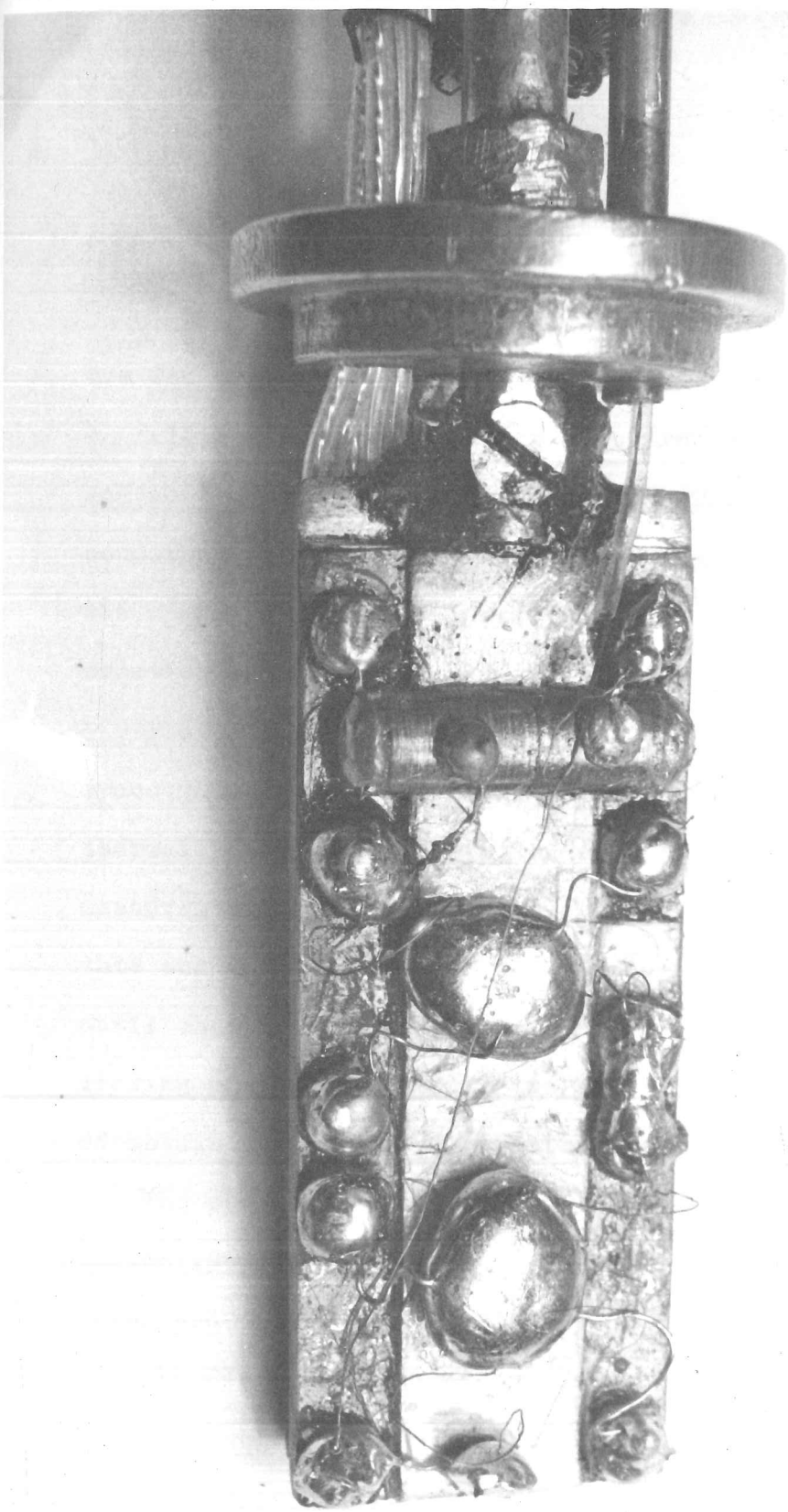

PLATE III

Chapter 2

EXPERIMENTAL DETAILS

2.a The Cryostat

Plate I shows a general view of the outside of the cryostat and some of the associated apparatus. The cryostat was of composite construction: the Nitrogen dewar with a narrow tail inserted into the magnet was made of glass but the Helium vessel itself was constructed mainly of copper.

Plate II and Figure 1 show the construction of the working space, which was situated in the Helium interspace in order to thermally isolate the specimen so that thermal conductivity measurements could be made. A full discussion of the reasons for this and the size of the specimens(about 10 cm long) is deferred until chapter 3. However it can be noted here that thermal weak-linking of the specimen to the bath is in any case the best way of obtaining a stable temperature(section 2.c).

The specimens were mounted in a similar way to that described by Walton(1965) using three lengths of 6 B.A. studding to hold the lower end of the specimen steady.

The Slugs and standard resistor(plate III) in their superconducting can were glued with Bostik I to a cigarette paper-covered copper plate which fitted into a re-entrant enclosure in the bottom of the Helium can. The purpose of this was to keep the

field distortion caused by the superconducting shield down to a minimum without sacrificing Helium content.

The two superconducting leads from the Slug box to the specimen consisted of a twisted pair of 0.004" diameter formvar coated Niobium wires(similar to that used in Slug manufacture). These were used rather than the ubiquitous tinned twisted Eureka(hereafter referred to as TTE) because the latter cannot be reliably coated with an insulating coating thin enough to keep the enclosed pick-up area down within the necessary limits. Niobium of course has the disadvantage that it is not easy to make reliable joints by soldering. However, after the technique described in section 2.d was discovered, there was not a single failure. The Niobium potential leads were joined to a pair of TTE wires(which could be bent in order to adjust the net pick-up area to a minimum) on insulating(Nylon) posts supported by the brass piece clearly seen half way up the specimen in plate II. These superconducting wires were then joined to the specimen side-arms.

The nether end of the specimen was soldered into a holder which was connected to the germanium thermometer by a thick piece of stranded copper wire. The thermometer was suspended by an arrangement of threads from the two main support rods in order to insulate it from the bath as well as possible. The leads to the thermometer were 42 SWG Eureka which, in the length necessary to reach the main tagboard, conducted away a negligible fraction of

the heat. The holder had an insulating collar, which could rotate about the specimen axis and had very thin Eureka wires connecting it to the three tensioning brass rods.

Electrical current could be fed into the specimen by 36 SWG TTE which could carry nearly an Amp in a 200 Gauss field while remaining superconducting. It had previously been found during an investigation of the critical current of TTE wire as a function of magnetic field(fig. 2) that 40 SWG was inadequate. The current left the specimen through the thermal weak link which consisted of 18 pieces of 24 SWG heavily tinned copper wire each $1\frac{1}{2}$ cm long. This link had a thermal resistance of about 150 mK/mW and replaced an earlier one consisting of a single piece of copper which had the same cross-sectional area but a measured thermal resistance more than an order of magnitude greater(presumably because of thermal resistance at the joints dominating the behaviour).

The sizes of the wires coming from the top of the cryostat were calculated by equating the heat generation with heat conduction (White 1968). 34 SWG Eureka was extensively used as it is a good compromise between ease of handling and the thermal requirements. Exceptions to this are: the voltage leads to the Slugs(44 SWG copper - low resistance to avoid signal loss), the thermometer voltage leads(44 SWG copper - all copper circuit to suppress thermal emfs) and the current leads to the specimen(40 SWG copper - higher current capacity without being excessively thick, as Eureka would be).

The wires entered the cryostat via the interspace pumping tube and were then stuck to the outside of the Helium can with Bostik I in order to provide a certain amount of thermal anchoring. The main bonding to Helium temperatures was however done by a specially constructed tagboard in which the current flowed along narrow superconducting strips(0.002" thick Pb/Bi foil) which were sandwiched between cigarette paper-coated copper sheets strongly bonded to the bath.

In order to make measurements of the pressure actually within the Helium bath(for thermometry purposes) a pressure sensing tube was incorporated in the design of the Helium bottle and this tube also carried the three 10 Ohm Allen-Bradley resistors used as level detectors.

If a room temperature seal were to be used a large diameter, poorly conducting tube would be needed to avoid excessive Nitrogen consumption and freezing of the O-ring. However copper-nickel tube was not made in the requisite size and stainless steel tube was ruled out because of difficulties experienced by others in the laboratory with leaking joints. Prof. Pippard suggested the use of a polythene gasket submerged in the liquid Nitrogen and this gave excellent results. Another advantage of this method was that the heat input to the Nitrogen was small as the few tubes needed were of small diameter. The three tubes(pumping,filling and level detectors/pressure sensing) which went through to the Helium

can were surrounded by small copper shields so that they remained cooled by Nitrogen until its level fell to below the top plate. Thus the Nitrogen capacity was increased without causing a loss of cooling(I am indebted to Mr. F.T.Sadler for this idea).

The Helium dewar had a capacity of 1.5 litres, its diameter being restricted by the size of the magnetic field coils. It needed a little over 4 litres(and 45 minutes) to fill it because of the rather large mass of copper. The cryostat was invariably pumped down to 1.2 K over a period of about an hour before any measurements were made. The calculated heat input was 120 mW(no heat to specimen included) and this agreed with the initial run length of 12 hours. However when many measurements were made at elevated temperatures the length of run decreased to about 7 hours and refilling was usually carried out(sometimes twice). This was very much quicker than the initial fill and required less than 2 litres of Helium. The total time necessary to refill and pump to 1.2 K was typically $\frac{3}{4}$ hour.

Although thermal bonding of the leads is more difficult with this type of cryostat(they could in any case be taken,using Stycast seals, through the Helium bath) it has great advantages over more conventional designs requiring Helium temperature gaskets or large messy soldered joints.

2.b The Magnetic Field

This section is split into two subsections for convenience:

2.b1 deals with the design and construction of the magnetic field coils, whereas

2.b2 is principally concerned with the sources and reduction of noise, which is naturally a very severe problem in these sensitive measurements.

However the dividing line is tenuous and the headings are really only a guide to the contents of the sub-sections.

2.b1 The production of the magnetic field

In order to set up a stable, uniform intermediate state structure in a cylindrical sample it is necessary to apply a homogeneous transverse magnetic field which can be rotated about the specimen axis at up to 30 R.P.M.(Walton,1965). It was decided that the design criterion should be for a field homogeneity of 1% over the specimen, which puts a considerable constraint on the diameter of the cryostat if the field coils are to be of a reasonable size.

2.b1.(i) Coil design

The off-axis field in the central plane of a pair of ideal coils(i.e. wound of wire of negligible radius) is conveniently expressed as an integral over current elements (although the integration is not trivial):

In e.m.u.:

$$H_z(y) = 2ni \int_0^{2\pi} \frac{b(b - y \operatorname{Sin}\theta)\, d\theta}{\left\{a^2+b^2+y^2-2by\operatorname{Sin}\theta\right\}^{3/2}}$$

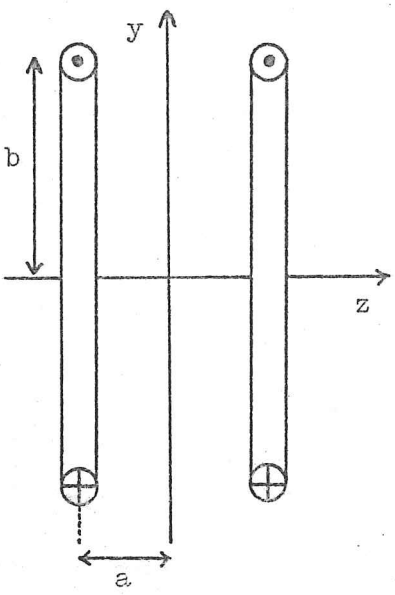

The effect of non-zero cross-section of the coils was allowed for by evaluating the average of the above integral over 25 points in a 5 X 5 mesh enclosed by the coil section.

At this stage in the calculation it became necessary to make a decision about the means of rotation of the field, as a rather attractive possibility was to have two stationary Helmholtz pairs at right angles fed in quadrature with alternating current(probably produced by motor driven sine-cosine potentiometers controlling the outputs of two matched current supplies). It was clear from the outset that the coils were going to be massive, and the prospect of rotating them at 30 R.P.M. was a little daunting. Another factor considered was the provision of electric current(and possibly cooling water) to the rotating magnet. However there are concomitant difficulties(as with all good ideas!):

(a) Two more coils are necessary.

(b) There is the physical difficulty of fitting two pairs at right angles - at least one pair would have to be very large indeed.

(c) As we shall see later the requirements on the power supply are strict and a pair of bilateral current supplies delivering 300 W each would be expensive and not easy to design.

Semi-empirical calculations indicated that water cooling would be unnecessary, especially as the resistance rise would have a negligible effect on the current delivered by the high output impedance supplies available. Accordingly the four coil idea abandoned and the appropriate calculations were carried out for a single pair, to be mechanically rotated.

It was found that spacing the coils slightly closer than Helmholtz(b = 2a in the above notation) gave a field within prescribed limits over a larger volume, at the expense of introducing small maxima away from the centre.

2.b1.(ii) Construction and mounting of the coils

The coil formers simply consisted of a short piece of tube to each end of which was fixed an annular cheek. Initially brass was used, since the right size of tube was readily available, but it proved impossible to prevent buckling after the cheeks were hard soldered in place. Accordingly duralumin was used for the actual formers(this had the slight disadvantage that the tube

had to be rolled first) and the cheeks were Argon arc-welded to the tube giving a very light and strong structure.

The formers were then lined with thin paxolin sheet in order to ensure that any chafing of the insulation of the wire during winding would be minimised. They were consecutively mounted in a lathe and were wound by hand, great care being taken to ensure that adequate tension was maintained on the rectangular section wire. When the last turn had been completed, the windings were secured in place by soldering the last two together, whilst still under tension.

The physical dimensions of the windings in each coil are listed in Table 1, together with some details of the pair as mounted together.

A rotating mounting for the coils was designed after a discussion with Prof. Pippard had produced much food for thought. The coils were mounted on the outside of a brass tube having an o.d. equal to the required coil separation and an i.d. a little larger than the Nitrogen dewar. This tube was then padded around its upper end to support the dewar at the top of its tail. The base plate at the foot of the tube had at its centre a Delrin insert which rested on a $\frac{1}{2}$" stainless steel half-ball in a plate fixed to the floor(thereby allowing the tube to pivot about the centre of its base). At the upper end of the tube the driving V-belt pulled the tube back against two rollers in order to

Details of Magnet Coils

Minimum Diameter	28.2 cm
Maximum Diameter	43.2 cm
Width	5.8 cm
Mass (including former)	42 Kg
Dimensions of Wire	.160 x .180 "
Number of Turns	486
Length of Wire	551 m
Mean Separation	17.8 cm
Clear Gap	10.8 cm
Inductance	30.4 mH
Resistance (20°C)	2.37 Ω
Field Strength per Unit Current	25.1 G/A
Thermal Conductance	7 W/°C
Constant Current for Thermal Runaway	25 A

Note : The last two entries were calculated (assuming heat loss and power input linearly proportional to the excess temperature) from measurement of the rate of rise of the coil resistance when a constant current of 10 A was passed.

TABLE 1

provide complete location. The tube base-plate(which was made of an insulator - bakelite) had attached to it two brass rings which dipped into mercury troughs in order to supply current to the rotating magnet. To the author's surprise(and relief) these were found to be safe to 100 A for at least a few seconds when the magnet supply was turned on after it had been left at full output by the previous user!

Since there was little clearance between the rotating glass dewar(which was not quite circular) and the stationary outer can of the Helium dewar, rather accurate alignment was required. This was accomplished by sliding the floor plate into the correct position before bolting it down and then adjusting the upper part of the tube by sliding the two roller supports appropriately. The cryostat itself could also be adjusted by means of the three supporting rods.

The main advantage of this method of coil mounting, apart from its obvious kinematic features, is that the Nitrogen dewar does not need a separate support.

The whole assembly was rotated by a compound wound d.c. motor driving through V-belts and a 50 to 1 reduction gear. The drive train was mounted separately from the cryostat to reduce vibration. The overall speed reduction ratio could be selected by slipping the first V-belt over the appropriate pulley pair and had three values: 50, 140 & 250. The speed of the motor was controlled by

two rheostats: one of which shunted its armature, and the other reduced the voltage applied to its terminals (from 220 V). By these means the magnet could be rotated at any rate between 1 and 30 R.P.M.

2.b1.(iii) Supply of current to the magnet

According to a Bell (Hall probe) Gaussmeter, the magnet gave 25.1 G/A, less than $\frac{1}{2}\%$ away from the calculated figure. All magnetic fields quoted in this thesis were calculated using this calibration constant.

Up to about 8 A the magnet current was usually supplied by a Hewlett-Packard 6286A power supply, which could be set to give a constant-current output irrespective of the magnet resistance. For currents larger than this (necessary below $2^{\circ}K$) the current was provided by a Newport Instruments C905 20KW motor-generator set. This had a transistor regulator built into the control console which reduced the ripple from the commutator of the generator. As the C905 control console was located in the next room from the present experiments, and could not be easily moved, it was necessary to control its output remotely. This was done quite conveniently by applying a voltage, derived from a Mallory cell and Helipot, to the appropriate terminals on the console. The residual instabilities in this supply were a few times more troublesome than those of the 6286A, presumably because of the low inductance of the coils (lower than that of the Newport magnet).

2.b2 Reduction of the noise due to the magnetic field

The great magnitude of this problem is shown by the following rule of thumb:

$$\text{Magnetically induced p.d.} = 6 \times 10^{-10} \text{ Volts(mm)}^{-2}\text{Gauss}^{-1}\text{Hz}^{-1}$$

There are four main sources of this noise to be considered here:

(a) Drift in the magnet current due to resistance change of the magnet or inherent drift of the current supply.

(b) Vibrations of the cryostat relative to the magnetic field

(c) Ripple on the magnet current.

(d) Stray a.c. fields.

For both the supplies used the output impedance was very large and effects of type (a) were negligible. One of the main ways of reducing the other types of noise is screening of the whole apparatus.

2.b2.(i) Screening

Most noise can be eliminated in experiments not requiring the application of large magnetic fields by enclosing the working space of the cryostat by superconductor. The next best thing is to allow only the d.c. component of the magnetic field to penetrate the region around the specimen, with the remainder of the circuit shielded by superconducting material. This was done by Wade(1969) who used a 1 cm thick high purity Aluminium can around the specimen space. The field ripple at 50 Hz was cut by an estimated 60 dB by this means. Wade also used a Pb/Bi eutectic can around the Slugs and standard resistors to screen that part of

the circuit. However the present experiments require a rotated field and therefore such a thick screen must be ruled out because of the torque and heat produced. Nevertheless superconducting screening of the Slugs is not ruled out and a can was constructed for the Slugs. This was designed to give much less than $\frac{1}{2}\%$ distortion of the field over the whole of the specimen volume.

Calculation of the eddy currents for the transverse geometry is not easy, but experimental tests revealed that the copper radiation shield which surrounded the cryostat working space was the right thickness, as the Helium boil-off rate was increased by 25% when a 300 Gauss field was rotated at 3 R.P.M.. Incidently, while these tests were being carried out, the following rather interesting effect was observed. The temperature of the copper shield fell by about 40 mK when the coils were rotated with no current passing through them. This was eventually ascribed to superheating of the Nitrogen(this apparently occurs very readily), which of course was stirred by rotation of the dewar(calculation revealed that the Reynold's number was about 4 000). To produce the observed temperature change it was estimated that a 1° K lowering of the Nitrogen would be needed - a not unreasonable figure.

A secondary method of stabilisation of the specimen field used by Wade(1969) was a superconducting coil incorporating a superconducting switch wound on a spherical former. When the

desired external field was reached the superconducting switch was closed and the small coil then screened out changing uniform magnetic fields(e.g. that due to ripple on the current supply). However, because of the large specimens to be used, this must be ruled out on account of its enormous size.

2.b2.(ii) Reduction of cryostat vibrations

It was somewhat amusing to find that the closing of a door about 20 yds away on the next floor could be detected by the Slug! In order to minimise this kind of vibration the free standing main support frame, which had been inherited from a previous experiment, was progressively stiffened. The frame was bolted to the wall after the surprising discovery that it was a smaller source of vibration than the floor. The main Helium pump-line, which had a number of bellows on it, was not at all troublesome. The residual contribution appeared to be due to the boiling of the Nitrogen, since for about an hour after filling the cryostat with Helium the Nitrogen did not boil and the noise level was lower.

In order to refrigerate the Nitrogen and thereby stop its boiling, a narrow cupro-nickel tube, partially closed at its lower end,was lowered to the bottom of the glass dewar. When this tube was pumped on, liquid entered the lower end, boiled under reduced pressure, and cooled the rest of the liquid by conduction through the walls of the tube. This sucessfully prevented boiling of the Nitrogen when there was no cryostat

inserted in the outer dewar, and in fact lowered its temperature to about 70 K(measured using a copper wire thermometer(Dauphinée & Preston-Thomas,1954)). However it had insufficient refrigeration capacity when the cryostat was inserted, and it proved impossible to adjust the small orifice to exactly the right size: too large and the pump could not lower the pressure enough and the Nitrogen was excessive; too small and the refrigeration rate was not great enough. It was discovered about this time that ripple on the C905 supply(which had been used exclusively up to this time) was the largest source of noise anyway, and so experiments with the de-bubbler were discontinued.

2.b2.(iii) Reduction of pick-up area

It is possible to reduce all forms of magnetic noise by making the effective area enclosed by the superconducting Slug circuit as small as possible. The transverse geometry makes this a rather difficult task. Walton tackled the problem in two ways:

(a) A proportion of the signal picked up in auxilliary coils around the outside of the dewar was fed into the circuit to cancel the noise. In the present experiments this was not possible as the Slug circuit has to be superconducting. A good deal of thought was put into ways of adjusting a signal injected in antiphase into the low temperature circuit(by superconducting switches or mechanical linkages) but no practicable method could be devised.

(b) The side-arms were put on opposite sides of the specimen so that the pick-up areas were nearly equal, and the field was stopped parallel to the side-arms when measurements were taken. However arranging exact cancellation of the two loops(each 4 cm X 0.5 cm) was not at all easy: a 5% inequality gives 10 $(mm)^2$ of effective pick-up area in the transverse direction. A few of the present measurements were made with the field far from parallel to the side-arms and,as expected, the noise level was much worse.

2.b2.(iv) Electrical interference

In practice the most troublesome form of noise(because it was irregular in time and difficult to track down) was that produced by other apparatus on the same mains circuit. Furnaces with Thyristor-controlled current regulators are especially bad in this respect: two in the Physics department and one in Metallurgy were tracked down with a small transistor radio and suppressed by a simple L-C filter in their mains leads.

Night cryostat runs were obligatory in order to reduce the noise level by typically a factor of 10 to 100. The value depended a little on magnetic field and so was probably due to vibrations of the building as well as to electrical pick-up. It was particularly annoying to find that some people operated noisy equipment at night, apparently in an effort to disturb as few people as possible!

2.b2.(v) Estimation of noise voltage

It is not inappropriate to point out at this stage that the noise voltage, V_n, referred to the Slug circuit, is $I_o S$ (where I_o is the minimum detectable current flowing into the current leads of the standard resistor S). This is not quite so trivial as it appears

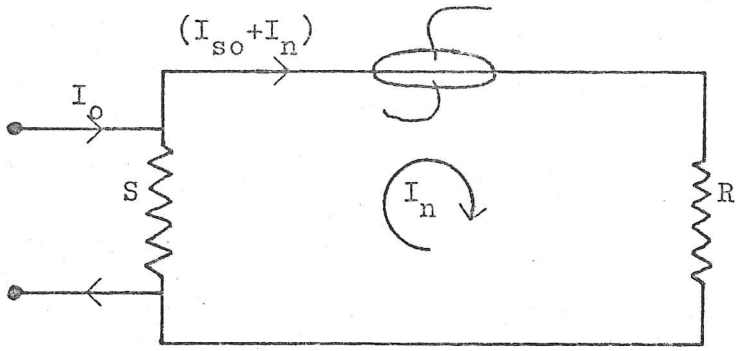

at first sight; for R may be very small, in which case virtually the whole of I_o flows through R instead of S. However when one bears in mind that the Slug senses current and not voltage the statement becomes clear once more.

Let I_{so} be the current flowing through the Slug in the absence of noise and let I_n be the circulating noise current due to the noise voltage, V_n:

$$\therefore \quad I_{so} = I_o \cdot \frac{S}{R+S} \qquad \& \qquad I_n = \frac{V_n}{R+S}$$

but we have chosen I_o such that $I_{so} = I_n$:

$$\therefore \quad V_n = I_o S$$

2.c Thermometry and Temperature Stabilisation

The accurate measurement and maintenance of temperatures within a few tens of millidegrees of the transition point turns out to be an important aspect of these experiments. Furthermore the techniques used to achieve this aim are of very general application. It is for these reasons that it is worthwhile examining them in some detail.

2.c.(i) The need for a good thermometer

Close to the transition temperature(T_c) the intermediate state resistance at fixed field is a rapid function of temperature. This is illustrated by the following approximate calculation:

$$R = 2 R_o \left\{ \frac{H}{H_c} - \frac{1}{2} \right\}$$

& $$H_c \sim 2 \frac{H_o}{T_c} \left\{ T_c - T \right\} \qquad \text{(near } T_c\text{)}$$

$$\frac{\partial R}{\partial T} = 2 R_o H \frac{\partial}{\partial T} \left[\frac{1}{H_c} \right] \sim \frac{R_o H T_c}{H_o (T_c - T)^2}$$

but $H \sim H_c$

$$\therefore \quad \frac{\partial R}{\partial T} \sim \frac{2 R_o}{(T_c - T)} \qquad \text{i.e.} \quad \frac{\Delta R}{R} \sim \frac{2 \Delta T}{(T_c - T)}$$

Hence the relative error in R is approximately double the relative error in the difference of the temperature from T_c.

The highest temperature at which measurements were repeatedly made was 20 mK below the transition, where a 1% change of resistance is produced by only a 100 μK change in temperature.

The minimum requirements for a thermometer for these experiments may thus be stated as follows:

(a) Sensitivity - 100 μK

(b) Differential accuracy of calibration(i.e. the slope of the residual error curve) - 1%

(c) Reproducibility - Under thermal cycling from 4 K to room temperature - 1 mK

(d) Accuracy unaffected by magnetic field(within the above limits).

Absolute accuracy of the calibration is relatively unimportant as the tin transition (in zero field) can be used as a reference point; this is convenient as absolute accuracy is often much more difficult to obtain than relative accuracy. Reproducibility is very convenient, but not strictly essential.

It was decided that a germanium resistance thermometer would be the most suitable device, with certain reservations about its magnetic field dependence. However tests revealed that the resistance did not change by more than 0.1% in a field of 400 Gauss, corresponding to a temperature error of less than 2 mK at all temperatures in the He range. Furthermore, as T_c is approached from below, the maximum magnetic field applied becomes progressively smaller as the temperature is required more and more accurately.

2.c.(ii) Measurement of thermometer resistance

The thermometer current was provided by the stable current supply described by Rumbo(1969) which consists of a 10 V supply feeding through high stability metal film resistors of values 1 M, 3.3 M, 10 M, 30 MΩ(according to the range selected). The current is monitored by dividing the 10 V rail by ρ (about 10) and comparing against a Weston standard cell with a digital voltmeter (D.V.M.) as shown below.

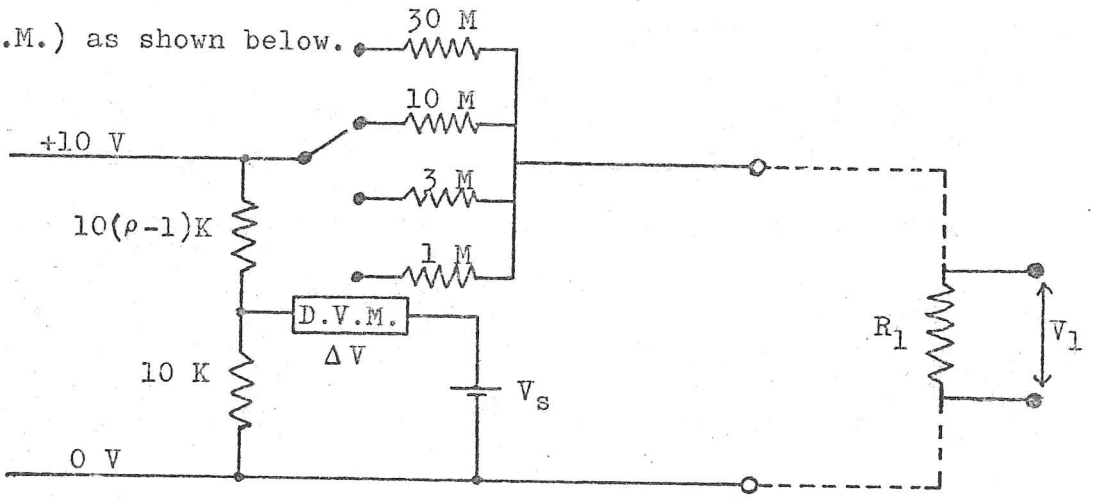

The necessary calibration of each range was done at intervals by measuring the voltage developed across a 1 KOhm standard resistor, with the same Tinsley Thermo-electric free Potentiometer used to measure the thermometer voltage. This calibration was found to change by only about 0.2% over two years, due to ageing of the metal film resistors. It is of course necessary to allow for the finite output impedance of the supply in order to calculate the thermometer resistance; the equation used being:

$$R_1 = V_1 \frac{R_1}{V_1'} \frac{\rho(\Delta V' + V_s) - V_1'}{\rho(\Delta V + V_s) - V_1}$$

(the dashed quantities being obtained in the calibration run)

This method of checking the current is much more convenient operationally than switching the potentiometer to measure the the voltage developed across a standard resistor. It is just as accurate since ρ is chosen so that ΔV is less than 20 mV and the most sensitive range of the D.V.M. can be used. The only disadvantage is that the device used to measure the voltage must be accurate as well as linear.

In order to minimise self heating of the thermometer, the p.d. across it was limited to 10 mV, where tripling the current had a negligible effect.

2.c.(iii) Thermometer calibration

Over the temperature range 4.25 to 13 K thermometer no.462 was calibrated against another Cryocal germanium thermometer(no.718), which was claimed by its manufacturers to be accurate to $\pm$ 5 mK. The holders of the two resistors were mounted on a specially constructed h.c. copper block and their leads were heat sunk by joining them to lengths of eureka wire wrapped around the block and secured by Bostik I. The elevated temperatures were obtained by weak linking the block to the He bath and using a

heater to provide a few mW of power.

In the He temperature range the laboratory possessed no standardised resistance thermometers and so it was calibrated against the vapour pressure of Helium. Because the Helium can of the cryostat was made of copper it was not possible to make the hydrostatic head correction by the usual technique of measuring the liquid level. Even if the level could be determined easily the correction is still reduced by an uncertain amount because of the good conductivity of the cryostat walls. Accordingly (since there is no head correction below the λ-point) the correction (20 mK) at 2.174 K was estimated by observing the apparent discontinuity in temperature (measured by vapour pressure) which occurs at this point in the thermometer calibration residual error curve. The magnitude of this correction corresponds to a head of 15 cm of Helium, consistent with estimates based on can dimensions, boil-off rate etc.. Similarly at 4.25 K there was a discontinuity(where the vapour pressure measurements met those using the standardised thermometer) amounting to some 26 mK. The hydrostatic head in the cryostat could have an upper limit of only 7 mK at 4.2 K and so there remained a rather large discrepancy at this end of the range. Unfortunately thermometer no.718 was not available for checking directly against Helium for a considerable time, but as the discrepancy amounted to an error in temperature <u>difference</u> of less than 1% $\left\{\frac{(26 - 7) \times 10^{-3}}{(4.2 - 2.174)}\right\}$ it was

decided that the temperatures would be corrected by adding an amount linearly interpolated between 20 mK at the λ-point and 26 mK at 4.25 K.

When the standard thermometer next became available it was found that it indicated a temperature about 17 mK too high, both when mounted as no.462 had been,and also when placed directly in contact with liquid Helium in a storage dewar. This confirmed that it was indeed the calibrated thermometer which was incorrect and not,for example, spurious heat input to the thermometer in the calibration rig. Thus the mystery was resolved,unfortunately too late for many measurements had already been taken. However, as already noted, the error was negligibly small and it was decided not to alter the calibration parameters. This explains why the tin transition temperature is later quoted as 3.731 K instead of the accepted value (3.722 K). When allowance is made for the wrong correction (and the earth's field) the agreement with the accepted value is perfect. The transition point of the specimens also provided a good check on the stability of the thermometer, which was found to be good to better than 1 mK over a period of a year and 40 cyclings between room temperature and 4 degrees(Fig. 17).

2.c.(iv) The fitting of the germanium resistor

It soon became clear from reading the references given by White(1968) that there is no simple formula analogous to that of Clement & Quinnell(1952)(for carbon resistors) which fits the

variation of germanium resistors at all well. Many of the references cited did not have small error curves and furthermore they gave R(T) rather than T(R). This point is not really a serious drawback, as T can be obtained from R by iteration, but it does contribute to unnecessary complication.

It was realised that one could probably achieve a significant improvement in accuracy by fitting an exponential first to remove the gross variation, and $R = A \exp(B/T)$ was tried. About this time a fortunate slight misinterpretation of a semiconductors lecture suggested it might be worth trying instead $R = A \exp(B/T^{\frac{1}{4}})$. This proved to be very successful;giving an rms deviation of 0.2 K over the range 1.2 to 13 K , an improvement by a factor of three over the straight exponential fit. The $T^{\frac{1}{4}}$ expression(hereafter called the initial fit) is easily invertible and leaves an error curve which was found to be approximately parabolic in log R,indicating the use of the following full expression:

$$T = \left[\frac{B}{\log R - \log A}\right]^4 + \sum_{i=1}^{M} Y_i (\log R)^{i-1}$$

where the Y_i are determined by a least squares fit to the initial residual error curve.

Before using the full expression it was necessary to estimate the magnitude of the corrections to be applied at 2.2 K and 4.2 K by plotting the error curve from the initial fit. When this had

been done it was found that the fit to the 52 calibration points with ten polynomial parameters(M=10) was excellent: rms deviation 2 mK with a peak deviation of 6 mK. That the residuals left by the full fit were the result of random scatter in the data was evidenced by the fact that the error curve crossed zero 19 times in the range, whereas with M=5 there were only 5 zeroes. The initial fit could of course be used alone if desired,to give a quickly calculated estimate of the temperature to within 4% using just two parameters.

2.c.(v) Temperature control

As noted earlier it is necessary to maintain the temperature of the specimen to within about 0.1 mK (when measuring near T_c) over the hour or so needed to take a set of readings. This presents a formidable problem for the designer of a temperature stabiliser (though no doubt it could be done). Since the Helium bath was pumped hard below the λ-point,it was reasoned that there would be a very stable environment for the specimen and so passing a constant current into a heater should give a stable excess temperature,which might be as good as one could get with a stabiliser. The constant current source used was a standard design using a stable variable voltage reference with an operational amplifier (709) to give a high output impedance and very low drift with room temperature. The temperature variation of the specimen (monitored by the potentiometer as the D.V.M.

had inadequate sensitivity) amounted to about 0.1 mK over a few minutes after a short settling time had elapsed. This temperature drift corresponds to a current change of only 20 ppm and was shown to be due to fluctuations in room temperature during one particular run on a hot summer evening: the specimen temperature was drifting very badly(a few mK in seconds) until the fan used to blow cool air over the experimenter was turned off. This had been circulating air over the current supply circuit, thereby increasing the thermal fluctuations and shortening their time constant!

In general this method of temperature control proved very adequate,although somewhat tedious and large external heat inputs had to be avoided where possible. It was certainly superior to the various stabilisers in use in the laboratory, by about an order of magnitude.

The excess temperature of the specimen stage was found to vary approximately linearly with heater current, as shown in Fig. 14.

2.d Slug Operating System

2.d(i) Description of the Slug characteristic

The Slug(Clarke,1966) is a low inductance(~10 nH), moderately sensitive(~1 μA) superconducting galvanometer. These properties enable it to be used in low resistance circuits($\sim 10^{-8}$ Ohm) whilst retaining an acceptable time constant(L/R ~ 1 sec). The voltage sensitivity is thus typically 10^{-14} Volt(10 nΩ X 1 μA).

The basis of the operation of the device(Josephson Effect) will not be discussed here; the Slug will merely be treated as a black box with the transfer characteristic(I-V) shown below. The usefulness of the Slug comes from the fact that the critical current(I_c) can be modulated by the bias current(I_H). Typically the variation is anything but sinusoidal, however in the present application the Slug is used purely as a null detector in a potentiometric circuit and so all we require is a large dI_c/dI_H.

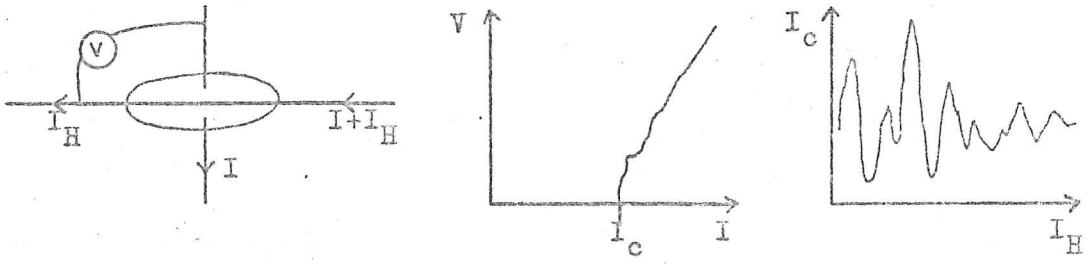

Various means can be used to produce a signal dependent on the instantaneous value of I_c(and therefore on I_H) but only the method actually used will be described here. It is possible to use this signal(suitably amplified) in a feedback system to keep the circuit automatically balanced, which saves a good deal of

effort, and a lot of work was put into trying to make the system stable in feedback mode. However, due to a lack of knowledge of feedback theory(especially in the design of the filter), the system could not be made stable with adequate gain(i.e. giving less than a 1% offset error);particular difficulty being encountered when the system was disturbed by magnetic field noise. Another source of difficulty was that the Slug characteristic(I_c v. I_H) was often changed, sometimes quite drastically, when the field was rotated. This necessitated resetting of the bias current(I_H) and is believed to be due to some of the magnetic field produced by the very large eddy currents in the circuit becoming trapped in the Slug junction.

Eventually the possibility of using feedback was abandoned (although it is now known why it would not work before) and all the measurements were made manually. Some idea of the tedium of this(the reason for the effort expended in the search for stability) can be gained from the fact that obtaining a couple of dozen points in a field sweep typically took two hours: feedback could have cut this by a factor of five, thus enabling five times as many measurements to be taken.

2.d(ii) Electronics

A block diagram of the electronics used to convert the critical current into an electrical signal, showing the waveforms at various parts of the circuit, is to be found in Fig. 3.

Following Wade(1969) and Rumbo(1969) a sawtooth oscillator (instead of sinusoidal) with D.C. bias was used to provide current to the Slug junction. The purpose of this is to avoid the noise which is sometimes observed on the reverse transition(N to S) of the Slug. The potential across the junction was amplified by a transformer-coupled(15:1 ratio) differential pre-amplifier(Rumbo, 1969) located close to the top of the cryostat to avoid the pick-up of electrical noise. This was followed by the saturating amplifier, two-stage active filter and d.c. amplifier with back-off control (to zero the output) which are shown in Fig. 4. The design of these stages was similar in principle to previous designs used in the Lab., except for the use of integrated circuit operational amplifiers (LM709C). The means by which an output proportional to the change in I_H is produced and the design of the d.c. amplifier are discussed in Appendix A.

2.d(iii) The calibration of the standard resistor

In order to make comparison of the low temperature specimen resistance with its room temperature value it is necessary to have a standard resistor in the Slug circuit. This resistor was calibrated by measuring the voltage across it with a d.c. chopper amplifier (Keithley 148 milli-microvoltmeter) whilst passing a current of about an Amp; the room temperature resistance of the specimen was measured in the same way. In order to eliminate thermal emfs and their drift it was necessary to take many readings, continually

reversing the current. The chopper amplifier was calibrated against a Weston cell with the Tinsley potentiometer used for thermometry measurements.

The standard resistor(Plate III) was constructed from a cylinder of copper-1% aluminium alloy, to keep its variation within the Helium range negligible. Because of the rather crude way in which the voltage contacts were soldered to the body of the resistor, there were some doubts about its reproducibility, particularly as wires had to be soldered onto it at intervals. However an independent check of the resistance of the dirtiest specimen using the chopper amplifier revealed that the standard resistor had retained its calibration to better than ½%.

2.d(iv) Noise in the Slug circuit

There are a number of sources of noise to be considered:

(a) Magnetic induction - this lumps under one heading all the forms of noise discussed in section 2.b2.

(b) Johnson noise - almost always negligible because of the small bandwidth, low temperature and low circuit resistance.

(c) Noise in the electronics - the pre-amplifier being by far the most important source because of the low signal level.

Clearly the choice of bias point of the Slug can have no effect on (a) and (b), as they are inherently in the Slug circuit itself. However if the Slug is set on an insensitive part of its characteristic (c) will be effectively increased, as it is the noise

referred to the Slug circuit which is important. At low fields and an insensitive Slug setting it is believed that (c) can be dominant but it usually does not concern us when working in magnetic fields.

In the present experiments the typical noise level was about 5 pV(i.e. about 0.02 mA into the 0.33 $\mu\Omega$standard resistor) in a 200 G field. This figure represents between two and three orders of magnitude improvement in usable sensitivity over conventional means(Walton,1964).

2.d(v) Miscellaneous observations

The following paragraphs form a selection of interesting and useful points discovered during the course of these experiments.

2.d(v)a Superconducting joints to Niobium wire

A certain amount of trouble is inevitably associated with the making of joints to the Niobium wires of the Slugs by soldering(some people have resorted to spot-welding) as only a mechanical joint is made. However it is well known that by cleaning the wire well and plunging it into a molten solder blob a reliable joint can often be made. What is not so well known is that the goodness of the joint can be tested by its room temperature resistance. With the size of the solder blobs used a resistance of 70 mΩ (measured by passing 10 mA around the Slug circuit, which had been broken at one point, and testing the voltage across the joints with a probe connected to a D.V.M.) always gave a satisfactory superconducting joint when cooled.

2.d(v)b Choice of Slug for a noisy environment

In early experiments it was found that the sensitivity of the Slug(to changes in the standard resistor current) decreased as the field(and noise) was increased. The particular Slug used had a period of a few hundred microamps,but only near the origin was its modulation appreciable. As the noise increased the localised modulation of the Slug became less important in determining the output and the sensitivity fell.

Ideally one would like a Slug with an infinite,linear characteristic so that the noise would average to zero, but this is not possible. However it may be noted that a long period is an essential criterion for the Slug to work satisfactorily in a noisy environment.

2.d(v)c Effect of short-circuits to earth

In experiments where one side of the specimen is connected to the cryostat, additional connections to earth must be avoided but are difficult to detect. They can give rise to unusual effects,for example in one run the specimen resistance(which had previously behaved quite normally) varied with field as shown below. This was

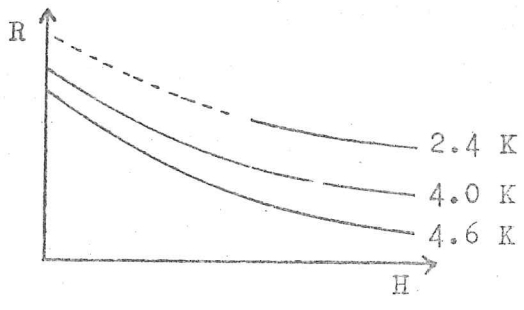

immediately recognised as being spurious, but its explanation was more difficult: When the circuit resistances are so small the drawing of an equivalent circuit incorporating

a short-circuit is difficult as the resistance of the short-circuit cannot be neglected. However consider the following circuit in which X is a hypothesised short(~1 $\mu\Omega$).

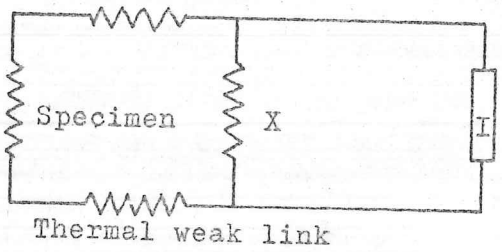

It will be recalled that the thermal link was coated with Sn/In ($T_c \simeq 3\frac{1}{2}$ K) and it had a temperature gradient along it; hence it was partially normal, depending on the temperature of the specimen and the magnetic field applied(~7 $\mu\Omega$ when fully normal). Estimates of the resistances involved revealed that this could indeed be the explanation, and when the cryostat was opened up the short-circuit was found(one of the wires to the specimen had become trapped by the radiation shield and the Teflon sleeving had been pierced!)

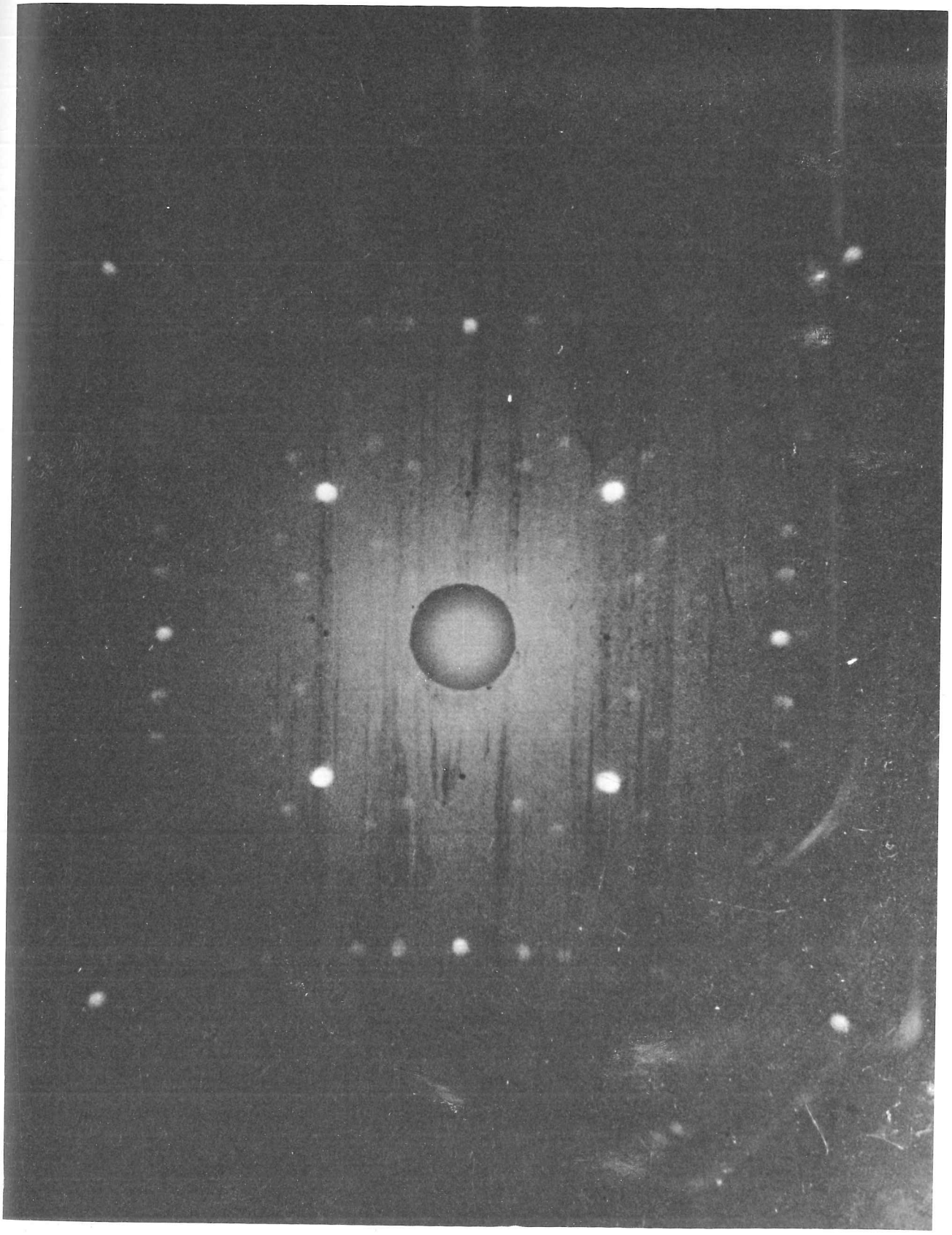

PLATE IV

Chapter 3

SPECIMENS

3.a Requirements

It was initially felt that it would be useful to have a facility for thermal conductivity measurements so that comparison with the results of Walton(1964) would enable a check to be made on the stability of the intermediate state structure. Furthermore, in order to make a direct comparison, it was decided that the specimens should be of similar size, provided that this did not compromise other design requirements. The restriction of heat input to minimise excessive bubbling of the Helium coupled with the need to produce an easily measurable temperature difference had lead Walton to choose specimens 2 mm in diameter with 10 cm between the side-arms. If made of the purest tin available, a specimen of these dimensions would have a Helium temperature resistance somewhat less than 10^{-7} Ohm, which is a convenient magnitude for Slug measurements.

Since we require the side-arms to be on opposite sides of the specimen, in order to reduce the magnetic pick-up area, the distance distance between them must be such that any transverse electric field* does not contribute appreciably to the potential difference measured. Furthermore the side-arms should be narrow to minimise

---

* This transverse electric field may be due to Hall effect or, in specimens where the axis is far from a principal axis, anisotropy.

distortion of the current flow and domain structure. Happily these are consistent with the criteria for thermal measurements. However a reduction to 8 cm in specimen length was judged to give a worthwhile gain in terms of the size of magnetic field coils needed, without compromising unduly the other specimen requirements. The dimensions of the specimens as cast are summarised below:

Overall length	11 cm
Distance between centres of side-arms	8.05 cm
Width of side-arms	0.2 cm
Diameter	0.203cm
Mean diameter after polishing	0.180cm

In order to minimise flux trapping the specimens should be as nearly perfect as possible; i.e. polished, defect-free single crystals. Furthermore to reduce effects due to crystalline anisotropy the specimen axis should be a principal direction, preferably the tetrad-[001]. This last requirement was relaxed for the last specimen studied(SnIII) in order to ascertain its effects. Polishing of the crystal surface is desirable in connection with the "0.58 effect": Andrew(1948) investigating the size dependence of the threshold field found that it did not vary with temperature (in contrast with the earlier results of Misener,1938) except for a specimen which had a poor surface. Indeed we obtained similar results with an early specimen(no. 2) which had a heavily etched

surface: the threshold field ranged from 0.64 to 0.76 H_c, depending on temperature and field orientation(Figs. 15 & 16). None of the electropolished crystals showed any significant departure from the figure of 0.52 H_c expected(Andrew,1948) from their diameter and the interphase surface energy in tin.

3.b Materials

The resistance ratios($R(293^\circ)/R(4.2^\circ)$ hereafter referred to as RR) of many batches of pure tin from Cominco and Vulcan were measured to provide a guide to selection of materials. However, because the RR of tin is 25% anisotropic, this was not always a reliable guide. This is the reason why there is a rather large gap in RR between specimens Sn 7 and Sn24: The material for Sn24 had a RR of less than 19 000 when cut from the ingot, but nearly 24 000 when cast! (in spite of the fact that the grains in the ingot were a few mm across).

To provide the lower purity materials a master alloy of 1% In in Sn was first produced and then appropriately diluted with more tin. The purpose of this is twofold: it gives a more even distribution of the In in Sn, and it is difficult to measure accurately the very small quantity of In needed to produce 40 gm of 35 ppm alloy. Inspection of various references revealed that:

$$RR \simeq 0.19 / (\text{In content})$$ as fraction by weight

and this was confirmed by a number of test samples which were dipped into a storage dewar.

3.c Orientation

The crystals were all oriented by back-reflection Laue X-ray photographs, taken on polaroid film, which is much more convenient to use than conventional plates. Plate IV shows a reproduction of a picture taken off the end of one of the specimens. The four-fold symmetry of the tetrad axis shows up well.

Orientation of the crystals proved to be an unexpectedly difficult task. The main source of confusion was probably caused by the axial ratio of tin(0.5456) being such as to give a number of zone angles close to 45° (the angle between $\langle 110 \rangle$ and $\langle 100 \rangle$). However once the tetrad was located there was never any doubt about it.

3.d The preparation of the seed crystals

Although it is very easy to grow tin single crystals there is a very strong tendency for one of the directions lying in the basal plane to grow parallel to the temperature gradient(i.e. along the length of the specimen). In order to grow an [001] specimen seeding is therefore obligatory, and furthermore the production of a seed is not easy. The most satisfactory seed was eventually produced by a lengthy process which is outlined below.

A large(3" long by 1" diam) piece of tin was cast to give a single crystal of random orientation(apart from a small polycrystalline core). This crystal had the tetrad almost perpendicular to its axis. It was cut with a Servomet spark machine

into a number of $\frac{3}{4}$" long, $\frac{1}{4}$" square section [001] seeds. These were inconveniently short, but after a number of trial attempts four specimens were produced simultaneously, one of which became Sn33. The polycrystalline section of the seeds(mainly low angle grain boundaries) had unfortunately dominated the seeding process and the crystals turned out to be 5° off [001].

Accordingly a large precise seed was grown from one of the spare specimens in a specially constructed graphite mould. This was then exactly oriented and one end was spark-planed accurately perpendicular to [001]. Seeds cut from this master were then used for all the other specimens: the seed for the off-[001] specimen (SnIII) being cut at a large angle to its length.

3.e Crystal growing

Because of the great length over which a uniform diameter is required, the Czochralski method is not practicable, although quite recently Tsivinskii and Stepanov(1965)have reported the use of a floating mask to grow very long thin germanium crystals of any desired cross-section.

At first the soft mould technique(packing the annular area between the specimen and a silica tube with magnesium oxide) was tried; but the surface finish was poor, leaving much to be polished off, and the drawing of the tin to the correct diameter was felt to be a potential source of impurities.

Mr T.E.Brown of the Cavendish Crystal Growing Unit then

suggested trying to grow the specimens in a split graphite mould (Bridgman method). This gives very precise control of the specimen dimensions and, provided that the tin could be persuaded to flow into the channels, the side-arms could be an integral part of the crystal. A mould(ref.no. CGU 16) in which four specimens could be grown simultaneously from the same seed was accurately fabricated from graphite by Mr.J.Pratt of the Unit. The precision of this mould is shown by the fact that the specimens were both round and uniform over their length to well within 1%.

The following paragraphs give a brief discription of the steps involved in the growing of each of the specimens. The seed was first placed in its holder(the seed block) and then the two halves of the mould were fastened together by means of the three graphite bands. In order to provide a gas-tight seal the joint was painted with Aquadag. The appropriate amount of material(about 40 gm) was put into the filler at the top and the whole inserted into a Bridgman 265 vacuum furnace., with heating provided by a Radyne R.F. power oscillator coupled to the tin by a few turns on the outside of the furnace. The necessary temperature gradient was provided by two means: the heater was near to the top of the mould and the seed block was sat on the water cooled chill.

The furnace was then evacuated by a diffusion pump and the temperature of the tin raised to somewhat above its melting point ($232^{\circ}C$). In order to ensure that the tin ran properly into the mould

it was found necessary to shut off the pumps and admit an inert gas(Argon). When this had been done a few times,the mould was slowly lowered by a motor until the tin had solidified whereupon the R.F. power was turned off and the tin allowed to cool slowly to avoid strain. Of course the settings of the power and the height of the heating coil had to be found by preliminary trial runs, but once this was done there was little trouble experienced with specimens not seeding on properly.

When the mould was thoroughly cool it was removed from the furnace and split open to remove the crystals. This was the most delicate part of the whole operation as they were extremely soft (especially the purest specimens). However, with a little practice and because four were grown simultaneously, it was always possible to get at least one(and usually three) out unstrained.

3.f Electropolishing

The final stage in the production of a specimen for mounting is electropolishing(Tegart,1956). A cell was constructed to hold the specimen(anode) vertically at the centre of a cylinder formed from rolled tin sheet. The tin cylinder(cathode) was 5 cm diam. and 10 cm long. The electrolyte was contained in a glass vessel surrounded by a beaker of ice. The entire cell could be rotated by hand(about 1 revolution every 5 secs.) with the specimen itself remaining stationary along with the top plate which carried a slip ring used to feed current to the cathode. The electrolyte

was one of those used by Fourie, Weinberg & Boswell(1960) with composition(by volume):

Ethanol	85%
Ethylene glycol monobutyl ether	10%
Perchloric acid	5%

Because of the low perchloric acid concentration this is very much safer than the more commonly used acetic acid/perchloric acid mixtures. Since the specimens as cast were very smooth, only a light polish was needed; principally to remove the "seam" where the two halves of the mould had come together. The optimum conditions were found by a series of trial experiments to be:

3 A for 2 mins followed by 1 A for 5 mins at 5°C.

The high initial rate removed the seam quickly without doing much to the overall diameter; the lower rate gave a final finishing polish. A total of about 0.01 cm was removed during polishing.

3.g Notes on the specimens

A summary of the specimen characteristics is to be found in Table 2. The [001] specimens have been numbered according to their RR in order to facilitate identification of the results. The other number in column 1 is the chronological order of the specimen. Specimens (1) and (2) are not shown in the table as they were really only used as tests of the measuring system. (1) was a polycrystalline drawn wire and (2) was crystallized(in a random

Specimen Characteristics

Number	Ψ deg.	Material	RR = $\frac{R(293^{\circ}K)}{R(4.2^{\circ}K)}$	R(293) mΩ	Diameter cm	Mean free path cm
3) Sn33	5	C	33 200	4.91	0.173	0.024
5) Sn24	0	V	23 900	4.51	0.181	0.017
6) Sn 7	0	V + 35ppm In	7 120	4.58	0.180	0.0051
4) Sn 1	0	V +170ppm In	1 380	4.37	0.185	0.0010
7) SnIII	69	C	22 500	3.28	0.181	0.022

Notes:

Materials - C Cominco 69 grade tin, batches HPM 2725 & 387

V Vulcan Spectrographic grade tin, batch VS 1793P

Ψ - Angle between specimen axis and [001]. The axis of SnIII lay about 2° from [111].

The diameter was calculated from the resistance; in each case this agreed with micrometer measurements(to $\pm$0.001 cm).

The mean free path was calculated using $\rho\ell = 10^{-11}\ \Omega(cm)^2$ (Chambers 1952)

TABLE 2

direction) by the soft mould technique. Both had etched surfaces and only (2) was measured in the intermediate state. These results are only referred to in connection with the 0.58 effect mentioned earlier. The only non - [001] specimen(7) has been distinguished by labelling it as SnIII since its axis lay close to [111].

To avoid contaminating the seed and mould(which had been leached out with boiling hydrochloric acid) it was decided that the first sample grown should be of the purest material(Cominco). However, as noted briefly earlier, it took an extra half dozen runs to get the conditions right. The RR dropped to about 33 000, presumably due to repeated contact of the hot tin with the mould removing a small quantity of impurities from the graphite. Because of this(and since the seed crystal was about 5^{o} off axis) it was intended that an attempt would be made later to grow a purer specimen. However when the results for Sn33 were analysed it was found that it was sufficiently near to the pure limit to make it unnecessary to try and do any better. In any case efforts to obtain purer starting material(similar to the Vulcan lot used by Guenault (1960), which had a RR of about 80 000) had drawn a blank, with the discovery that the purest material now supplied by Vulcan had a RR of only 22 000 - a factor of two worse than the Cominco lot used.

Once the longer seed had been grown it proved a much more routine task to produce the remaining four specimens.

Chapter 4

THE THEORY OF BOUNDARY RESISTANCE

4.a A Review of the Theory of S-N Interface Reflection($T \ll T_c$)

The difference in behaviour between the electrical and thermal resistance at low temperatures* was explained by the work of Andreev(1964) on the mechanism of reflection of electronic excitations by an S-N interface. This work, together with a later paper(Andreev,1966), showed why the interface is most effective in destroying a heat current, but quite consistent with the flow of an electrical current. With a view to later discussion it is convenient to present here Andreev's analysis in qualitative terms, considering an excitation incident on the interface from the normal side(Fig. 6). The interface is to be regarded as a region where the energy gap, Δ, varies within a few coherence lengths(ξ) from zero to its equilibrium value, Δ_∞, far within the superconducting region(S).

Insofar as it is legitimate to think of a local excitation spectrum, the value of Δ at any point defines its hyperbolic variation $\epsilon(\delta k)$, δk being measured radially from a point on the fermi surface. The variation of Δ with position is due to the electron-electron interaction responsible for superconductivity,

* We implicitly exclude the phonon thermal conductivity, which is an important contribution at very low temperatures, in the whole of the discussion.

and the excitation must therefore be considered as subjected to a force-field imposed collectively by the electrons in the superconductor; since it is interacting with a massive object it retains the same total energy whilst its momentum changes. In these terms we can picture the excitation changing its k-state in accordance with Fig. 6. If its energy is less than Δ_∞ it cannot penetrate further into the S-region than the reflection point x_ε, and the whole process of reflection can be seen as an adiabatic transition from the initial electron-like state A through A' to A'' (which is the same as B'') and back through B' to the final hole-like state B. Particle conservation is achieved by the injection of a pair of electrons into the superconducting condensate. In terms of the electron occupation picture(conventional for normal metals) the superconductor imposes on the distribution function in the N-region the boundary condition that if a state just outside the fermi surface at $\underline{k} + \delta\underline{k}_\perp$ is occupied ($\delta\underline{k}_\perp$ being a vector normal to the plane of the interface), then the state just inside at $-\underline{k} + \delta\underline{k}_\perp$ shall be unoccupied. On the other hand, if its energy is greater than Δ_∞, the excitation can pass freely through the interface which imposes no such condition.

This discussion as an adiabatic process is only strictly valid if Δ changes so slowly that there is no tendency for the states A and B to be mixed together. However, since the difference in $\underline{k}$ between A and B is of the order of $1/\xi$, there must be some mixing as the interface is only of order ξ wide: this has the consequence

that when $\epsilon > \Delta_\infty$ the excitation may be partially reflected(there is a certain amount of similarity to ordinary potential scattering). Andreev has calculated the reflection coefficient(Fig. 9) R for a sharp interface, which gives the maximum value to be expected: R is of course unity for $\epsilon < \Delta_\infty$, and falls nearly to zero by the time ϵ has reached $2\,\Delta_\infty$.

Figure 7 shows the modified electron distribution in a normal metal carrying an electrical current and a heat current, from which it is clear that in the former case the matching of filled and unfilled states on opposite sides of the fermi surface, as demanded by the boundary condition, is already satisfied; while in the latter it is wholly violated. This provides the explanation of the difference in behaviour between the two which is found experimentally. One must remember however that this boundary condition applies only for $\epsilon < \Delta_\infty$, and does not affect most of the excitations at temperatures near T_c.

4.b Andreev Reflection and Magnetoresistance

With a sample exhibiting strong magnetoresistance it is not entirely clear(Walton,1965) why the intermediate state electrical resistance should be linear even though there is a constant field(H_c) in the bulk of the N-domains, which are assumed to exhibit the magnetoresistance of the bulk material. The thermal resistivity measurements show the existence of strong interference by the phase boundaries, which may be separated by much less than the cyclotron

radius. Consequently one must explain why the resistance variation neither lies below the linear nor has a sharp rise near H_c.

With the aid of the accompanying diagram we give a simple explanation of why Andreev reflection should have no effect on the magnetoresistance of the normal domains.

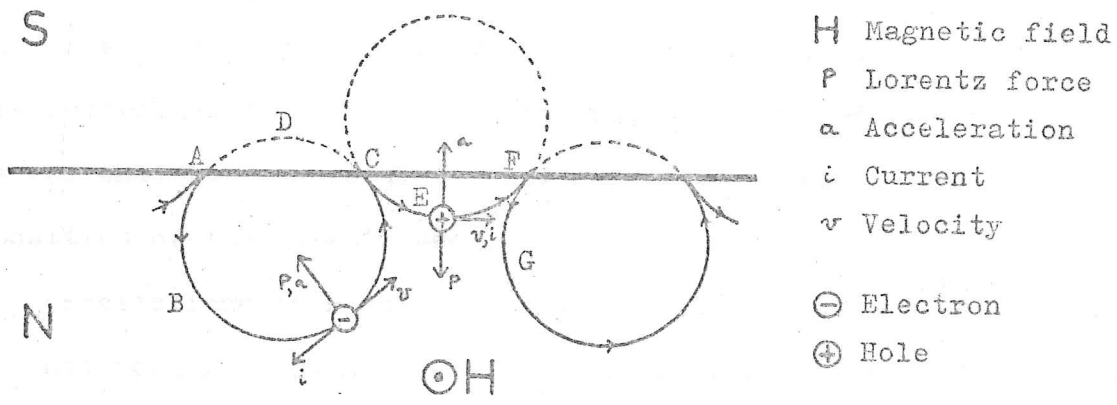

An electron arrives at C and is reflected as a hole, which then follows a peculiar trajectory because of its negative mass. The current however completes effectively the same orbit in the normal metal(by following the path $\overleftarrow{ABCEFG}$) as the electron would have done in the absence of the boundary($\overleftarrow{ABCDAB}$). On reaching F the hole is reflected as an electron which moves towards G, in just the same manner as it moved from A to B before the first reflection. Furthermore, by drawing another phase boundary less than two cyclotron radii away from the first, it can readily be seen that the current always effectively completes its orbits in the N-material.

4.c Theoretical Model of an S-N Interface

We assume that near the interface Δ varies as in Fig. 6, being strictly zero in a normal region $N(x < x_B)$ and rising in the superconducting region $S(x > x_B)$ to its bulk value Δ_∞. An electric field may exist in N but not in S. There can be little doubt that in reality the boundary is a complex fluctuating situation, not to be described in this classical way, which we are forced to adopt in order to make some progress. The value of Δ in the fluctuating region will be determined by factors such as thermal disordering and reduction by a current, but the result is not sensitive either to the value or position of the cut-off used.

Excitations in N suffer elastic collisions with a relaxation time τ_1 and mean free path $\ell_1 = v_f \tau_1$, which is also the free path for such collisions in S(Bardeen,Rickayzen & Tewordt,1959). We must also allow for the fact that some electrons will be totally, and others only partially, reflected as holes from the S-N interface. These interface effects have an important consequence, not usually found in conduction processes in normal metals, that the total occupation of an energy shell need not stay constant. It is therefore necessary to allow for the existence of inelastic scattering processes which help to restore the true equilibrium state, and we shall incorporate these through a second relaxation time τ_2(and corresponding free paths ℓ_2^N and ℓ_2^S, which need not be the same in the N and S states of the same material. We take τ_2 as the overall relaxation time for the

removal of excitations from a particular energy shell ~~state~~, strictly we should allow for three separate processes in S:

a) Elastic scattering around a single energy shell.

b) Inelastic scattering between different energies on the same excitation branch.

c) Exchange of excitations in pairs with the ground state;

of these only (b) and (c) contribute to τ_2.

The last may be a very slow process, and in real metals may be bypassed if the energy gap is at all anisotropic(Phillips,1969).

If the probability of occupation, $f(\varepsilon)$, of a given state$(\varepsilon,\underline{k})$ differs from its equilibrium value, $f_0(\varepsilon)$ the fermi function, by an amount $g(\underline{k})$, we shall write the collision term in the Boltzmann equation in the form:

$$\left[\dot{g}(\underline{k})\right]_{coll} = -\left[g(\underline{k}) - \bar{g}\right]/\tau_1 - g(\underline{k})/\tau_2 \qquad (4.1)$$

where $\bar{g}$ is the average of $g(\underline{k})$ around the energy shell ε.

Particular interest attaches to those excitations with $\varepsilon > \Delta_\infty$, which penetrate into the superconductor and are scattered there; for the randomization due to scattering certainly generates entropy, yet we have excluded the possibility that the resulting resistance may be manifested locally as an electric field. We shall show that the electric field in N is not modified in our model(in contrast to what we understand from Landau(1970) to be the behaviour of Nozieres' model), but that the extra resistance appears as a potential discontinuity at the interface x_B; in exact analogy to the temperature

discontinuity in Andreev's(1964) analysis of the thermal problem.

To describe the distribution $g(\underline{k})$ we shall use the excitation model in both N and S, as illustrated in Fig. 6. In N there is a clear distinction between electron-like(e.g. A) and hole-like(e.g. B) states which are separated by the cusp at $\varepsilon = 0$; in S there is continuity from one branch to the other. However the important property of normal metals is retained(at least in an isotropic superconductor) that no scattering can transfer an excitation from one to the other. In Equn.(4.1) therefore $\bar{g}$ is the average around one shell only, not both. This property is not preserved at the S-N interface, where such transfers are caused by Andreev reflection.

The mathematical difficulties of the model will now be reduced very considerably by restricting it to one dimension; supposing excitations to move only parallel to the x-axis, normal to the interface. The fermi surface is reduced to two points(Fig. 8 - F & F') and the spectrum to four branches: (1) & (4) just outside the fermi points representing typical electron-like excitations, (2) & (3) just inside representing hole-like ones. The arrows represent the direction of particle motion. The departure from equilibrium for a particular excitation energy ε at any point is now characterized by four functions: g_1, g_2, g_3, g_4. Under the influence of an electric field, E, and in the presence of both elastic(relaxation time τ_1) and inelastic(τ_2) scattering these are solutions of the following Boltzmann transport equations:

$$
\begin{aligned}
-v_f \frac{dg_1}{dx} - eEv_f f_o' &= -\frac{g_1 - \frac{1}{2}(g_1+g_4)}{\tau_1} - \frac{g_1}{\tau_2} \\
v_f \frac{dg_2}{dx} - eEv_f f_o' &= -\frac{g_2 - \frac{1}{2}(g_2+g_3)}{\tau_1} - \frac{g_2}{\tau_2} \\
-v_f \frac{dg_3}{dx} + eEv_f f_o' &= -\frac{g_3 - \frac{1}{2}(g_2+g_3)}{\tau_1} - \frac{g_3}{\tau_2} \\
v_f \frac{dg_4}{dx} + eEv_f f_o' &= -\frac{g_4 - \frac{1}{2}(g_1+g_4)}{\tau_1} - \frac{g_4}{\tau_2}
\end{aligned}
\qquad (4.2)
$$

where $f_o' = \frac{df_o}{d\epsilon}$,

The usual current-carrying solution of these equations has

$$g_1 = -g_3 = g_2 = -g_4$$

and we also note that the equations do not couple excitation branches of opposite character : g_1 is coupled by collisions to g_4 only, and g_2 to g_3 only. However this full symmetry does not hold in the presence of an S-N interface, where the Andreev reflection transfers excitations between branches 1 and 2 and between 3 and 4. Nevertheless we may retain the conditions

$g_1 = -g_3$ and $g_2 = -g_4$ everywhere because this is not inconsistent with either the reflection process or the symmetry of the equations. This enables us to reduce the four

equations to two involving only g_1 and g_2:

$$\left.\begin{aligned} \frac{dg_1}{dx} + eEf_o' &= \frac{g_1 + g_2}{2\ell_1} + \frac{g_1}{\ell_2} \\ \frac{dg_2}{dx} - eEf_o' &= -\frac{g_1 + g_2}{2\ell_1} - \frac{g_2}{\ell_2} \end{aligned}\right\} \qquad (4.3)$$

(These equations are equally valid in the superconductor, where E = 0) Certain general properties of these equations may be noted immediately. Adding and subtracting we find:

$$\frac{dj}{dx} = \frac{q}{\ell_2} \qquad (4.4)$$

$$\frac{dq}{dx} + 2eEf_o' = \frac{j}{\ell_o} \qquad (4.5)$$

where $1/\ell_o = 1/\ell_1 + 1/\ell_2$ and we have written j for $(g_1 + g_2)$ and q for $(g_1 - g_2)$; these are respectively the contributions to the current and charge density of excitations of energy ε. In N charge uniformity requires that dQ/dx vanish identically, where $Q = \int q d\varepsilon$. Integration of Equn.(4.5) over energy then shows that the electric field is uniquely determined by the current density J, which is proportional to $\int j d\varepsilon$. On the other hand dQ/dx need not vanish in S, where charge uniformity is preserved by motions of the ground state. The absence of electric field shows that Q must vary if J does not

vanish. Unusual boundary conditions are therefore unable to modify the electric field in either N or S: it is necessarily the same almost everywhere as it would be in the absence of interface effects.

It follows from Equns.(4.4) & (4.5) that in both N and S:

$$\frac{d^2q}{dx^2} = \frac{q}{\lambda^2} \qquad (4.6)$$

$$\frac{d^2j}{dx^2} - \frac{j}{\lambda^2} = -\frac{2ef_o'E}{\ell_2} \qquad (4.7)$$

where $\lambda = (\ell_o \ell_2)^{\frac{1}{2}}$ is the diffusion length over which an excitation travels by random walk before being inelastically scattered.

4.d Boundary Conditions

Although the extra resistance cannot be accounted for by modifications to the electric field in either N or S, there remains the possibility of a potential discontinuity, proportional to J, at the boundary, as shown in Fig. 6. Indeed the discontinuity is needed to satisfy the boundary conditions set by the reflection process. The height of the potential step, $h = V(x_B^-) - V(x_B^+)$, depends on the number of excitations having sufficient energy to penetrate into S and suffer scattering there. The existence of such a step complicates the consideration of the boundary conditions at the interface; for it causes a sudden shift of the g-functions such that j is unaffected, but q changes by an amount $2ef_o'h$ (this is easily seen by integrating Equn.(4.5) with respect to x):

$$q(x_B^+) = q(x_B^-) - 2ef_o'h \quad \& \quad j(x_B^+) = j(x_B^-) \qquad (4.8)$$

There is also the boundary condition at the reflection point, x_ε, to be considered; this is determined by the Andreev reflection. The excitations on branch 1 with a certain $\varepsilon > \Delta_\infty$, leaving the interface for the normal metal, are supplied by those arriving from N on branch 2(of which a fraction R are reflected) and those arriving from S on branch 1(of which a fraction 1-R are transmitted); thus:

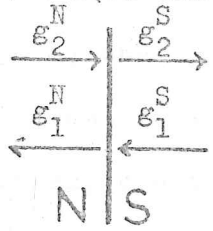

$$\left.\begin{aligned} g_1^N &= Rg_2^N + (1-R)g_1^S \\ g_2^S &= Rg_1^S + (1-R)g_2^N \end{aligned}\right\} \qquad (4.9)$$

Rearranging these equations* one finds that:

$$\left.\begin{aligned} q^N &= q^S \\ j^N &= j^S - \alpha q^S \end{aligned}\right\} \qquad (4.10)$$

where $\alpha = 2R/(1-R)$. Figure 10 illustrates the boundary conditions (Equns.(4.8) & (4.10)), together with sketches of the solution in the clean limit.

It is only at this point that the theory for the SNS sandwich results parts company with the intermediate state theory, for we now impose a further condition: that the solution has the periodicity of the intermediate state structure($a^N + a^S$). This forces $q = 0$(i.e. $g_1 = g_2$) at the centre of each domain, since excitations on branches

* Note that the exact form of these equations depends on whether N has been chosen to the left or right. The actual choice made is irrelevant of course but, as it is tied up with the choice of suffixes for the g's(1 & 2), one must be consistent.

(1) and (2) go through identical histories before they arrive at the centre of any domain, with the important exception that they see the electric field in opposite directions with respect to their own motion.

4.e The Solution of the Equations

Now that the equations have been set up and the boundary conditions found, all that remains to be done is to solve them for the potential step, h, and hence to deduce an expression for the variation of the additional resistance, $\delta R/R_o$ (Fig. 5) with the fraction of normal material, $\eta = a^N/(a^N + a^S) = \left\{\frac{H}{H_c} - \frac{1}{2}\right\}$.

The solution to Equns.(4.4)-(4.7) for j and q may be written:

$$\left.\begin{aligned} q &= A\,\mathrm{Sinh}(x/\lambda) + B\,\mathrm{Cosh}(x/\lambda) \\ j &= \frac{\ell_o B}{\lambda}\,\mathrm{Sinh}(x/\lambda) + \frac{\ell_o A}{\lambda}\,\mathrm{Cosh}(x/\lambda) + 2ef'_o E\ell_o \end{aligned}\right\} \qquad (4.11)$$

where the integration constants A and B take different values(A^N & A^S and B^N & B^S) in N and S since λ and ℓ_o may not be the same in both.

At the centre of an N domain($x = -a^N/2$) $q = 0$:-

$$\left.\begin{aligned} \therefore \quad B^N &= A^N\,\mathrm{Tanh}(a^N/2\lambda^N) \\ \text{\& similarly at } x = (a^S/2): \quad B^S &= -A^S\,\mathrm{Tanh}(a^S/2\lambda^S) \end{aligned}\right\} \qquad (4.12)$$

As q is continuous through the reflection point x_ε, from Equn.(4.11a) evaluated at the boundary($x = x_B \approx 0$) we have:

$$q^N(x_B^-) = B^N \qquad \text{and} \qquad q^S(x_B^+) = B^S \qquad (4.13)$$

Substituting Equn.(4.12) into Equn.(4.11) for j:

$$j^N = \frac{\ell_o^N A^N}{\lambda^N}\left(\text{Cosh}(x/\lambda^N) + \text{Tanh}(a^N/2\lambda^N)\,\text{Sinh}(x/\lambda^N)\right) + 2ef_o'E\ell_o^N \quad (4.14)$$

and similarly(with E = 0 and Tanh replaced by -Tanh) for j^S.

At the reflection point($x = x_\varepsilon \approx 0$) we have:

$$\left.\begin{aligned} j^N(x_\varepsilon^-) &= \frac{\ell_o^N A^N}{\lambda^N} + 2ef_o'E\ell_o^N \\ j^S(x_\varepsilon^+) &= \frac{\ell_o^S A^S}{\lambda^S} \end{aligned}\right\} \quad (4.15)$$

The boundary conditions can now be imposed on these solutions:

$$\left.\begin{aligned} &\text{from (4.8):} \quad -A^S\text{Tanh}(a^S/2\lambda^S) = A^N\text{Tanh}(a^N/2\lambda^N) - 2ef_o'h \\ &\text{from (4.10):} \quad \frac{\ell_o^S A^S}{\lambda^S} - \frac{\ell_o^N A^N}{\lambda^N} - 2ef_o'E\ell_o^N = -\alpha A^S\text{Tanh}(a^S/2\lambda^S) \end{aligned}\right\} \quad (4.16)$$

These equations(4.16) can be written in matrix form as:

$$\begin{bmatrix} \text{Tanh}(a^N/2\lambda^N) & \text{Tanh}(a^S/2\lambda^S) \\ -\dfrac{\ell_o^N}{\lambda^N} & \left\{\dfrac{\ell_o^S}{\lambda^S} + \alpha\text{Tanh}(a^S/2\lambda^S)\right\} \end{bmatrix} \begin{bmatrix} A^N \\ A^S \end{bmatrix} = \begin{bmatrix} 2ef_o'h \\ 2ef_o'E\ell_o^N \end{bmatrix} \quad (4.17)$$

Since we know that $dQ/dx = 0$(p.58) we also have $\int A^N d\varepsilon = 0$, and this gives a condition for h. Hence we now solve (4.17) for A^N:

$$A^N = \frac{\begin{vmatrix} 2ef_o'h & \text{Tanh}(a^S/2\lambda^S) \\ 2ef_o'E\ell_o^N & \{\ell_o^S/\lambda^S + \alpha\text{Tanh}(a^S/2\lambda^S)\} \end{vmatrix}}{\begin{vmatrix} \text{Tanh}(a^N/2\lambda^N) & \text{Tanh}(a^S/2\lambda^S) \\ -\ell_o^N/\lambda^N & \{\ell_o^S/\lambda^S + \alpha\text{Tanh}(a^S/2\lambda^S)\} \end{vmatrix}} \quad (4.18)$$

Equating $\int A^N d\varepsilon$ to zero gives:

$$\int \frac{f_o' h \left\{ (\ell_o^S/\lambda^S) + a\,\mathrm{Tanh}(a^S/2\lambda^S) \right\} d\varepsilon}{\Gamma} = \int \frac{f_o' E \ell_o^N \,\mathrm{Tanh}(a^S/2\lambda^S)\, d\varepsilon}{\Gamma} \qquad (4.19)$$

where $\Gamma = (\ell_o^S/\lambda^S)\mathrm{Tanh}(a^N/2\lambda^N) + (\ell_o^N/\lambda^N)\mathrm{Tanh}(a^S/2\lambda^S) +$

$$a\,\mathrm{Tanh}(a^N/2\lambda^N)\mathrm{Tanh}(a^S/2\lambda^S)$$

Multiplying numerator and denominator on each side of (4.19) by $\left[\frac{\lambda^N\lambda^S}{\ell^N\ell_o^S}\right]$ and both numerators by $\mathrm{Tanh}(a^N/2\lambda^N)$:-

$$\frac{h}{E\ell_o^N} = \left[\frac{I}{1-I}\right]\Lambda^N \quad \text{where } I = -\int \frac{f_o' \Lambda^S\, d\varepsilon}{\Lambda^S + \Lambda^N + a\Lambda^S\Lambda^N} \qquad (4.20)$$

$$\text{and } \Lambda = (\lambda/\ell_o)\mathrm{Tanh}(a/2\lambda)$$

It is easily seen that we have an additional potential drop, h, for every half period, $(a^N + a^S)/2$, of the structure(Fig. 10).

$$\therefore \frac{\delta R}{R_o} = \frac{h}{E(a^N + a^S)/2} = \frac{2h\eta}{Ea^N} = \left[\frac{2\,\lambda^N \eta\,\mathrm{Tanh}(a^N/2\lambda^N)}{a^N}\right]\cdot\left[\frac{I}{1-I}\right] \qquad (4.21a)$$

If we now assume that $\lambda^N = \lambda^S$ and $\ell_o^N = \ell_o^S$ the integral becomes:

$$I = -\int \frac{f_o'\,\mathrm{Tanh}(a^S/2\lambda)\, d\varepsilon}{\mathrm{Tanh}(a^N/2\lambda) + \mathrm{Tanh}(a^S/2\lambda) + \left[a\lambda/\ell_o\right]\mathrm{Tanh}(a^N/2\lambda)\mathrm{Tanh}(a^S/2\lambda)} \qquad (4.21b)$$

This integral is turned into a form more amenable to calculation in Appendix B (Equn.(B.5)), but some of its simpler properties are investigated in the next section.

4.f Evaluation of the Additional Resistance

In view of the apparent complexity of the expression for the additional resistance(Equn.(4.21), also referred to as the "exact" expression) it is worthwhile examining its behaviour in two limiting cases:

i) Long diffusion length(or "clean") limit: $a \ll \lambda$, $\mathrm{Tanh}(a/2\lambda) \approx a/2\lambda$

ii) Short diffusion length(or "dirty") limit: $a \gg \lambda$, $\mathrm{Tanh}(a/2\lambda) \approx 1$

Examination of a graph of Tanh(x) soon shows that the great majority of specimens will fall close to either one or the other of these cases. Calculations(and experimental results - see Chapter 6) show that the dividing line between (i) and (ii) comes at a RR of about 25 000 in tin.

However even when these approximations are made the integrals cannot be evaluated analytically because of the form of the Andreev reflection coefficient(Equn.(B.1)). Hence we further approximate by using the "Square Model" for R(Fig. 9):-

$$a = \begin{cases} \infty & \varepsilon < \Delta_\infty \\ 0 & \varepsilon > \Delta_\infty \end{cases} \qquad (4.22)$$

(from now on Δ, without subscript, will be used to denote the value in the bulk of S). As we shall see this simplifies the integrands so much that their integration becomes trivial.

4.f(i) The clean limit($\lambda \gg a$)

In the limit $\mathrm{Tanh}(a/2\lambda) \approx a/2\lambda$ the g, j, and q functions become linear, as illustrated in Fig. 10, and Equn.(4.21) becomes:

$$\left.\begin{aligned} \frac{\delta R}{R_o} &\approx \eta \frac{I}{1 - I} \\ \text{where} \quad I &\approx \int \frac{-f_o' \, d\varepsilon}{(1 - \eta)^{-1} + (\alpha \eta a / 2 \ell_o)} \end{aligned}\right\} \qquad (4.23)$$

In the Square model(Equn.(4.22)) the integrand vanishes for $\varepsilon < \Delta$ and is equal to $-(1 - \eta)df_o$ for $\varepsilon > \Delta$.

$$\left.\begin{aligned} I &\approx 2 (1 - \eta) f_o(\Delta) \\ \text{and so} \quad \frac{\delta R}{R_o} &\approx \eta \frac{2 (1 - \eta) f_o(\Delta)}{1 - 2(1 - \eta) f_o(\Delta)} \end{aligned}\right\} \qquad (4.24)$$

(The factor of two arises from integration over both electron and hole branches of the excitation spectrum). The behaviour of Equn.(4.24) over a wide temperature range is shown in Fig. 11.

Another important feature of this equation is that it is valid for any reflection coefficient in the limit $\ell_o \gg a$. This fact undoubtedly contributes to its good agreement with the results for the purest specimen, Sn33,(and made it unnecessary to grow a purer one - see Chapter 3) in spite of both the apparent crudeness of the Square model and also the absence of adjustable parameters(in fact the value of Δ is open to a certain amount of discussion because of its anisotropy in tin). It is interesting to observe that because $\lambda \gg a$, so that the excitations can pass right through the S regions, the additional resistance is independent of the period, a, of the intermediate state structure(i.e. independent of the number of

boundaries). There is therefore no necessity to make estimates of the domain sizes, which are open to considerable doubt(as discussed further in Chapter 6).

Since α is infinite for $\varepsilon<\Delta$ the effect of using a better estimate for α(having a positive non-zero value in the supergap region, $\varepsilon > \Delta$) is to reduce I, and hence(since I lies between 0 and 1) the additional resistance, of any specimen not pure enough to be fully in the clean limit. The consequence of using the exact expression (4.21) instead of the clean limit expression (4.24) is to reduce the maximum value of $\delta R/R_o$ in specimen Sn33 by only about 10%(see Figs. 25 a & d, which also show separately the effects of doubling the domain size and increasing Δ), bringing it into rather better agreement with the experimental points.

4.f(ii) The dirty limit($\lambda \ll a$)

In the limit $\mathrm{Tanh}(a/2\lambda) \approx 1$ the excitations injected into S decay away so quickly that the boundaries become completely decoupled. Thus we expect that the additional resistance will be proportional to the number of boundaries(i.e. inversely proportional to a) and indeed this is the case:

$$\left.\begin{aligned} \frac{\delta R}{R_o} &\approx \frac{2\lambda}{a}\cdot\frac{I}{1-I} \\ \text{where} \qquad I &\approx \int \frac{-f_o'\,d\varepsilon}{2+(a\lambda/\ell_o)} \end{aligned}\right\} \qquad (4.25)$$

It will be noted that this expression only depends on η through the

variation of the domain period, a, since I is now independent of η.

In the Square model* I simply reduces to the fermi function:

$$I \approx f_o(\Delta) \tag{4.26}$$

and so $$\frac{\delta R}{R_o} \approx \frac{2\lambda}{a} \cdot \frac{f_o(\Delta)}{1 - f_o(\Delta)} = \frac{4\lambda}{a} \cdot \left[\frac{\delta R}{R_o}\right]_{\square\ \eta=\frac{1}{2}}^{\text{clean}}$$

(where $\left[\begin{smallmatrix}\text{clean}\\ \square\ \eta=\frac{1}{2}\end{smallmatrix}\right]$ means Equn.(4.24) evaluated at $\eta = \frac{1}{2}$).

Once again if α is not identically zero in the supergap region the effect is to reduce I and $\delta R/R_o$, although this time by the same factor for all η. Equn.(4.26) leads us to believe that measurements of impure specimens may give information about the scale of the structure(Fig. 12 shows some possible theoretical variations). However the theory given above may not be valid and so it is better to try to check it by using the theoretical domain size variation(Lifshitz et al.,1951 as modified by Pippard,1955). This is discussed in more detail in the next two chapters.

---

* Or $\lambda \ll \ell_o$; which is unphysical, because ℓ_2 is much larger than ℓ_o for the cases where $\lambda \ll a$. This points to the additional resistance in the dirty limit being sensitive to the true variation of α as well as a.

Chapter 5

EXPERIMENTAL RESULTS

5.a General Remarks

In almost all the intermediate state results shown in the Figures the resistance of the specimen is scaled in terms of its value, R_o, obtained by linear extrapolation back to the critical field, H_c, from two points just above H_c(Fig. 5). The critical field itself was calculated using the relation given by Lock et al.(1951), with H_o = 306 G and T_c = 3.731 K(the zero field transitions of the specimens are shown in Fig. 17), and this calculated value was consistent with the curves for all the specimens in spite of the fact that the specimen was not screened from the earth's field: This produces only a small effect even at a temperature as high as $0.995T_c$ because it forms a large angle with the horizontal applied field. The purpose of the extrapolation was to make some allowance for magnetoresistance, since it is unlikely that the resistance would be measured exactly at H_c, and great care was taken to ensure that there were always two points above H_c close enough to make the error in this process very small indeed. The threshold field, H_{th}, was consistent with the expected value($0.52H_c$) for all the electropolished specimens(see p. 42).

Figure 13 shows examples of the noise level(referred to the Slug circuit) with superposed square waves for calibration purposes produced by reversing a measured current through the standard resistor.

These traces are not entirely representative for two reasons:

(a) The chart recorder used introduced a certain amount of interference and this is probably the main source of noise in the upper traces(zero field).

(b) Almost the first observation made of the intermediate state was that there was more noise than with the specimen in the superconducting state. Furthermore the noise level was often actually less when the applied field exceeded H_c. Domain motion(e.g. Sharvin,1965, and Shikina et al.,1968) may be responsible for this extra noise.

In order to estimate the amount of scattering produced by phonons the resistances of the specimens were measured as a function of temperature(e.g. Fig. 18 for Sn33) and plotted against T^5(Fig. 19). This investigation shows that the ideal resistance ratio of tin between 293 K and T_c is about 2×10^5. The linear variations do not quite lie parallel to the results of Aleksandrov et al.(1962) on very pure material(or to each other for that matter), most probably because of the breakdown of Mattiesson's Rule when the two scattering mechanisms occur in comparable amounts.

Because of the strong temperature dependence of the resistance it is essential to measure the resistance ratio of the specimens between the same two definite temperatures, if comparison of behaviour is to be meaningful. Accordingly for all the RR's quoted the low temperature value was obtained by interpolation of the R v. T^5 curves.

It is important to bear this in mind when comparing the resistance ratios of the specimens with those of other workers, e.g. Landau (1970) quotes R(300)/R(0) for his In specimen(Sn33 quoted in the same way would give 45 000). The anisotropy of RR(26% greater for the tetrad direction) accounts for that of SnIII being much lower than that of Sn33, which was made from essentially the same material. These figures show just how anisotropic the normal state scattering processes actually are.

The anisotropy of resistance in a magnetic field is shown for Sn33 in Fig. 20. The magnetoresistance of all specimens was fortunately close to a maximum when the field lay parallel to the side-arms($\Theta = 0^{o}$); so that any small errors in the positioning of the field had a negligible effect on the results without having to stop the field in a direction where the pick-up area was larger. Figure 20 also shows the effect of temperature on the magnetoresistance: as the temperature is raised the zero field resistance increases directly because of phonon scattering, but at high enough fields it decreases because of the reduction of $\omega_c \tau$ by the phonons.

The effect of impurities on the magnetoresistance of the three purest symmetrical specimens(Sn33, Sn24 & Sn 7) is illustrated in Figure 21, which may be called a Kohler plot. Kohler's Rule is an approximation which states that $(\rho(H) - \rho(0))/\rho(0)$ is a function of $H/\rho(0)$ only, i.e. it is not dependent on the specimen purity. Any departures from this simple rule are evidence that the different

scattering mechanisms have different effects on different groups of carriers. For specimens of the same orientation there is little deviation shown in Fig. 21(although closer examination of the points near to the origin does reveal some significant differences), but changing the field orientation(Figs. 20 & 39) does reveal a large change in the amount of magnetoresistance. Furthermore it appears that the lower the magnetoresistance the less parabolic is its variation with magnetic field.

5.b Conditions employed in setting up the intermediate state

5.b.(i) A brief review of previous work

When the present investigation was commenced all published measurements had been confined to the regime below about 0.8 T_c and probably until the work of Walton(1965) nobody had succeeded in measuring the electrical resistance of a stacked structure of disc shaped domains. Since a narrow superconducting "bridge" can easily remove the effect of a thick normal region one would expect that it would be more difficult to obtain reproducible electrical results than to obtain similar thermal measurements(where the superconductor does not constitute a short circuit). Also we might expect that the resistance would lie below rather than above the linear variation.

These expectations are borne out by the lack of consistency between the results of early investigations(de Haas et al.,1934, Misener,1938, Andrew,1948, etc.) which shared the common feature that the resistance lay below linear and increased with measuring

current. These measurements had also revealed a phenomenon which came to be known as the "0.58 Effect"(see e.g. Shoenberg,1952) whereby resistance was first restored in a cylindrical wire at a field somewhat above $\frac{1}{2} H_c$(in fact at about 0.58 H_c for the particular diameter of wire used).

The more recent investigations of Walton(1964,1965), in which particular attention was paid to the setting up of a reproducible domain structure, have revealed that the use of a large current and field rotation between measuring points both increase the electrical resistance of the intermediate state region towards the expected linear variation at low tempertures. Because of the lack of sensitivity of conventional galvanometers(Walton used much thicker specimens than the earlier workers) a measuring current of at least 50 mA had to be used(this value is actually marked as $I_s = 0$ in both the paper and thesis) and this was rather close to the value of the electrical current needed to produce "saturation" of the thermal behaviour(between about 100 & 250 mA according to specimen). Furthermore in the case of the purest specimens readings could not be obtained with sufficient accuracy with a current less than the saturation value.

5.b.(ii) <u>The present work far below the transition temperature</u>

Since the ideal behaviour in this regime is well established(at least for symmetrical specimens) it was decided that it should provide a basis for the present investigations. Measurements on an early

non-electropolished specimen(Fig. 15) have already been briefly referred to in connection with the value of its threshold field(p. 41) but they are mentioned again because they show the first manifestation of a phenomenon which was to cause considerable trouble and is still not fully understood. This specimen had been measured using a static field when quite irreversible results were obtained but field rotation had caused the behaviour to become reversible and reproducible except just below H_c. In this regime the noise level was especially bad and it proved impossible to get reproducible results. Since Walton(1965 - figs. 13 & 14) had shown that there were "steps" in the thermal resistance just below H_c where it decreased rapidly, it was concluded that the different values taken by the electrical resistance perhaps corresponded to the thermal resistance levels. This will be discussed further in connection with the results on Sn 1, which shows quite definitely that the resistance in this region can take on a number of quite different values which depend on the particular conditions employed.

In Figure 22 we compare the resistance of Sn33(measured with a very small current) under two different conditions(hereafter the words "boost current" refer to the current of about 0.5 A passed through the specimen between measurement points to remove superconducting bridges across the normal domains):

26A : 6 rotations @ 8 sec/rev with no boost current

28 : 3 rotations @ 20 sec/rev with a 10 sec boost current.

According to Walton(1964) both rotation rates used here should have been slow enough to produce saturation. The 26A results show the characteristic droop below linear(although rather more than might have been expected from the behaviour of Walton's purest specimen) but in addition there is the marked tendency for the resistance to drop when approaching H_c and in fact the resistance in this region sometimes was only 75% of that shown in Figure 22. However both these effects are removed by the passage of the boost current and the 28 results show a linear variation in both increasing and decreasing field, except just above H_{th} where it appears that there are still a few superconducting bridges left.

It was shortly discovered that the rotation did not make a significant improvement in linearity; for example the 32C results (Fig. 25(f)) were obtained with a static magnetic field and boost current between points. Figure 23 shows the most impure specimen,Sn 1, under similar conditions and once again the variation is very close to linear in both increasing and decreasing field(it is to be noted that the difference in behaviour between them near H_{th} was in fact very reproducible although this is not understood).

The linearity of this curve(without field rotation) is really the only point of disagreement with Walton's results(1965 - fig. 9D) since his measuring current was probably always large enough to eliminate the behaviour found in the present experiments near to H_c and also above the saturation value for the purest specimen. Further

evidence supporting the conclusion that rotation is not strictly necessary, providing that a boost current or large measuring current is employed, is seen in Figure 30(a) for Sn 1. However as this is at elevated temperatures a full discussion of it is postponed until the next section.

In spite of the fact that the regime near H_c is inherently rather unstable(the thermal resistance results show that the number of boundaries is falling rapidly) it is difficult to see why the passage of the boost current should remove the tendency for the resistance to decrease, since this is the regime where the S domains have almost disappeared anyway. Perhaps if there are superconducting filaments left when the S domains become very thin a thread-like structure would have lower energy than an array of thin discs, because of the larger surface area of the discs. If, on the other hand, the superconducting bridges are removed by a boost current(or large measuring current) there could well be a large energy barrier to the re-arrangement of the structure from laminar(high resistance) to filamentary(low resistance). This is really only speculation but the free energies of quite different models differ very little(Andrew,1948). It is interesting also to note that in results discussed later it is shown that a boost current was certainly not required above 0.7 H_c in order to eliminate the irregularities just below H_c.

5.b.(iii) The present work in the vicinity of the transition point

As the transition temperature is approached from below the

requirement on the specimen current becomes progressively more stringent, if the structure is not to be modified by its magnetic field. In Figure 24 we show the effect of increasing the measuring current, when the specimen temperature was only 21 mK below T_c;* after increasing the field a boost current was passed before any readings were taken. The upper limit of the measuring current(100 mA) would give a field at the sample surface of 0.2 G - about 7% of the critical. Because of the sensitivity of the electrical resistance to changes in the structure this is reasonably consistent with the observation of Shalnikov(1957) that a current of about 15% I_c was necessary to produce visible changes in the powder patterns on the surface of a tin cylinder. However it does suggest that there could be some rather smaller superconducting regions deep in the material, which would have a higher field at their surface when carrying a current, similar to those observed by Meshkovsky(1949) and Meshkovsky et al. (1947) in tin spheres. These could shrink as the measuring current is increased and, because the I-V characteristic of the specimen was reversible, grow again when the current is reduced.

Although it is not well shown in Figure 24, because of the overlapping curves near the origin, the specimen resistance was

* Non-linearities like this can arise spuriously because heating of the Slug(e.g. by the large standard resistor current) causes its characteristic to alter. The linearity of the variation in the normal state however shows that this was not the case in this experiment.

constant up to about 15 mA throughout the whole of the intermediate state region - showing that the 10 mA measuring current usually employed had a negligible effect on the resistance of the structure.

At this temperature there is a considerable additional resistance (about 35% in Sn33) due to boundary scattering and so there are other possible explanations of the non-linearity. However the theory presented in Chapter 4 could not account for this as it is clearly linear in the current. It is also reasonably independent of the domain size(for a specimen of this purity) and so a change in the domain structure would not be expected to change the contribution made by the boundaries to the resistance of the whole.

As noted earlier it was found unnecessary to rotate the field at low temperatures in order to obtain linear behaviour, provided that a boost current was passed through the specimen between points. However, when very close to T_c and H_c, the passage of a large current can cause the material to become fully normal(both by the slight heating produced and also the magnetic field) and then to remain in the normal state(i.e. supercool) when the boost current is turned off. This can be seen in Figure 25(b)(although it would be more easily seen in an R v. h plot) where there is a rather sudden jump in the resistance up to its normal state value at $\eta = 0.85$. Because this also coincides with the theoretical variation it looks at first sight as though the specimen suddenly jumps to a new structure which is perhaps more nearly "ideal". However this should be regarded as a

coincidence due to the fact that at these temperatures the theoretical variation of R with h is very nearly flat itself. In order to prevent the occurence of this phenomenon it was decided to try only passing the boost current between points just above the threshold(up to about h = 0.7) since this should still adequately remove the superconducting threads. As already noted this was successful in removing the flatness at H_c as well as not allowing the reintroduction of the irregularities just below.

The plots in Figures 25, 26 & 29, showing the behaviour of the additional resistance as a function of temperature, will be more fully discussed in the next chapter. However we should observe at this stage that they were all set up with a static field(with the exception of Fig. 25(c) results 30B) with a current boost between points(a summary of the conditions used is to be found in Table 3).

Because of the length of time needed to take a set of measurements (see p. 34) no detailed investigation of the decreasing field variation was made. Figures 27 & 28 show that sometimes very odd things can happen: a boost current was only used in increasing field to about h = 0.7 and when H_c had been exceeded the field was reduced statically with no current boost(as it might have been expected that there would be no superconducting bridges to be eliminated - the behaviour is a little more evidence for a filamentary structure existing under certain circumstances). This behaviour however does bear out Walton's(1965 - fig. 9A) findings: if one superposes the

theoretical additional resistance variation(Fig. 27) on top of Walton's decreasing field plot the resulting curve looks very similar to the decreasing field plot of Figure 28. Also results 30B(Fig. 25(c)) show that when rotation and current boost are employed the variation is quite reversible.

We now come to deal with the results on the "awkward" specimen, Sn 1. Figure 31 summarises most of the measurements made on this sample - however we hasten to add that things are not quite so chaotic as they appear in that diagram as it was found possible to produce a particular resistance state by the appropriate choice of conditions. The behaviour of this specimen is not fully understood but it appears that it was produced by a variety of circumstances.

The range of variation may be divided into the following three regimes:

I : h=0.5 to h=0.62 where the behaviour is largely independent of the conditions. This will not be discussed at any length.

II : h=0.62 to h=0.8 where the variation follows one or the other of two paths(Fig. 32)

III : h=0.8 to h=0.95 where it appears that almost anything can happen.

Since the specimen resistance was high(about 3 $\mu\Omega$) compared with that of the standard resistor(about 0.3 $\mu\Omega$) the boost current went almost entirely through the Slugs and the standard resistor in preference to the specimen. This was particularly bad as it was later

found that Walton had needed as much as ¼ A to ensure saturation of his most impure specimen, Sn0.3. Since the superconducting current leads could not be made to carry much more current easily and as it was not convenient to change the standard resistor for a larger one, a resistance of about a microOhm was inserted into the specimen voltage leads(this also reduces the sensitivity of course - but with such a large specimen resistance the full sensitivity is not needed). The results 42(Fig. 31) show a marked improvement over 40B, 41A & 41C, but there is still much unreproducibility in regime III.

For measurements 43 the Slug circuit was disconnected and a Keithley model 148 millimicroVoltmeter was used to measure the p.d. across the specimen when an 80 mA current was passed. Even with an all copper circuit many readings had to be averaged at each field value(incidently the measurements above T_c gave a good check on the value of the standard resistor). A static field was employed with a boost current(which this time went only through the specimen) and the measurements showed no sign of any irregularity, even in region III. However Figure 24 shows that the measuring current was almost certainly enough to raise the specimen resistance significantly and this may explain why these results lie rather above the others(Fig. 31).

After this investigation the Slug circuit was reconnected with about 2 microOhm in the voltage leads to the specimen. The results 44B(Fig. 32) were obtained - again with static field and current

boost to h=0.7. This was repeated in 44C except that the field was rotated four times(@ 10 sec/rev) between points, with the boost current being turned off after the first two field rotations. It was very apparent that in region II there were two quite separate variations of resistance which one could select by the conditions: at a fixed field turning the boost current off after the second rotation always gave the same higher resistance, whilst four rotations with boost current invariably produced the lower curve. However at h=0.87 the resistance dropped once again and the four points were obtained in the order shown by the arrows with four field rotations(two with current boost) between each.

A further investigation(Fig. 33) revealed a number of interesting features. At fixed field value "A" the first point gradually drifted down to about 80% of the value shown. Accordingly four rotations were used to increase the resistance to point no. 2. When a current boost was then passed this was reduced to the same value as no. 1; two further sets of rotations increased this through 3 to 4. At the field marked "B" a similar effect of the boost current was found: point no. 3 followed a passage of the boost current and the later points(4,5 & 6) show the effect of subsequent sets of rotations.

At field value "C" the first three points were obtained with rotation alone and then a boost was passed which drastically reduced the resistance(to point no. 7). It had been noted before that the passage of the boost current caused the specimen temperature

boost to h=0.7. This was repeated in 44C except that the field was rotated four times(@ 10 sec/rev) between points, with the boost current being turned off after the first two field rotations. It was very apparent that in region II there were two quite separate variations of resistance which one could select by the conditions: at a fixed field turning the boost current off after the second rotation always gave the same higher resistance, whilst four rotations with boost current invariably produced the lower curve. However at h=0.87 the resistance dropped once again and the four points were obtained in the order shown by the arrows with four field rotations(two with current boost) between each.

A further investigation(Fig. 33) revealed a number of interesting features. At fixed field value "A" the first point gradually drifted down to about 80% of the value shown. Accordingly four rotations were used to increase the resistance to point no. 2. When a current boost was then passed this was reduced to the same value as no. 1; two further sets of rotations increased this through 3 to 4. At the field marked "B" a similar effect of the boost current was found: point no. 3 followed a passage of the boost current and the later points(4,5 & 6) show the effect of subsequent sets of rotations.

At field value "C" the first three points were obtained with rotation alone and then a boost was passed which drastically reduced the resistance(to point no. 7). It had been noted before that the passage of the boost current caused the specimen temperature

to rise by a few mK, but the temperature was always restored to its original value before making a measurement and it was not suspected that this small temperature rise could be a source of trouble. However the difference between points 8 and 9 is solely due to heating the specimen by a few mK and restoring it to its previous value before making the measurements. Points 10, 11 and 12 show the effect of reducing and restoring the temperature - again by less than 10 mK. Two final sets of rotation were used before each of points 13 and 14.

It appears that temperature control is an exceedingly important factor in the behaviour of the intermediate state under the conditions employed here - even more important than the simple calculation of section 2.c.(i) would suggest. It is comforting however to observe that there is little difference between results 43 and the highest obtained under other conditions at the same value of magnetic field. There seem to be two possible reasons for the differences in behaviour:

(a) The boost current was not large enough to achieve saturation in the Slug measurements(Walton's impure specimen needed 250 mA but even this might not be enough at our higher temperature).

(b) The measuring current used in results 43 was probably enough to affect the structure and keep it in only one of its possible states in regime III, where the free energy of

different structures in the absence of the magnetic field due to the measuring current is probably very small. At any rate it would appear from measurements on other specimens that a measuring current of 2 mA should give identical results to those obtained with 10 mA.

The strong dependence of the resistance on the temperature history of the specimen is puzzling, not particularly because of its existence, but because of its sign and magnitude: heating(and cooling to the measuring temperature) of the specimen reduces its resistance, often by almost a factor of three. This would tend to indicate that new superconducting bridges were forming - which seems highly unlikely. The interphase surface energy is a rapidly increasing function of temperature and this, together with the fact that this is likely to be the most inhomogeneous specimen(because of its In content), may account for the fact that the "ideal" behaviour appears to have been drastically upset. One thing is clear: the intermediate state resistance of Sn 1 is not as clearly a defined function of magnetic field just below H_c as is the behaviour of the purer specimens Sn 7, Sn24 and Sn33.

5.c The unsymmetrical specimen, SnIII

In this context we mean by "unsymmetrical" a specimen in which the axis is far from a principal crystallographic direction. Figure 35 shows a standard stereographic projection of the main features of SnIII. It is to be noted that, although the specimen axis was

determined to about 1°, the directions of the side-arms(i.e. the direction $\Theta = 0^{\circ}$ of the magnetic field) are subject to an error of about 10° because their short length made alignment about the specimen axis difficult. This is believed to be responsible for the minimum magnetoresistance direction($\Theta = 115^{\circ} \pm 5^{\circ}$) lying not quite at the closest point of the field trajectory to [001].

The behaviour of this specimen at high temperatures(Fig. 34 - static field at $\Theta = 0^{\circ}$, with current boost between points to about $h = 0.7$) appears to be about as expected: the calculated curves have not been changed in any way to allow for the different orientation of this specimen.

However the main interest focussed on the low temperature behaviour, especially as a function of field angle, Θ. Figures 36, 37(a) and 40 show the difference between measurements near to the maximum ($\Theta = 0^{\circ}$) and at the minimum($\Theta = 115^{\circ}$) of the magnetoresistance. The behaviour at $\Theta = 115^{\circ}$ attracts particular interest:

(a) No other results show a decrease in resistance actually at the critical field.

(b) No other low temperature variations show any marked rise above linear, especially in the region near H_c.

The results 51(Fig. 38) were intended to ascertain the behaviour of the specimen in the normal state in order to find the position of minimum magnetoresistance and consequently little care was taken with the intermediate state points which show a good deal of scatter

and little correlation with the normal state variation. Since the more careful investigations 50D and 52(Figs. 36 & 37(a)) of the two extreme magnetoresistance values reveal no difference until $\eta = 0.4$(the current boost was used until 0.7) it seems reasonable to conclude that this is true for all orientations of the field(but only in a scaled resistance plot - see also Fig. 40). Figure 40 shows that the variation at $\Theta = 115^{\circ}$ is quite linear above $h = 0.75$, but with a gradient about 15% larger than one would expect.

This type of additional linearity has not been reported before at all. This is almost certainly because the specimens used previously have all been oriented near to a principal axis - either deliberately as in Walton's case, or an unseeded crystal has grown near a $\langle 110 \rangle$ (seeding is virtually obligatory to obtain a "random" tin crystal as noted on p. 43 and for example Pippard,1955, reports results in which about two dozen unseeded tin crystals had an angle of 80° to 90° between [001] and the specimen axis). A further factor must surely be that the present measurements were made at a lower temperature(where H_c is larger) with quite a pure specimen, so that magnetoresistance and its anisotropy are near to the maximum possible in the intermediate state of tin.

It is possible that the effect could be due to the boundary condition imposed on the electromagnetic equations by the S-N interfaces. As a simple example consider a uniform stack of discs, alternately S and N, forming a cylinder analogous to the intermediate

state in a wire. The surface of the S regions is an equipotential and so the electric field, $\underline{E}$, lies parallel to the specimen axis, $\underline{s}$, in the N regions(the discs are considered to be so thin in relation to their diameter that edge effects are negligible). In an anisotropic medium the current, $\underline{J}$, need not lie parallel to $\underline{E}$ and so there is a difference between $(\text{conductance})^{-1}$ and resistance: In the stacked array one measures $R_E = (\text{conductance})^{-1}$ but above H_c, where the specimen is wholly normal, $\underline{J}$ is forced parallel to $\underline{s}$ and one measures R_J, the resistance. Clearly the presence of the magnetic field in the true intermediate state case further complicates the situation since $\underline{J}$ is not parallel to $\underline{E}$, even in an isotropic medium, if there is a magnetic field applied. A simple calculation based on the above model(Appendix C) shows that R_J always exceeds R_E in an anisotropic medium and this obviously does not explain the results shown in Figure 40.

This model is certainly too naïve but before investigating further we should consider another quite different explanation of the observations, which appears to be difficult to rule out by experiment. Figure 38 shows that near the minimum($\Theta = 115^\circ$) the magnetoresistance of the normal state of SnIII varies very rapidly with angle, whereas at $\Theta = 0^\circ$ it varies but slowly. Now if for some reason the magnetic field in the N domains were to deviate by about 20° around the vertical axis(or a comparable amount about a horizontal axis) from the applied field direction, the resistance would be

increased by about the right amount to account for the rise in the region between h = 0.75 and h = 1. This small deviation would undoubtedly raise the magnetic energy of the system, because it requires bending of the field lines near the ends of the N domains, but it is quite possible that for example anisotropy of the interphase surface energy would more than compensate for this increase. In any case it is well known(Shoenberg,1952) that many of the different models of the intermediate state have closely similar free energies.

We must therefore reluctantly conclude that until further experiments are made on this type of sample at low temperatures that this explanation cannot be ruled out.

Chapter 6

DISCUSSION OF THE EXPERIMENTAL RESULTS

6.a Introduction

The purpose of this chapter is to apply the theory developed in Chapter 4 to the experimental results obtained in the vicinity of the transition temperature on the additional resistance of the intermediate state due to boundary reflection of electronic excitations. Firstly estimates are made of the parameters required for the full theoretical fit(shown by the solid lines in the Figures). The dependence of the calculated additional resistance on the various parameters is then discussed with reference to the other theoretical variations shown in some of the Figures. Lastly the recent paper of Landau(1970) on the subject of resistance due to interface reflection is briefly discussed.

6.b The parameters used in the full theoretical fit

The analysis of the limiting cases given in section 4.f shows that the additional resistance given by our model is rather insensitive to many of the quantities in the full expression(Equn. 4.21), especially when the specimen is reasonably pure. However we have as yet not made a practical estimate of the position expected for the dividing line between the Clean and Dirty limits in tin. To do this we must first estimate domain sizes and diffusion lengths, as the division between the cases occurs at $\lambda \sim a$. Since there was

no provision made for measuring the domain size directly in the present experiments an estimate was made based on the results of Faber(1958) on the measurement of domain size in flat plates of tin.

The various theories of the variation of domain size, a, with the fraction of normal material, η, invariably minimise the free energy of a flat plate of thickness d with respect to a parameter related to the domain size; such as the ϕ of Lifshitz et al.(1951) - based on the model of Landau(1937). It is usually assumed that this is equally applicable to a cylinder of diameter of the order of d; it is here that our first approximation comes in, we shall investigate this further in due course. Lifshitz et al.(1951) obtained the following value for a(we use σ for the interphase surface energy parameter instead of the more usual Δ in order to avoid confusion):

$$a = \sqrt{\frac{\sigma d}{\phi}}$$

Figure 12 shows the variation of $\phi^{-\frac{1}{2}}$, together with the modification derived empirically by Pippard(1955), in which in both increasing and decreasing field when the domain period reaches its minimum value($\phi^{-\frac{1}{2}} = 6.6$) it remains there for the rest of the variation of η. This modified variation is compatible with the results of Walton (1965) as the constancy of the number of boundaries above $\eta = 0.4$ accounted for the rather flat top of the additional thermal resistance and the sudden decrease just below H_c. The measurements of

Faber(1958) show that the surface energy parameter in tin is:

$$\sigma = 2.3 \times 10^{-5} \left(1 - t^{\frac{3}{2}}\right)^{-\frac{1}{2}} \text{ cm}$$

We must now estimate the mean free paths; this was done principally by the use of the result of Chambers(1952) that $\rho_o \ell_1 = 10^{-11}$ $(\text{cm})^2$ where ρ_o is the residual resistivity. As remarked earlier Bardeen et al.(1959) show that ℓ_1^S is equal to ℓ_1^N but this gives us no information about the inelastic mean free path. Fortunately the theoretical variation is not sensitive to the values of ℓ_2^N and ℓ_2^S for pure specimens and varies only as $(\ell_2)^{\frac{1}{2}}$ in the dirty limit.

The interfaces forced us to introduce inelastic scattering in order to restore equilibrium(p. 54); this scattering has little effect on the electrical conductivity of normal metals but the present situation, with S-N boundaries, is more akin to the thermal conductivity problem in a normal metal where the small angle phonon scattering also restores equilibrium and the Wiedemann-Franz law breaks down. The results of Guenault(1960) on the thermal conductivity of tin enable an estimate of the mean free path required for the interface problem to be made, but only rather approximately. It was decided to use the ideal resistance ratio(2×10^5 at T_c), substituted into the formula of Chambers(1952), to estimate the inelastic mean free path: this will be an over-estimate for the reasons outlined above but because in the dirty limit the domain size always occurs with λ in the denominator(see Equn. 4.26), and in the

clean limit the additional resistance is independent of λ and very weakly dependent on a(Equn. 4.23), we shall allow for this error by varying the value of a used in the full theoretical fit(especially since there are doubts about the domain size anyway). Quite arbitrarily we take the inelastic mean free paths to be the same in both N and S.

We are now in a position to estimate the position of the division between clean and dirty in tin, where $\lambda \sim a$:

$$\sqrt{\frac{l_o l_2}{3}} \sim 6.6\sqrt{\sigma d}$$

(The factor of 3 arises from diffusion in three dimensions). The use of the various estimates derived above gives RR $\lesssim 2 \times 10^4$ at the changeover point; we shall see that this is borne out by the experimental results.

The variation of the energy gap parameter, Δ, with temperature was taken to be BCS-like(Muhlschlegel,1959 - fitted by Equn. B.6) which is known to be well obeyed in tin. The energy gap is however known to be anisotropic(e.g. ultrasonic attenuation measurements of Morse et al.,1959 and Bezugli et al.,1959) and we make some estimate of the effect of this later.

In the absence of any more realistic calculations of the interface reflection coefficient the variation due to Andreev(1964) for a sharp step(which gives the maximum value of R and α) was used.

6.c The theoretical variations shown in the Figures

Figures 25, 26, 29, 30 and 34 show the theoretical curves and experimental points for the variation of high temperature scaled additional intermediate state resistance for each of the five specimens. The axes are only labelled in Figures 25(a) & (b) in order to save unnecessary repetition. In some of the Figures the full theoretical fit is accompanied by modified variations which are coded as below:

(a) ———— Full theoretical fit(section 6.d)

(b) ····· Square model - clean limit(Equn. 4.24)

(c) -·-·-·- As (a) but Δ_o/kT_c increased to 2.15 from 1.76, preserving the BCS temperature variation(section 6.e.(i)).

(d) – – – – – As (a) but with double domain thickness(section 6.e.(ii)).

6.d Discussion of the full theoretical fit

In view of the sweeping approximations made in the development of the theory and in the estimation of the parameters involved the fit to the experimental results is surprisingly good, especially for the purest specimens Sn33 and Sn24. Since the clean limit Square model(Equn. 4.24) for these specimens is not altered drastically by the effects of a finite diffusion length this good agreement is to some extent expected. On the other hand the clean limit Square model contains no adjustable parameters and so this gives confidence that the physical basis of the theory is sound.

Because of the difficulties encountered with the most impure specimen Sn 1 recounted in the last chapter we hesitate to attach much importance to the results shown in Figure 30(especially above $h = 0.75$); however it is interesting to note that the behaviour is qualitatively correct: the scaled additional resistance is lower than that of the purer specimens and the behaviour is different in increasing and decreasing fields in the correct way.

The behaviour of SnIII(the curves have not been corrected for the different orientation) also goes according to plan, except for Figure 34(a). The discrepancy here is almost certainly due to lack of care with the temperature control as the main purpose of this specimen was to give information at low temperatures.

It is apparent that virtually all the theoretical curves are over-estimates and so we go on in the next section to examine the effect of varying some of the parameters.

6.e Discussion of the modified variations

Extensive calculations were carried out on two modified models in order to ascertain separately the effects of the energy gap and domain size/diffusion length.

6.e.(i) Effect of a larger energy gap

Since the energy gap is known to be anisotropic we should consider what effect a change in Δ has on the additional resistance. If the energy gap is widened fewer excitations will be able to penetrate into S and be scattered there, so that the size of the

additional resistance will be reduced.

This was investigated by preserving the BCS temperature variation but raising the absolute zero value, Δ_o, to the highest value(2.15 kT_c) measured in ultrasonic attenuation work on tin. This is not intended to be the "correct" value, but it does serve to show that the theoretical dependence on Δ is quite small in spite of the fact that δ appears in the argument of an exponential in the integrand(Equn. 4.24 etc.). The curves show that even this large change in Δ is unable to account for the results, especially those on Sn 7, and so we conclude that we must look elsewhere for the explanation.

6.e.(ii) Effect of changing the domain size

As we saw before(p. 90) changing the domain size is almost equivalent to correcting our estimate for the diffusion length because of the way in which the equations depend on a/λ. The curves (------) show the additional resistance to be expected when σ is quadrupled(i.e. a doubled or λ halved). A comparison of Figures 25(a) and 29(b) shows that the effect of changing Δ is purity independent, whereas changing the domain size gives a much larger reduction for Sn 7 than for Sn33. This is because in Sn 7 the variation is more nearly proportional to the number of boundaries present, i.e. it is closer to the dirty limit with decoupled boundaries.

Although the domain size is uncertain because it was not measured in the present experiments(and because the theory of domain size really applies to flat plates) we do know that λ is

over-estimated. Hence the most reasonable single explanation of the differences between experiment and the full theoretical fit is that ℓ_2 has been over-estimated by a factor of about five.

6.e.(iii) Discussion of the reflection coefficient

Deviations from the full theoretical variation could also be regarded(especially for the purer specimens Sn33 and Sn24) as evidence that the Andreev reflection coefficient is in error. However(as shown by Equn. 4.23) this is so inextricably bound up with the values of domain period and mean free path that we cannot really comment on the validity of the Andreev expression.

6.f Comparison with the results of Landau(1970)

Very recently Landau(1970) has reported preliminary measurements of the additional resistance in the intermediate state of Indium. Although he used a superconducting chopper amplifier he used such a large measuring current($0.1\ I_c$) that the structure was strongly modified by its passage(e.g. strong hysteresis at the threshold field). However the results are at least qualitatively similar to ours.

He fits his results to a formula obtained by Nozieres(cited as a private communication which makes a full discussion rather difficult) by using the reflection coefficient, R, as a variable parameter. This gives a variation of R with temperature which has a distinct similarity to the variation of the fraction of excitations in N with $\varepsilon < \Delta$ shown in fig. 2 of the paper. As far as can be gathered from

the text the difference is accounted for satisfactorily by partial Andreev reflection, although no evidence for this is shown.

Landau's specimen corresponds rather closely to Sn33 in its physical properties, except that it was made of Indium. This might be expected to have detailed differences with tin because of the different electronic structures of the two elements. However the Nozieres expression reduces to ours in the clean limit(which would apply to Landau's specimen of course) and so the agreement found by Landau points to the different metals behaving quite similarly in respect of the additional resistance in the vicinity of the transition.

Chapter 7

CONCLUDING REMARKS

Since the measurements of de Haas et al.(1934) almost forty years ago the electrical resistance of the intermediate state of superconductors has been investigated many times and it is interesting to ponder why the additional resistance due to the S-N interfaces has been discovered only recently. There are a number of factors which spring to mind: lack of sensitivity, problems of accurate temperature control and the reluctance of the intermediate state resistance to follow the linear variation at low temperatures. Really the first of these can be ruled out since it is possible to observe the additional resistance with only nanoVolt sensitivity, if one is prepared to tolerate large measuring current densities. The most likely explanation is that no additional resistance was ever found up to the largest temperatures examined, where temperature control becomes progressively more troublesome; in addition there seemed little reason to expect that the behaviour closer to the transition would be much different.

The work of Andreev(1964) undoubtedly stimulated interest in the S-N boundary problem but a later paper(Andreev,1966) did little more than put onto a more mathematical basis what had been generally accepted for many years: that far from the transition the resistance was a linear function of the applied field. On the experimental side

the arrival of superconducting quantum interference galvanometers, which were very sensitive and yet easy to use(one can say this in retrospect even though a Slug at times receives rather more uncomplimentary names!), renewed interest in the accurate measurement of very small resistances.

The work near the transition point, which forms the backbone of this thesis, was made much more coherent by the theory of boundary resistance set out in Chapter 4. This had its origins in a parallel study of SNS sandwiches(Shepherd,1971) and it is particularly satisfying that the results on the two closely related systems, which however differed considerably in technical matters, could be united with a common theory(Pippard et al.,1971). This gives added confidence to the belief that the basis of the theory is sound: that the additional resistance arises from the scattering of supergap excitations in the superconducting regions.

There are many points in the theory where it was necessary to make rather drastic assumptions in order to simplify the analysis. However the results presented here show that the theory is surprisingly accurate in predicting the behaviour of the intermediate state resistance. It would appear in particular that the assumption of an exactly periodic stacked array of domains is not so restrictive as one might have inferred from the small difference in free energy between the various possible intermediate state structures. In addition one might have expected that anisotropy of the energy gap

would invalidate the results of any one dimensional model, but as we have shown its good agreement with experiment is consistent with its rather unexpectedly small dependence on the value of Δ.

The specimens spanned a good range of purity enabling the effect of diffusion length to be investigated. It is rather unfortunate however that the RR of Sn24 turned out larger than expected because the results show(and rough calculations indicate) that the borderline between Clean and Dirty limits occurs somewhere between this specimen and Sn7. A closer investigation of this intervening region would probably provide a further check on the details of the theory, although the results might be difficult to interpret because of the many contributing factors.

In addition a further investigation of specimens similar to Sn 1 might have revealed whether for instance inhomogeneities in the crystal were responsible for its tendency toward different resistance states at the same value of field. However it is not possible to interpret electrical resistance results on an unknown structure uniquely because of the zero resistance of the S regions and an investigation of the structure is better carried out by other means. The best of these methods is probably thermal conductivity, since direct observation of the structure with magnetoresistive probes, powder patterns or magneto-optic glasses give only information about the structure at the surface. Because the additional thermal resistance is small near T_c where the electrical resistance is large, parallel

studies could give little information particularly as we have shown that the structure can be very sensitive to its temperature history: the temperature difference needed for accurate thermal measurements could disturb the structure enough to affect the electrical resistance drastically. In any case for such an impure specimen the boundaries only contribute a small amount to the relatively large thermal resistance: unlike the electrical case the additional thermal resistance is directly dependent on the number of boundaries and is consequently independent of purity.

We now turn to the subsidiary study made of the unsymmetrical specimen SnIII at low temperatures where the use of direct domain observation could have verified the hypothesis of field tilting made to explain the large excess resistance observed at the angle of minimum magnetoresistance. It could however not fully disprove the hypothesis because internal changes in the structure need not be manifested on the surface. The thermal boundary resistance at this temperature is very large and there should be little problem with the heat current disturbing the structure so that thermal measurements could provide sensitive information about any internal domain rearrangement. However one would have to choose a temperature at which the magnetothermal effects(which would give information about the field directions in the N domains in the same way as the magnetoresistance),which increase relatively slowly with decreasing temperature(as the H_c v. T curve is almost flat in this region), were

not completely overcome by the thermal boundary resistance(which rises exponentially with decreasing temperature).

An attempt was made to measure the thermopower of the intermediate state in the present investigations but without adequate automatic temperature stabilisation the rise in mean temperature of the specimen as the thermal current was increased(this had to be done slowly since feedback could not be used in the Slug circuit) meant that the critical field of the specimen changed, and there was a consequent effect on the structure. This disadvantage would not have attended the measurement of thermal conductivity as the heat could then be switched quickly between two matched heaters at each end of the specimen, preserving the mean temperature. The thermopower is undoubtedly one stage more difficult to measure than resistance and the results would also probably be difficult to interpret. Nevertheless there is a complete lack of experimental work on this aspect of the intermediate state and this in itself makes it of great interest.

APPENDIX A

ANALYSIS OF SLUG CIRCUITRY

The behaviour of the Slug system is analysed in terms of a simple model in which the Slug has a sinusoidal variation of I_c with I_H and its V-I characteristic consists simply of two linear sections:

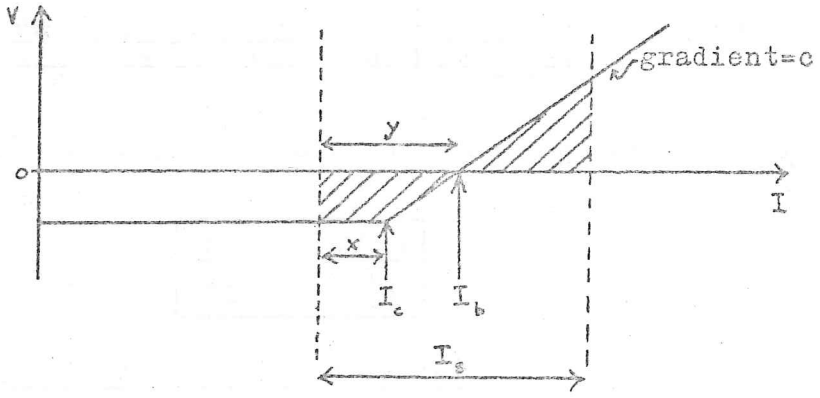

The Slug junction current is swept $I_s/2$ either side of I_b; I_b is the point at which the saturating amplifier switches from -ve to +ve. Because the pre-amplifier is a.c. coupled to the saturating amplifier the two shaded areas must be equal(no d.c. can flow) and this gives a condition from which the mark-space ratio,M, can be determined:

$$x(y - x)c + \tfrac{1}{2}(y - x)^2 c = \tfrac{1}{2}(I_s - y)^2 c$$

$$\therefore \quad y = \frac{I_s^2 + x^2}{2I_s}$$

but M is defined as $\left\{\dfrac{I_s - y}{y}\right\}$ $\quad \therefore \quad \boxed{M = \dfrac{I_s^2 - x^2}{I_s^2 + x^2}}$ A.1

We assume that the critical current of the Slug is given by:

$$I_c = I_{co} + I'_{co} \cos\left(\frac{2\pi I_H}{I_p}\right)$$

where I_p is the period of the Slug. We can now define a "goodness factor" of the Slug as $a = I'_{co} / I_p$, and so $\left(\frac{dI_c}{dI_H}\right)_{max} = 2\pi a$

$$\therefore \frac{dM}{dI_H} = \frac{dM}{dx}\cdot\frac{dx}{dI_c}\cdot\frac{dI_c}{dI_H} = \frac{d}{dx}\left[\frac{I_s^2 - x^2}{I_s^2 + x^2}\right] \cdot 1 \cdot 2\pi a$$

It is easy to show that this has a maximum at $x = I_s/\sqrt{3}$, where

$$\boxed{\frac{dM}{dI_H} = \frac{3\sqrt{3}\pi a}{2I_s}} \qquad A.2$$

The saturating amplifier and filter

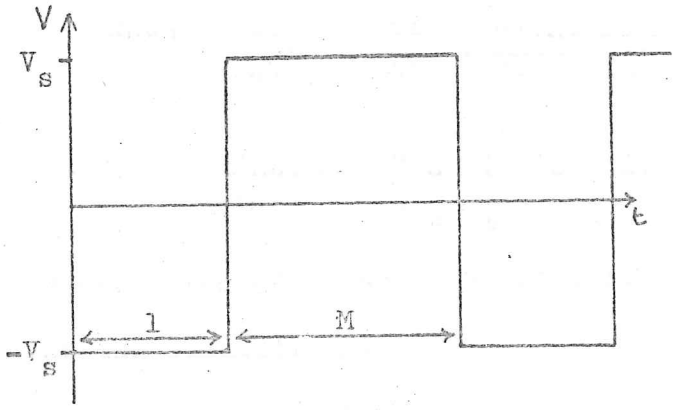

The output from the saturating amplifier is a square wave of amplitude $2V_s$ and mark-space ratio M. The low-pass filter removes the sweep frequency and leaves a d.c. level, V, determined by M and V_s:

$$V = \frac{V_s M - V_s}{M + 1} = V_s\left(\frac{M - 1}{M + 1}\right)$$

The signal is thus contained in this variation of V with M:

$$\frac{dV}{dM} = \frac{V_s(I_s^2 + x^2)^2}{2\, I_s^4} \qquad A.3$$

where equn. A.1 has been used to eliminate M.

The d.c. amplifier

The quantity which is most important in the design of a d.c. amplifier for the feedback system is the loop current gain dI_o/dI_H, where $I_o = \frac{I_{out}S}{R+S}$ is the current flowing along the Slug wire due to a current I_{out} being fedback to the standard resistor,S, by the(high output impedance) d.c. amplifier. The loop current gain must exceed 100 if the measurement of the specimen resistance,R, is not to be in error by more than 1%.

Now: $$\frac{dI_o}{dI_H} = \frac{dI_o}{dI_{out}} \cdot \frac{dI_{out}}{dV} \cdot \frac{dV}{dM} \cdot \frac{dM}{dI_H}$$

$$\therefore \quad \frac{dI_{out}}{dV} = \frac{dI_o}{dI_H} \cdot \left[\frac{dI_o}{dI_{out}} \cdot \frac{dV}{dM} \cdot \frac{dM}{dI_H} \right]^{-1} \qquad A.4$$

Combination of equns. A.2 A.3 & A.4,with the following estimates of the quantities involved, shows that the transconductance of the d.c. amplifier should be of the order of at least 0.1 A/V.

($a = 0.1$, $I_s = 10^{-4}$ A, $x = I_s/\sqrt{3}$, $V_s = 10$ V, S = R & loop gain = 100.)

It is interesting to note that equn. A.2 shows that best sensitivity is obtained with a small value of current sweep,I_s.

The integral in Equn. (4.21b) is over excitation energies in the normal state. In this appendix ε and E are synonymous and mean the excitation energy.

Appendix B

EVALUATION of I for ANDREEV REFLECTION

Equn.(4.21b) defines $$I = -\int \frac{f_o' \, \mathrm{Tanh}(a^S/2\lambda)\, d\varepsilon}{\left(\mathrm{Tanh}\left\{\frac{a^N}{2\lambda}\right\} + \mathrm{Tanh}\left\{\frac{a^S}{2\lambda}\right\} + \frac{a\lambda}{\ell_o}\mathrm{Tanh}\left\{\frac{a^N}{2\lambda}\right\}\mathrm{Tanh}\left\{\frac{a^S}{2\lambda}\right\}\right)}$$

Andreev(1964) gives the value of the reflection coefficient as:

$$R = \begin{cases} \dfrac{2\sqrt{E^2 - \Delta_\infty^2}}{E + \sqrt{E^2 - \Delta_\infty^2}} & E > \Delta_\infty \\ 0 & E < \Delta_\infty \end{cases}$$

$$\therefore \; a = \frac{2R}{1-R} = \begin{cases} \dfrac{x - \sqrt{x^2 - 1}}{\sqrt{x^2 - 1}} & x > 1 \quad \text{where } x = E/\Delta \\ \infty & x < 1 \end{cases} \qquad (B.1)$$

Also the derivative of the fermi function with respect to energy is:

$$\frac{\partial f_o}{\partial \varepsilon} = -\frac{\exp(E/kT)}{kT\left[\exp(E/kT)+1\right]^2} \qquad (B.2)$$

$$\therefore \; I = \int \frac{\exp(E/kT)\, d\varepsilon}{kT\left[\exp(E/kT)+1\right]^2 \left[\beta + \frac{a\lambda}{\ell_o}\mathrm{Tanh}\left\{\frac{a^N}{2\lambda}\right\}\right]} \qquad (B.3)$$

where $\beta = 1 + \dfrac{\mathrm{Tanh}(\eta a/2\lambda)}{\mathrm{Tanh}\left\{\frac{(1-\eta)a}{2\lambda}\right\}}$

Let Δ_o be the value of the energy gap of the superconductor(now denoted by Δ with no subscript) at absolute zero:

$$I = \frac{1}{kT_c}\int_{-\infty}^{\infty} \left(\frac{T_c}{T}\right) \frac{\exp(\Xi)\;\; d(x\Delta)}{\left[\exp(\Xi)+1\right]^2 \left[\beta + \frac{a\lambda}{\ell_o}\mathrm{Tanh}\left\{\frac{\eta a}{2\lambda}\right\}\right]} \qquad (B.4)$$

where $\Xi = \left\{\frac{E}{\Delta}\right\}\left\{\frac{\Delta}{\Delta_o}\right\}\left\{\frac{\Delta_o}{kT_c}\right\}\left\{\frac{T_c}{T}\right\} = 1.76\,\frac{\delta}{t}\,x$ (1.76 being the BCS value)

The limits of integration in (B.4) are intended to remind one that both excitation branches(electrons and holes) must be integrated over.

Now: $$\int_{-\infty}^{\infty} = \int_{-\infty}^{-1} + \int_{-1}^{0} + \int_{0}^{1} + \int_{1}^{\infty}$$

$$= 2\int_{1}^{\infty}$$

This simplification occurs because of the properties of a(symmetry with respect to +ve and -ve energies;and equation (B.1)).

$$\therefore \quad I = 3.52\,\frac{\delta}{t}\int_{1}^{\infty}\frac{\exp(1.76\,x\delta/t)\,dx}{\left[\exp(1.76\frac{\delta}{t}x)+1\right]^2\left(1+\left[\frac{\mathrm{Tanh}\left\{\frac{\eta a}{2\lambda}\right\}}{\mathrm{Tanh}\left\{\frac{(1-\eta)a}{2\lambda}\right\}}\right]+\frac{\lambda}{\ell_o}\mathrm{Tanh}\left\{\frac{\eta a}{2\lambda}\right\}\left[\frac{x-\sqrt{x^2-1}}{\sqrt{x^2-1}}\right]\right)} \qquad (B.5)$$

In order to evaluate this integral at any temperature it is necessary to interpolate in the table(Muhlschlegel,1959) of reduced BCS energy gap, $\delta(=\Delta/\Delta_o)$ versus reduced temperature, $t(=T/T_c)$. In order to make use of the known asymptotic form of δ near T_c the following expression was fitted to the tabulated points(to a precision of four decimal places from t=0.5 to t=1.0):

$$\delta = S(1.7385 - S(0.0246 + S(0.6053 + 0.1846\ S)))$$

where $$S = (1 - t)^{\frac{1}{2}} \qquad \text{(B.6)}$$

The integration was performed numerically by Weddle's Rule(similar to Simpson's Rule, but more accurate) with variable step length. This was checked in two ways:

a) against the analytic integration which can be performed in the clean limit($\ell_o \gg a$).

b) graphically(i.e. counting squares) for one general case.

APPENDIX C

THE EFFECT OF ANISOTROPY ON RESISTANCE

The difference between $(\text{conductance})^{-1}$ and resistance in an anisotropic crystal is investigated in the following two dimensional model:

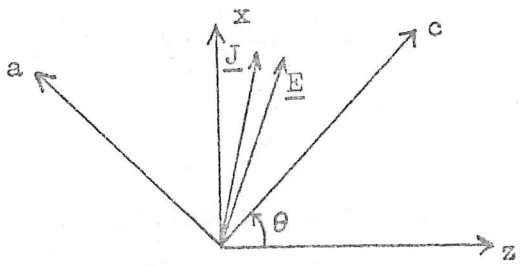

a & c : crystalline axes

z : specimen axis

Resolving along the specimen axes:

$$\left.\begin{aligned} E_x &= E_c \,\mathrm{Sin}(\theta) + E_a \,\mathrm{Cos}(\theta) \\ E_z &= E_c \,\mathrm{Cos}(\theta) - E_a \,\mathrm{Sin}(\theta) \end{aligned}\right\} \qquad (C.1)$$

and similarly for J. The measured resistance along z is thus:

$$R = \frac{E_z}{J_z} = \frac{-E_a \,\mathrm{Sin}(\theta) + E_c \,\mathrm{Cos}(\theta)}{-J_a \,\mathrm{Sin}(\theta) + J_c \,\mathrm{Cos}(\theta)} \qquad (C.2)$$

Case 1: J forced parallel to z

Equation (C.2) becomes:

$$R_J = \frac{-\rho_a J_a \,\mathrm{Sin}(\theta) + \rho_c J_c \,\mathrm{Cos}(\theta)}{-J_a \,\mathrm{Sin}(\theta) + J_c \,\mathrm{Cos}(\theta)} \qquad (C.3)$$

Since $J_x = 0$ we have (from the analogue of (C.1) for J):

$$J_c = -J_a \frac{\mathrm{Cos}(\theta)}{\mathrm{Sin}(\theta)} \qquad (C.4)$$

$$\therefore \qquad \underline{R_J = (\rho_c - \rho_a)\,\mathrm{Cos}^2(\theta) + \rho_a} \qquad (C.5)$$

Case 2:E forced parallel to z

In this case $E_x = 0$ and Equn.(C.1) gives:

$$E_c = -E_a \frac{\mathrm{Cos}(\theta)}{\mathrm{Sin}(\theta)} \qquad (C.6)$$

$$\therefore \qquad \underline{R_E = \left((1/\rho_c - 1/\rho_a)\,\mathrm{Cos}^2(\theta) + 1/\rho_a\right)^{-1}} \qquad (C.7)$$

Summary

The ratio of the two resistances is:

$$\boxed{\frac{R_J}{R_E} = \frac{(\rho_c - \rho_a)^2}{\rho_a \rho_c}\,\mathrm{Cos}^2(\theta)\mathrm{Sin}^2(\theta) + 1} \qquad (C.8)$$

It will be noted that this expression is at least unity for all values of resistivity.

REFERENCES

Aleksandrov,B.N. & D'Yakov,I.G. 1962 Zh.Eksp.Teor.Fiz. 43, 852; Soviet Phys.-JETP 16, 603

Alekseevskii,N.E., Gaidukov,Yu.P., Lifshitz,I.M. & Peschanskii,V.G. 1960 Zh.Eksp.Teor.Fiz. 39, 1201; Soviet Phys.-JETP 12, 837

Andreev,A.F. 1964 Zh.Eksp.Teor.Fiz. 46, 1823; Sov. Phys.-JETP 19, 1228

Andreev,A.F. 1966 Zh.Eksp.Teor.Fiz. 51, 1510; Sov. Phys.-JETP 24, 1019

Andrew,E.R. 1948 Proc. Roy. Soc. A, 194, 80 & 98

Bardeen,J., Rickayzen,G. & Tewordt,L. 1959 Phys. Rev. 113, 982

Bezugli,P.O., Galkin,A.A. & Karolyuk,A.P. 1959 Zh.Eksp.Teor.Fiz. 36, 1951; Soviet Phys.-JETP 9, 1388

Chambers,R.G. 1952 Proc. Roy. Soc. A, 215, 481

Clarke,J. 1966 Phil. Mag. 13, 115

Clement,J.R. & Quinnell,E.H. 1952 Rev. Sci. Instrum. 23, 213

Dauphinee,T.M. & Preston-Thomas,H. 1954 Rev. Sci. Instrum. 25, 884

de Haas,W.J., Voogd,J. & Jonker,J.M. 1934 Physica 1, 281

Faber,T.E. 1958 Proc. Roy. Soc. A, 248, 460

Fourie,J.T., Weinberg,F. & Boswell,F.W.C. 1960 J. Appl. Phys. 31, 1136

Guenault,A.M. 1960 Thesis, University of Cambridge

Landau,I.L. 1970 JETP Letters 11, 437

Landau,L.D. 1937 Zh.Eksp.Teor.Fiz. 7, 371

Lifshitz,E.M. & Sharvin,Yu,V. 1951 Dokl.Akad.Nauk. S.S.S.R. 79, 783

Lock,J.M., Pippard,A.B. & Shoenberg,D. 1951 Proc.Camb.Phil.Soc. 47, 81

Mendelssohn,K. & Olsen,J.L. 1950 Phys. Rev. 80, 859

Meshkovsky,A.G. 1949 Zh.Eksp.Teor.Fiz. 19, 1

Meshkovsky,A.G. & Shalnikov,A.I. 1947 J. Phys. USSR 11, 1

Misener,A.D. 1938 Proc. Roy. Soc. A, 166, 43

Morse,R.W., Olsen,T. & Gavenda,J.P. 1959 Phys. Rev. Lett. 3, 15 & 4, 193

Muhlschlegel,B. 1959 Z. Phys. 155, 313

Phillips,W.A. 1969 Proc. Roy. Soc. A, 309, 259

Pippard,A.B. 1955 Phil. Trans. Roy. Soc. A, 248, 97

Pippard,A.B., Shepherd,J.G. & Tindall,D.A. 1971 Proc. Roy. Soc. (To be published)

Rumbo,E.R. 1969 Thesis, University of Cambridge

Shalnikov,A.J. 1957 Zh.Eksp.Teor.Fiz. 33, 1071; Soviet Phys.-JETP 6, 827

Sharvin,Yu.V. 1965 JETP Letters 2, 183

Shepherd,J.G. 1971 Thesis, University of Cambridge

Shikina,N.I. & Shikin,V.B. 1968 Zh.Eksp.Teor.Fiz. 54, 1114; Soviet Phys.-JETP 27, 597

Shoenberg,D. 1952 "Superconductivity" 2 nd Ed. Cambridge Univ. Press

Tegart,W.J.McG. 1956 "The Electrolytic and Chemical Polishing of Metals in Research and Industry" 1 st Ed. Pergamon Press

Tsivinskii,S.V. & Stepanov,A.V. 1964 Fiz.Tverdogo Tela 7, 194; Soviet Phys. Solid State 7, 148

Wade,J.M.A. 1969 Thesis, University of Cambridge

Walton,A.J. 1964 Thesis, University of Cambridge

Walton,A.J. 1965 Proc. Roy. Soc. A, 289, 377

White,G.K. 1968 "Experimental Techniques in Low Temperature Physics" 2 nd Ed. Oxford University Press

FIGURES

Notes on the Figures

a) Most of the additional resistance($\delta R/R_o$ v. η) plots have unlabelled axes to avoid unnecessary repetition. Figures 25(a) & (b) show clearly the labelling of the axes: the vertical($\delta R/R_o$) axis is divided into units of 0.1 with the origin at the intersection with the horizontal(η) axis, which is also divided into tenths.

b) Unless otherwise stated:

i) Specimen current, I_s = 10 mA.

ii) Field angle(measured from the side-arm direction), $\Theta = 0^o$

c) In the additional resistance plots(with the exception of Fig. 37) the key for the theoretical variations shown is as follows:

i) ····· Square model

ii) ——— Full theoretical fit

iii) -·-·-·- As (ii) but with an increased value(2.15) for Δ_o.

iv) – – – – – As (ii) but with doubled domain thicknesses.

d) All points were taken in increasing field except where marked by ↓. (↑ is used for increasing field points in these circumstances).

e) Table 3(overleaf) gives a very brief summary of the conditions employed in setting up the intermediate state structure. A fuller description is given in Chapter 5.

TABLE 3

Summary of Conditions Used in Making the Measurements

Fig.	Ref. no.	No. of Rotns. between pts.	Rotn. vel. Sec/rev	Length of "boost" current(secs.)		Specimen
				h = 0.5 to 0.7	h = 0.7 to 1.0	
15	17	6	8	0	0	(2)
22	26A	6	8	0	10	Sn33
	28	3	20	10	10	
23	41D	0	-	5	5	Sn 1
25(a)	32B	0	-	30	30	Sn33
	33	0	-	30	0	
(b)	31B	0	-	30	30	
	32A	0	-	30	30	
(c)	30B	3	20	30	30	
	32D	0	-	30	30	
(d)	39A	0	-	30	0	
(e)	32E	0	-	30	30	
(f)	32C	0	-	30	30	
	39B	0	-	30	0	
26(a)	46C	0	-	30	0	Sn24
(b)	46A					
(c)	46B					
27 & 28	46D	0	-	30	0	Sn24
29(a)	47B	0	-	15	0	Sn 7
(b)	47A					
(c)	47C					
(d)	47D					
30(a)	43	0	-	15	15	Sn 1
(b)	40A	0	-			
34(a)	49B	0	-	15	0	SnIII
(b)	50A					
(c)	50B					
(d)	50C					

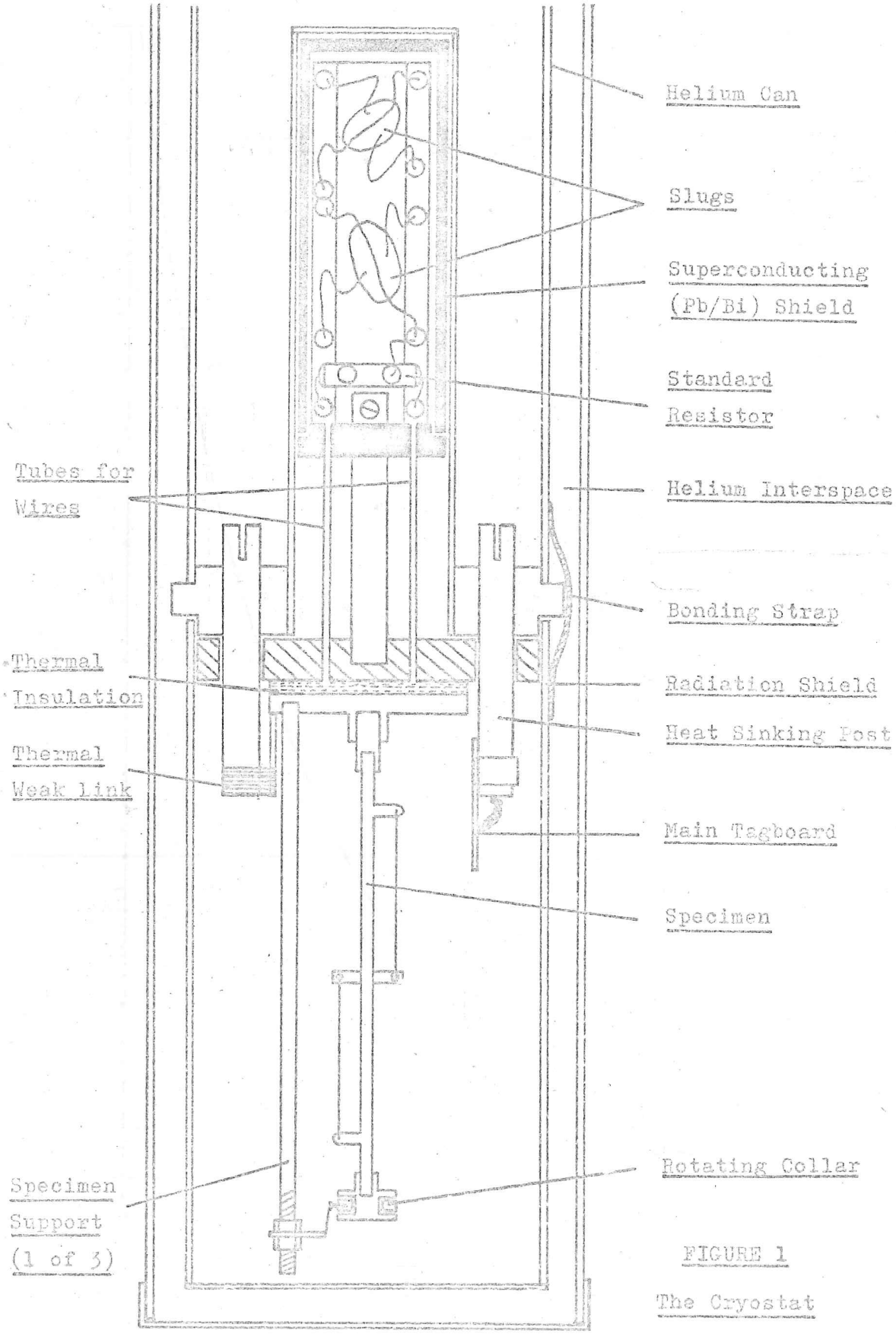

FIGURE 1

The Cryostat

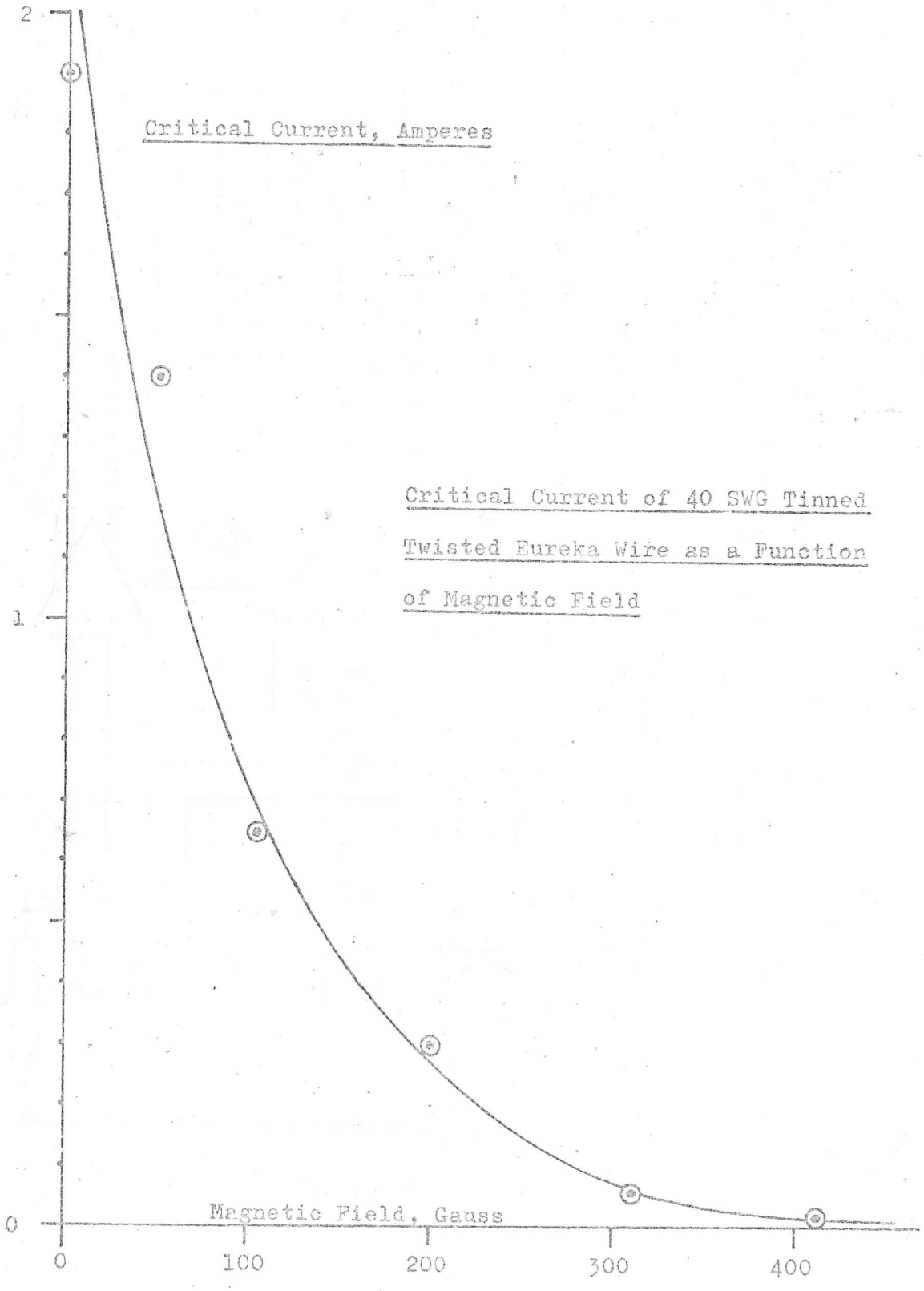

Critical Current of 40 SWG Tinned Twisted Eureka Wire as a Function of Magnetic Field

FIGURE 2

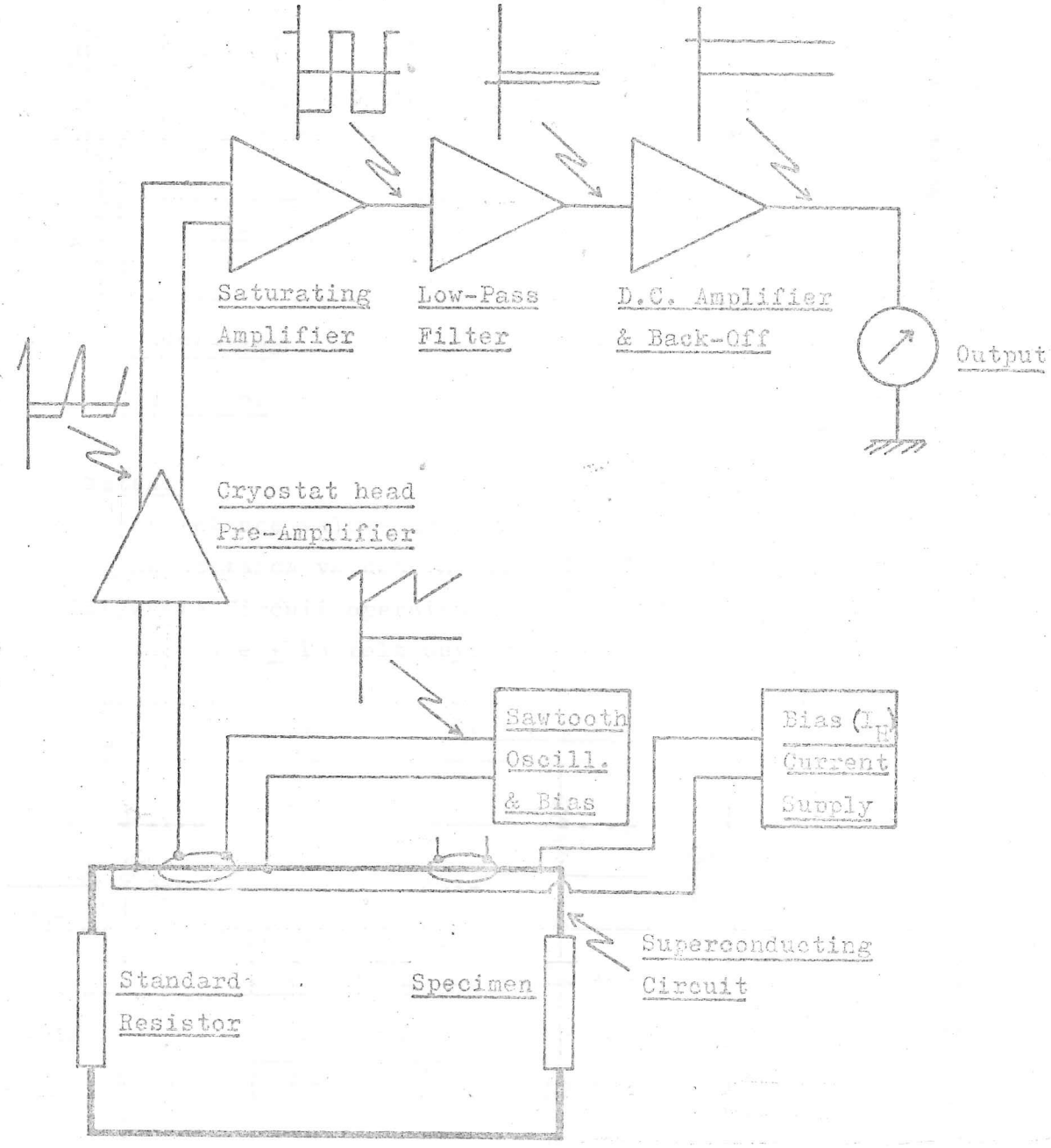

FIGURE 3

Block Diagram of the Slug Circuit

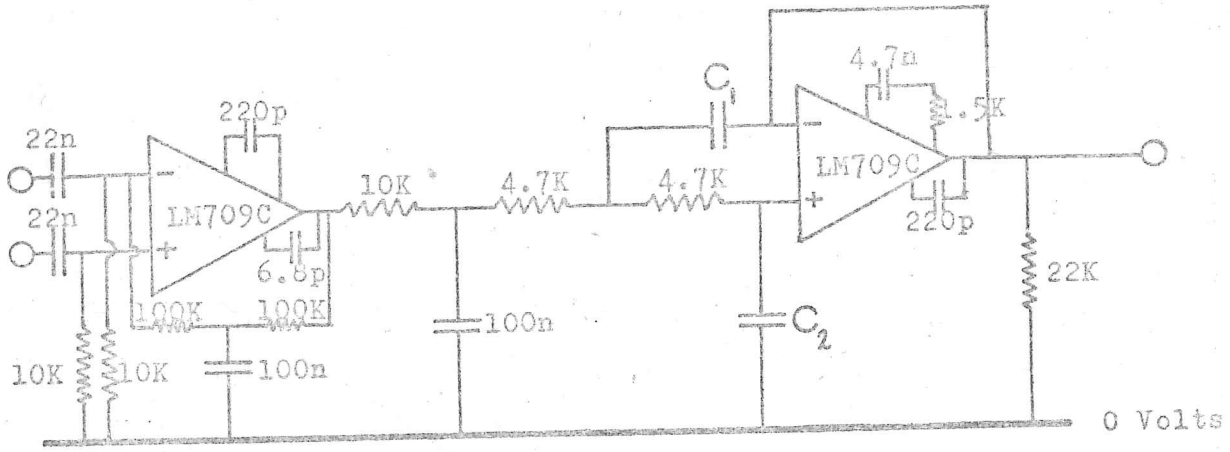

Saturating Amplifier

Two Stage Active Filter

(Q = 1.6)

Freq(Hz)	$C_1(\mu F)$	$C_2(\mu F)$
1	100	10
10	10	1
100	1	0.1
1000	0.1	0.01

Notes:

i) Resistance values in Ohms

ii) Capacitance values in Farads

iii) Whole Circuit operates off the same ± 15 Volt supply.

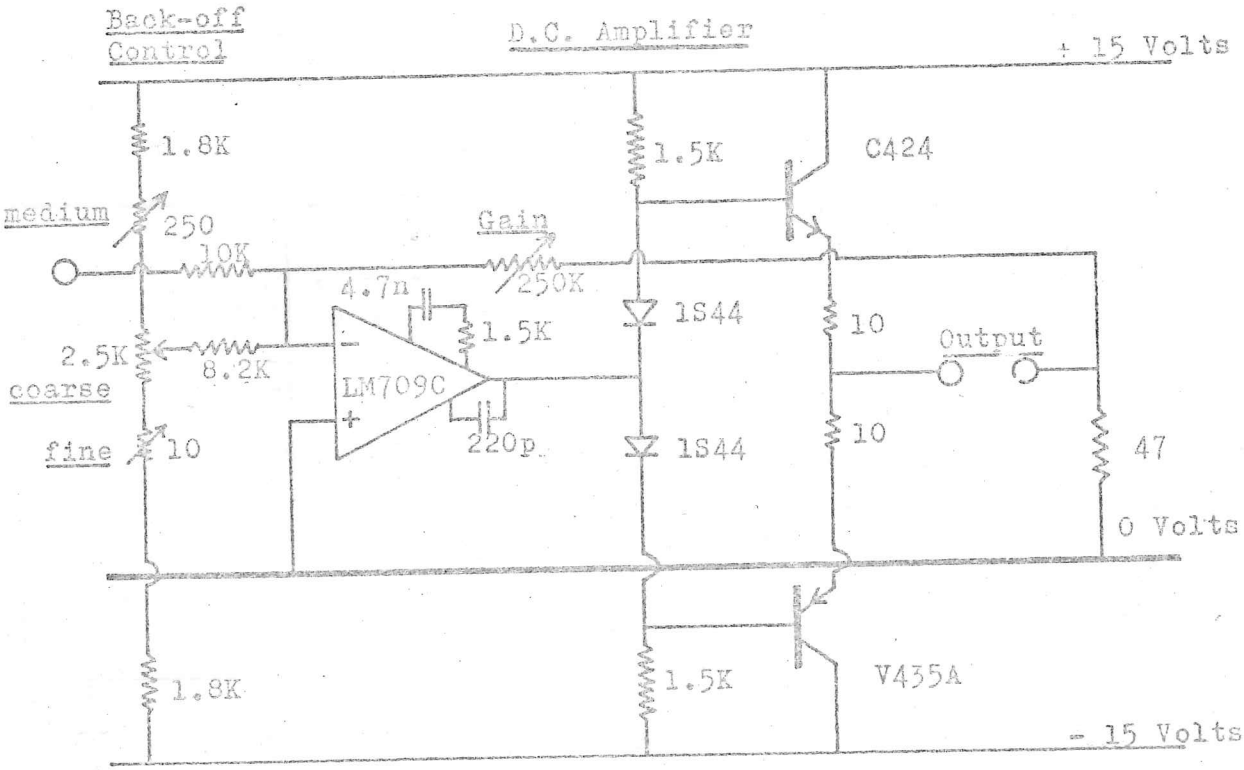

FIGURE 4

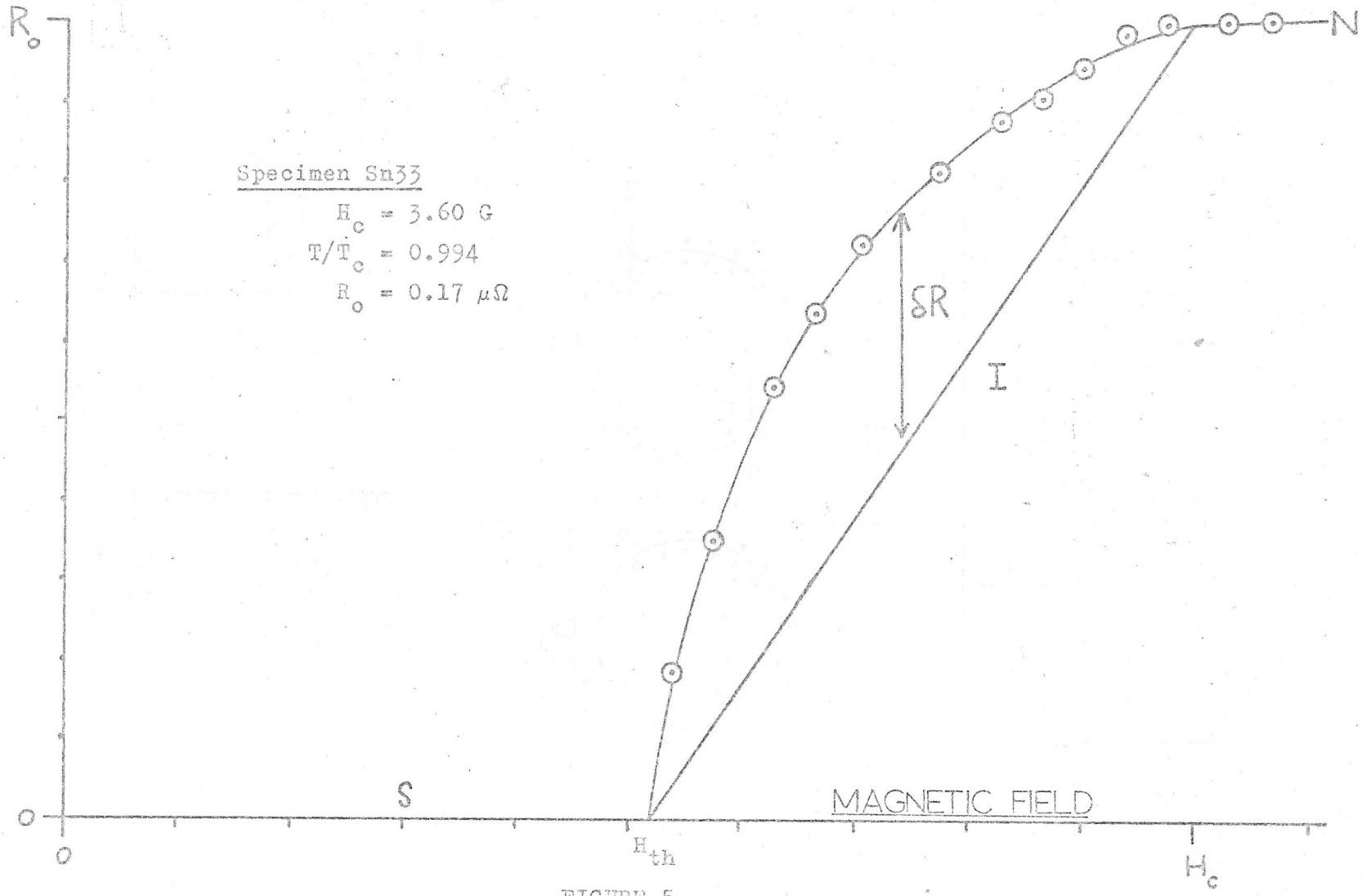
R
o
Specimen Sn33
H
c
= 3.60 G
T/T
c
= 0.994
R
o
= 0.17 μΩ
N
δR
I
S
MAGNETIC FIELD
0
0
H
th
H
c

FIGURE 5

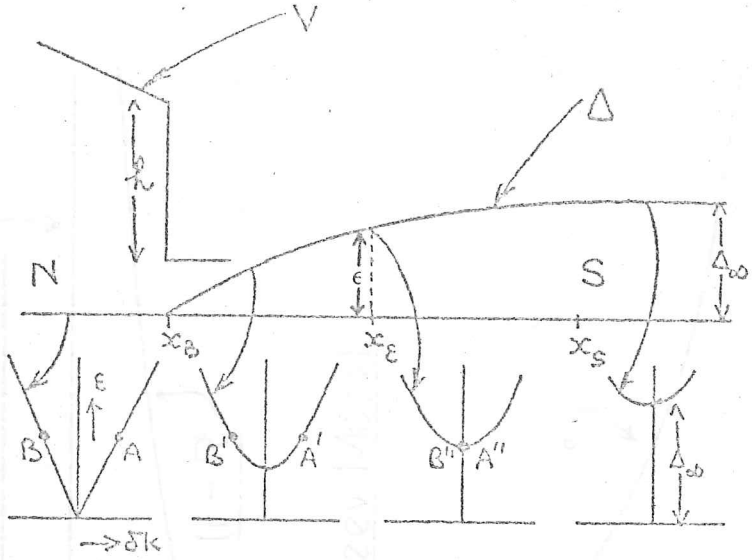

FIGURE 6

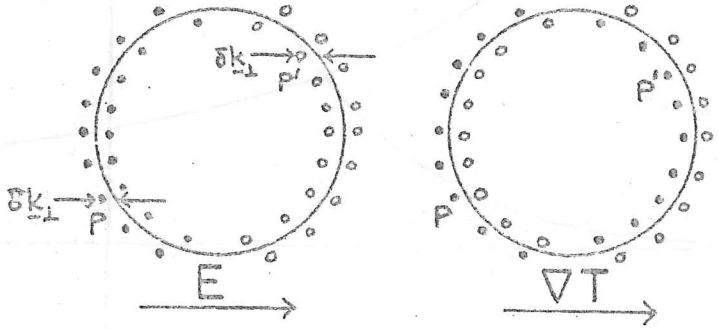

FIGURE 7

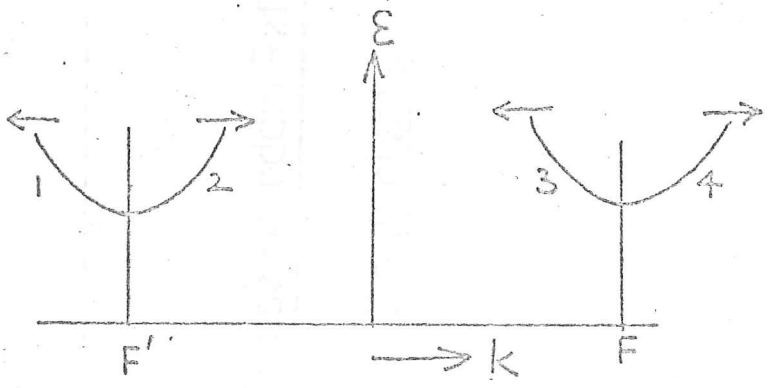

FIGURE 8

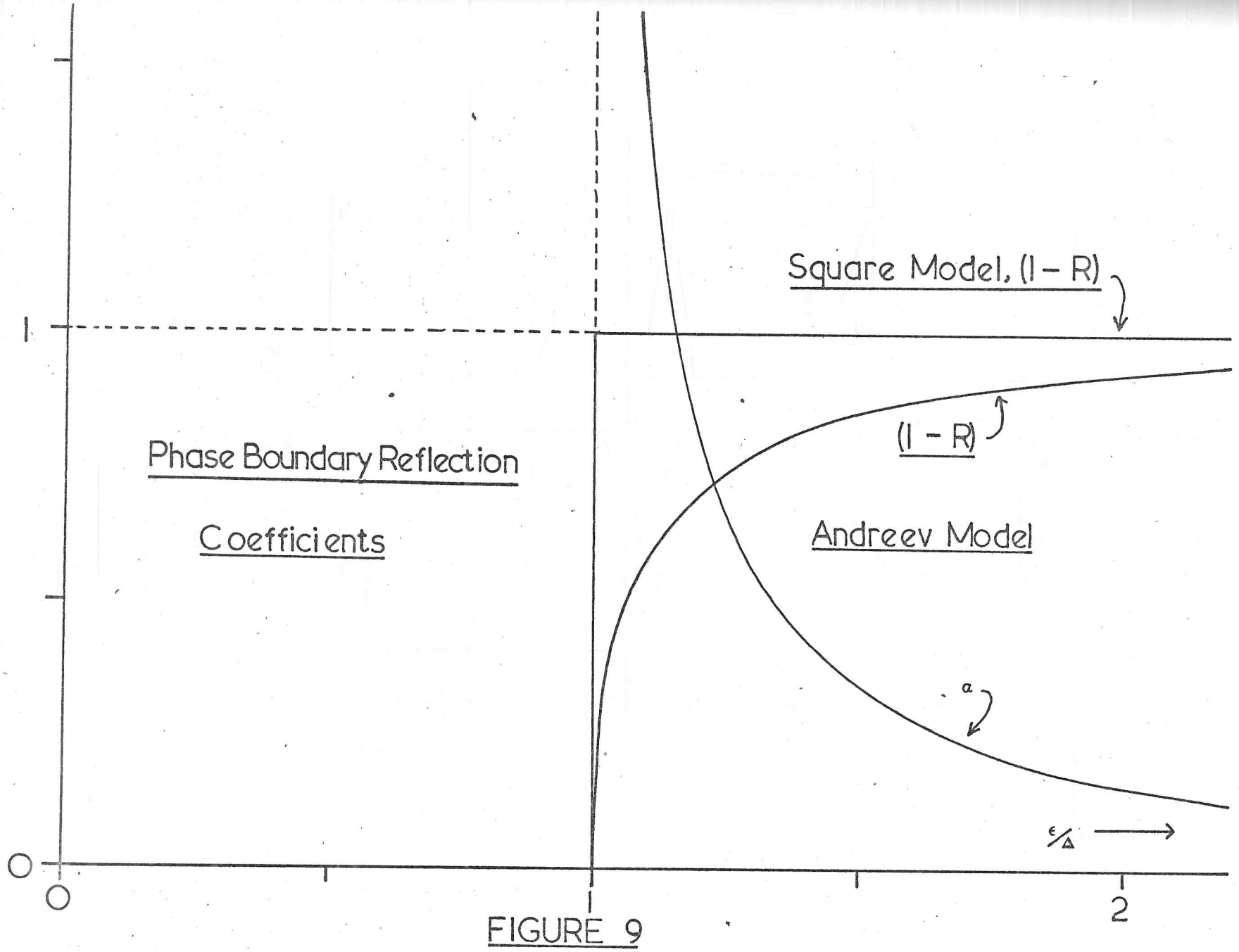
Square Model, (1 – R)
1
(1 – R)
Phase Boundary Reflection
Coefficients
Andreev Model
a
ε/Δ
0
0
2

FIGURE 9

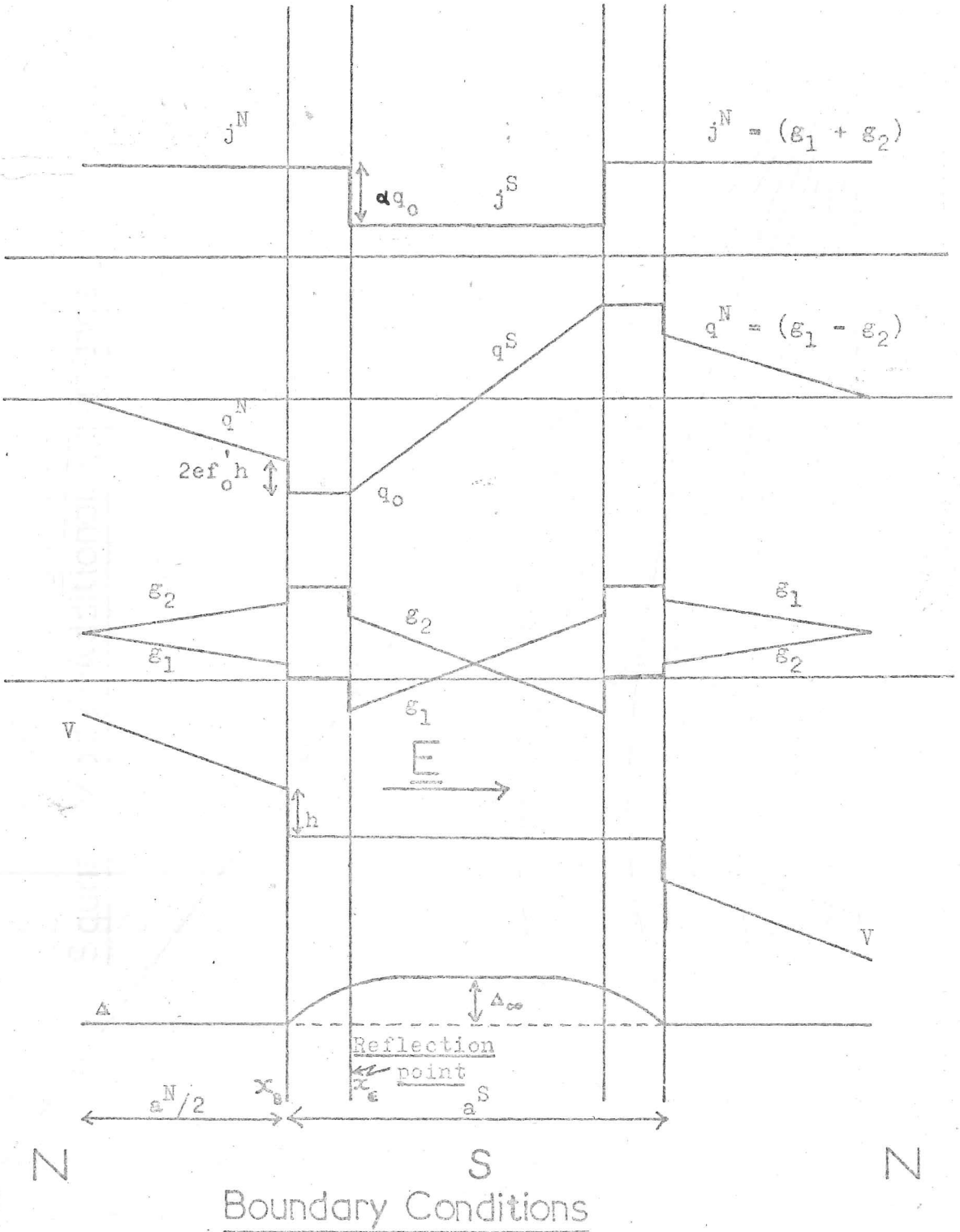
j^N
$j^N = (\varepsilon_1 + \varepsilon_2)$
αq_o
j^S
$q^N = (\varepsilon_1 - \varepsilon_2)$
q^S
q^N
$2ef_o'h$
q_o
ε_2
ε_1
ε_2
ε_1
ε_1
ε_2
V
E
h
V
Δ
Δ_∞
Reflection point
x_ε
$a^N/2$
x_s
a^S
N
S
N
Boundary Conditions

FIGURE 10

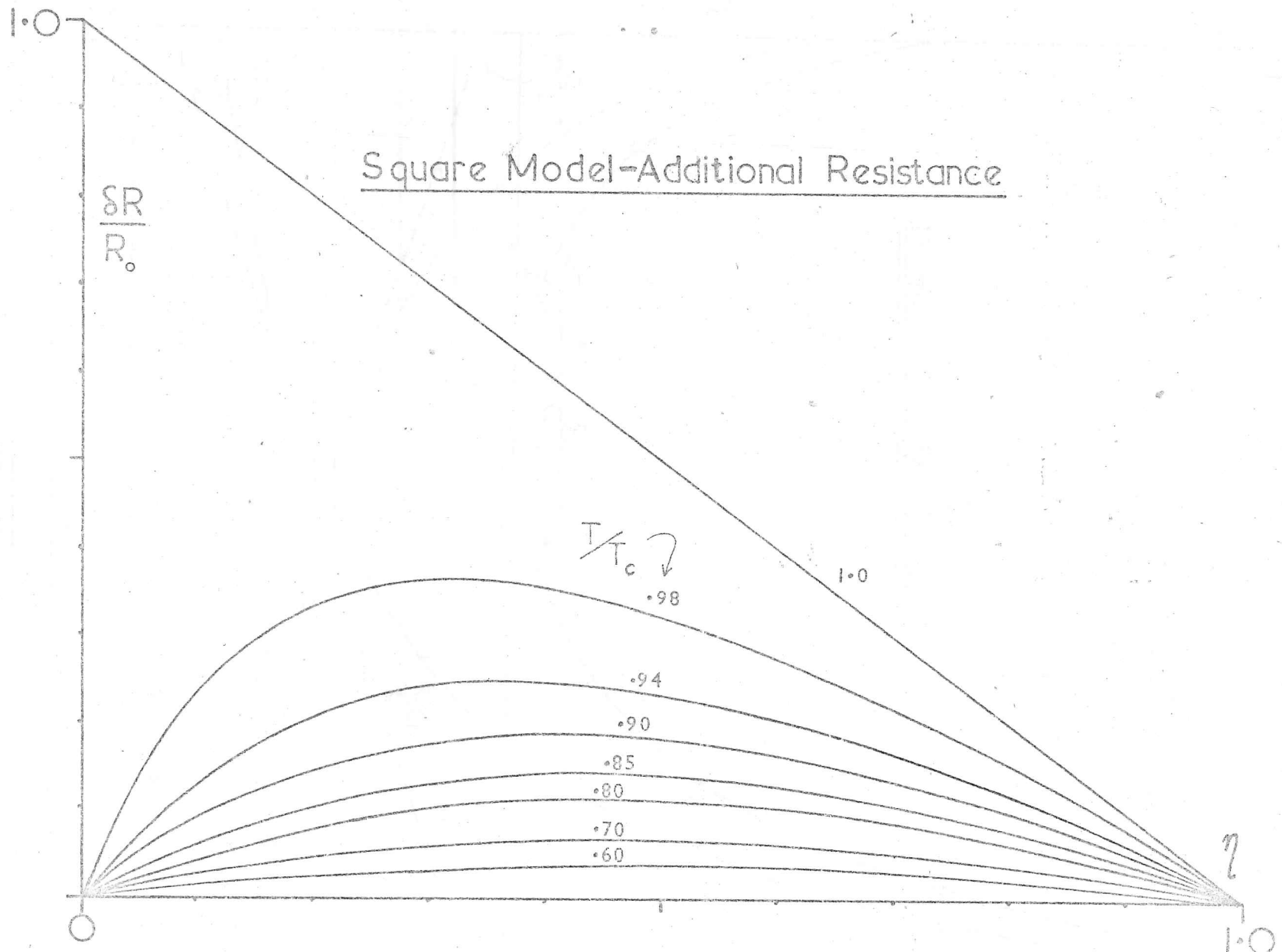
Square Model-Additional Resistance
1·0
δR/R₀
T/Tc
1·0
·98
·94
·90
·85
·80
·70
·60
η
1·0

FIGURE 11

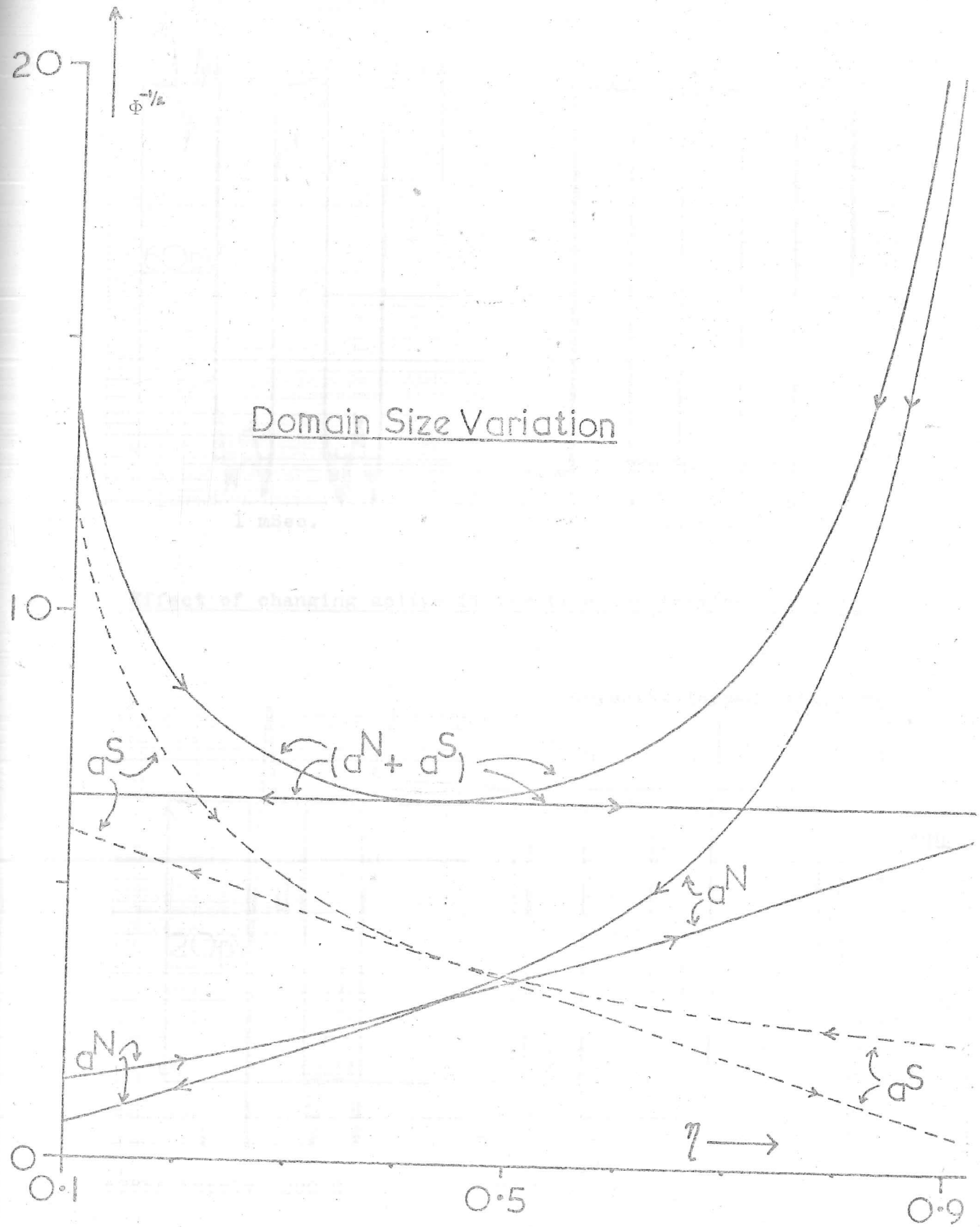
20
$\Phi^{-1/2}$
Domain Size Variation
10
a^S
$(a^N + a^S)$
a^N
a^N
a^S
$\eta \longrightarrow$
0
0·1
0·5
0·9

FIGURE 12

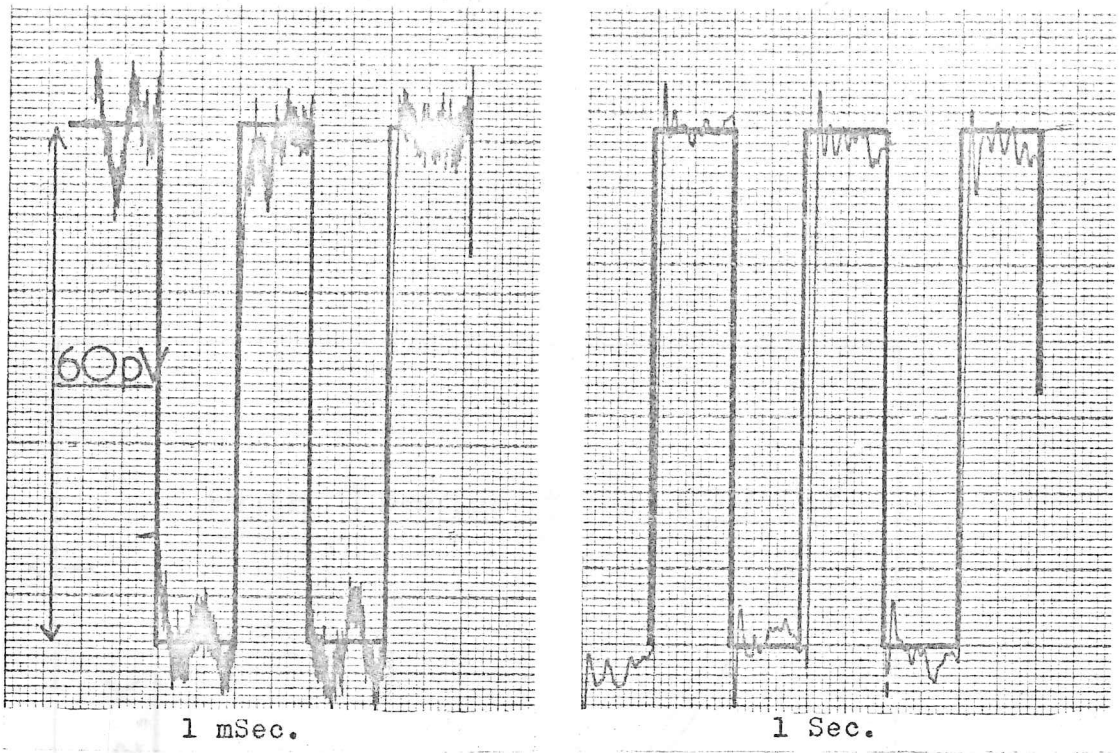

Effect of changing active filter time constant(zero field)

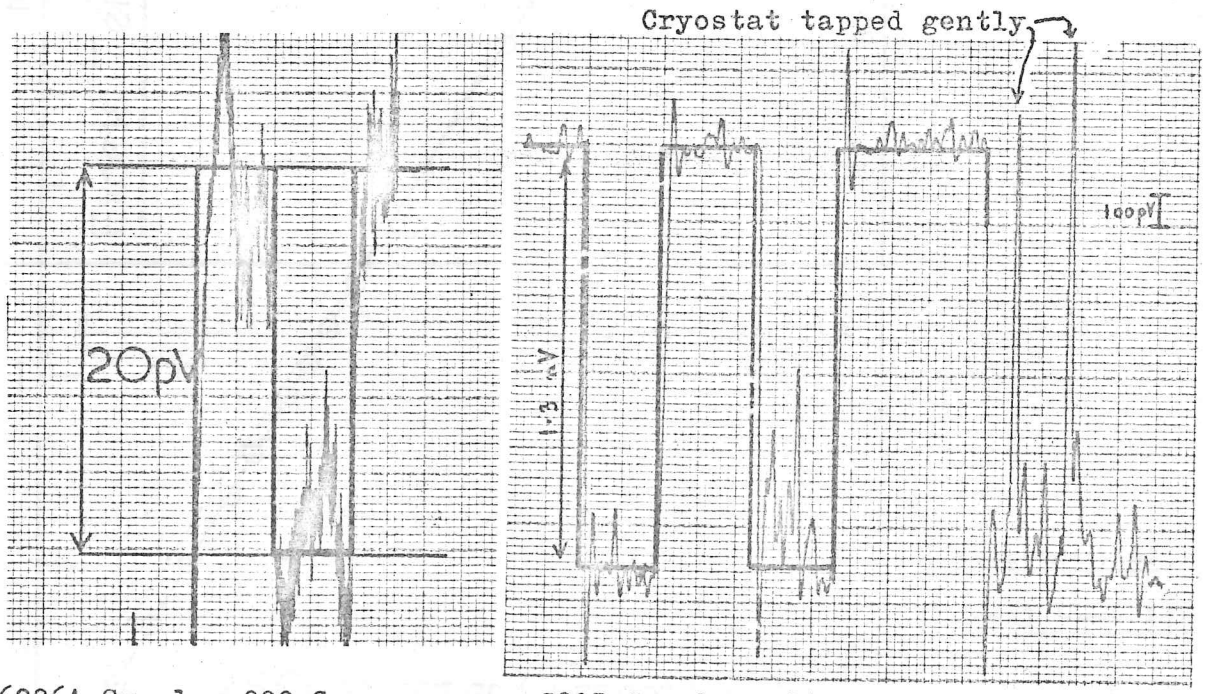

6286A Supply 200 G

C905 Supply 350 G

SLUG CIRCUIT NOISE

FIGURE 13

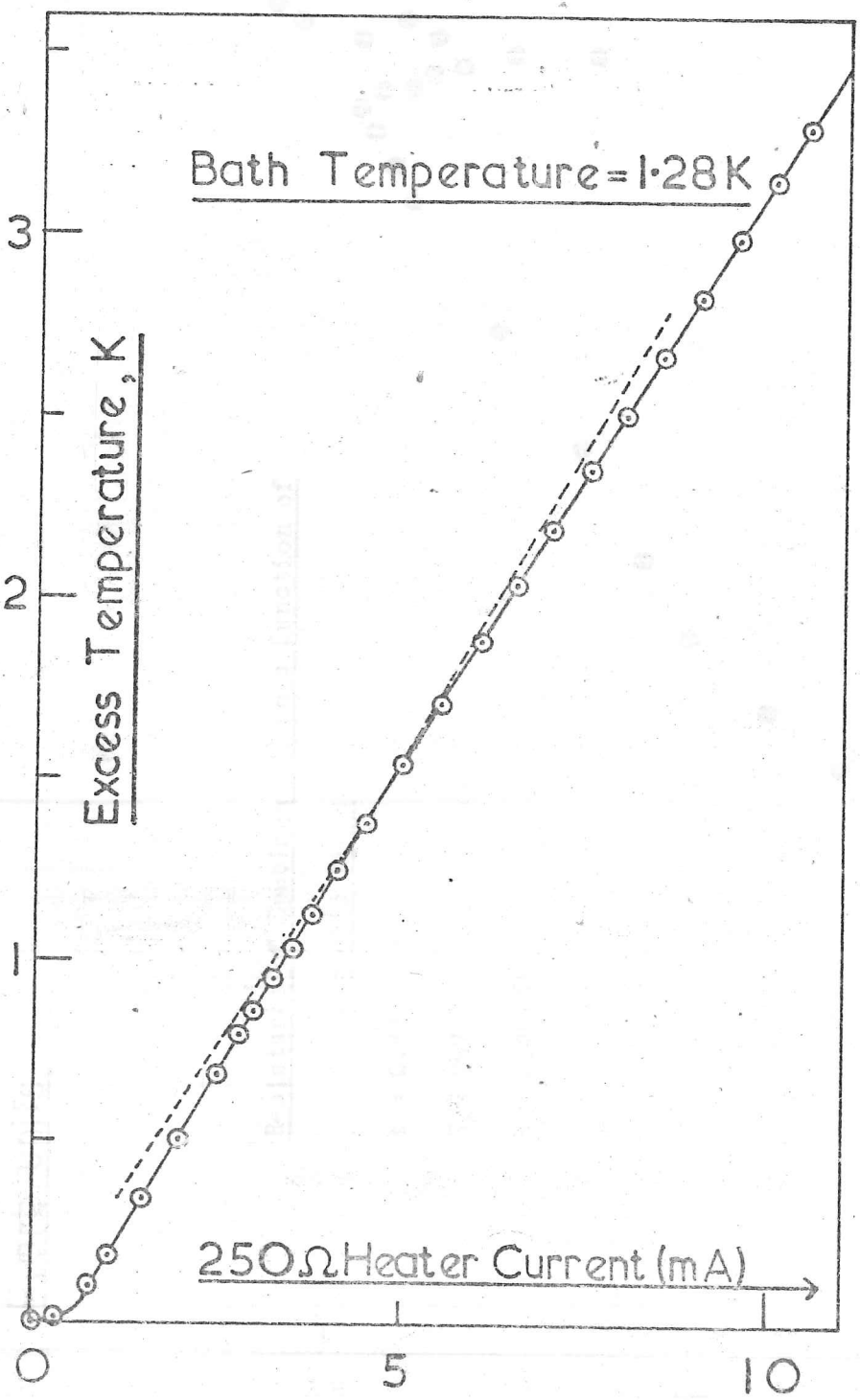

Measurement of Thermal Weak Link

FIGURE 14

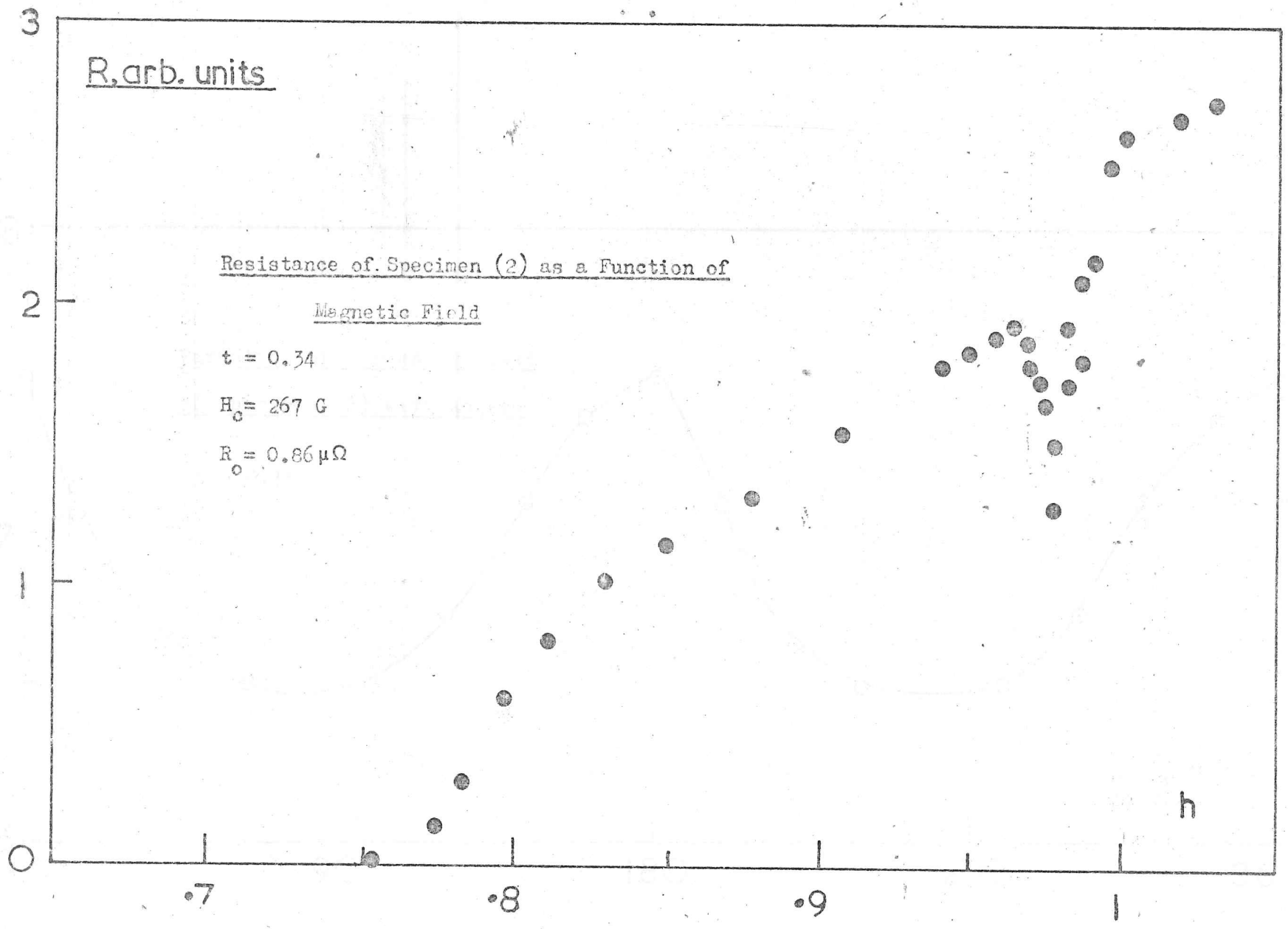
R, arb. units
3
2
1
0
Resistance of Specimen (2) as a Function of
Magnetic Field
t = 0.34
H_o = 267 G
R_o = 0.86 μΩ
h
.7
.8
.9
1

FIGURE 15

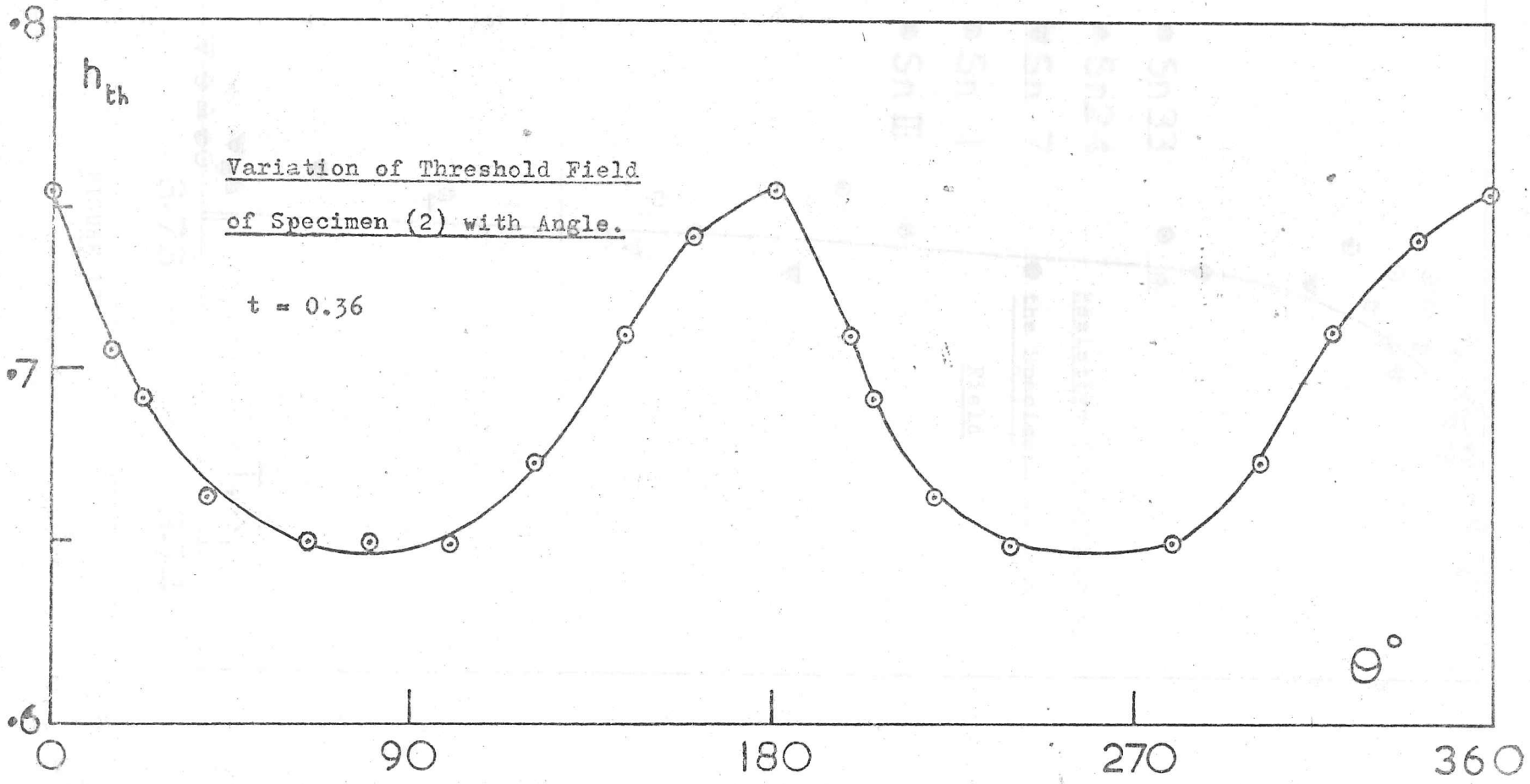
·8
h_{th}
Variation of Threshold Field
of Specimen (2) with Angle.
t = 0.36
·7
·6
0
90
180
270
360
θ°

FIGURE 16

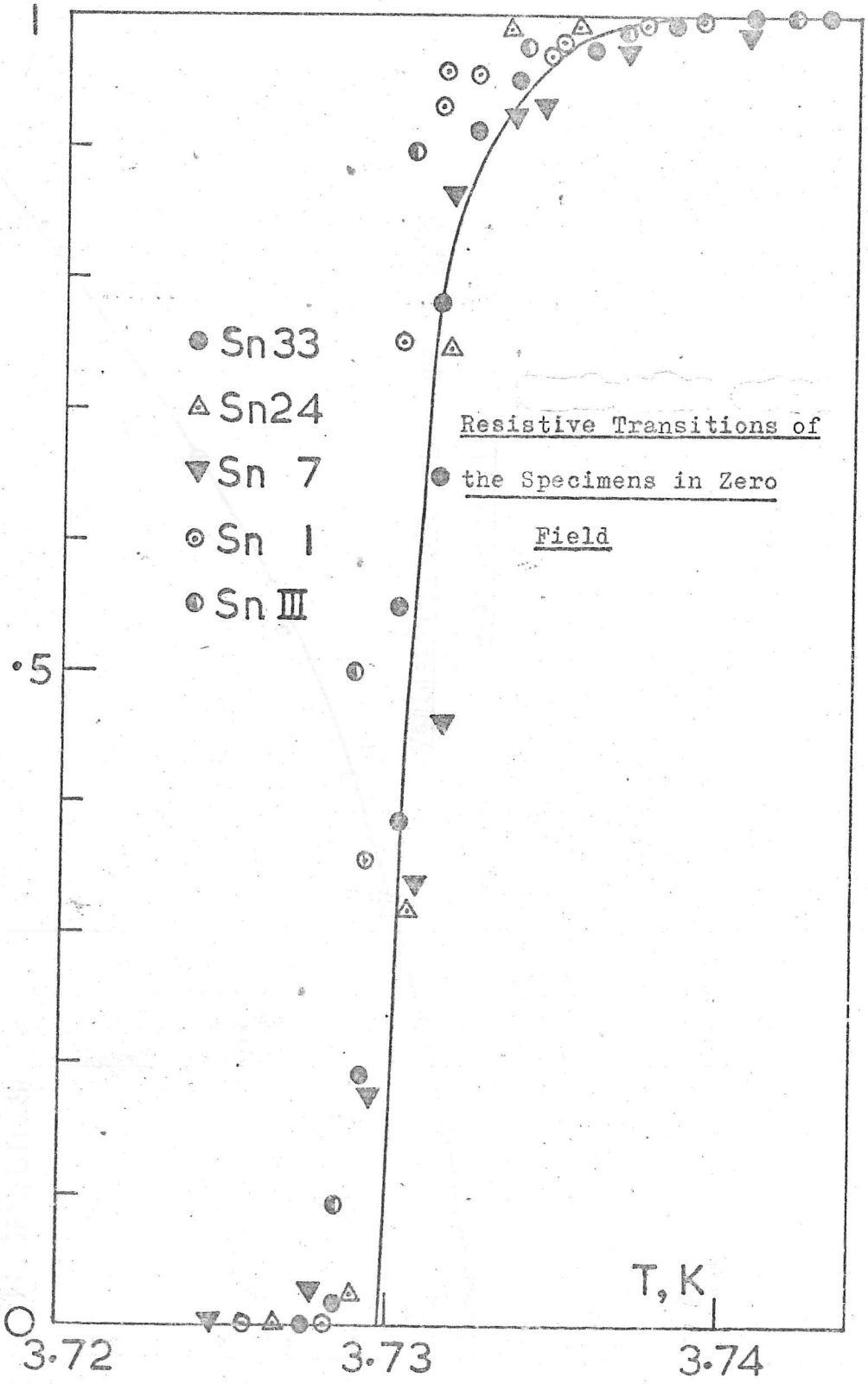
1
·5
0
Sn33
Sn24
Sn 7
Sn 1
Sn III
Resistive Transitions of
the Specimens in Zero
Field
T, K
3.72
3.73
3.74

FIGURE 17

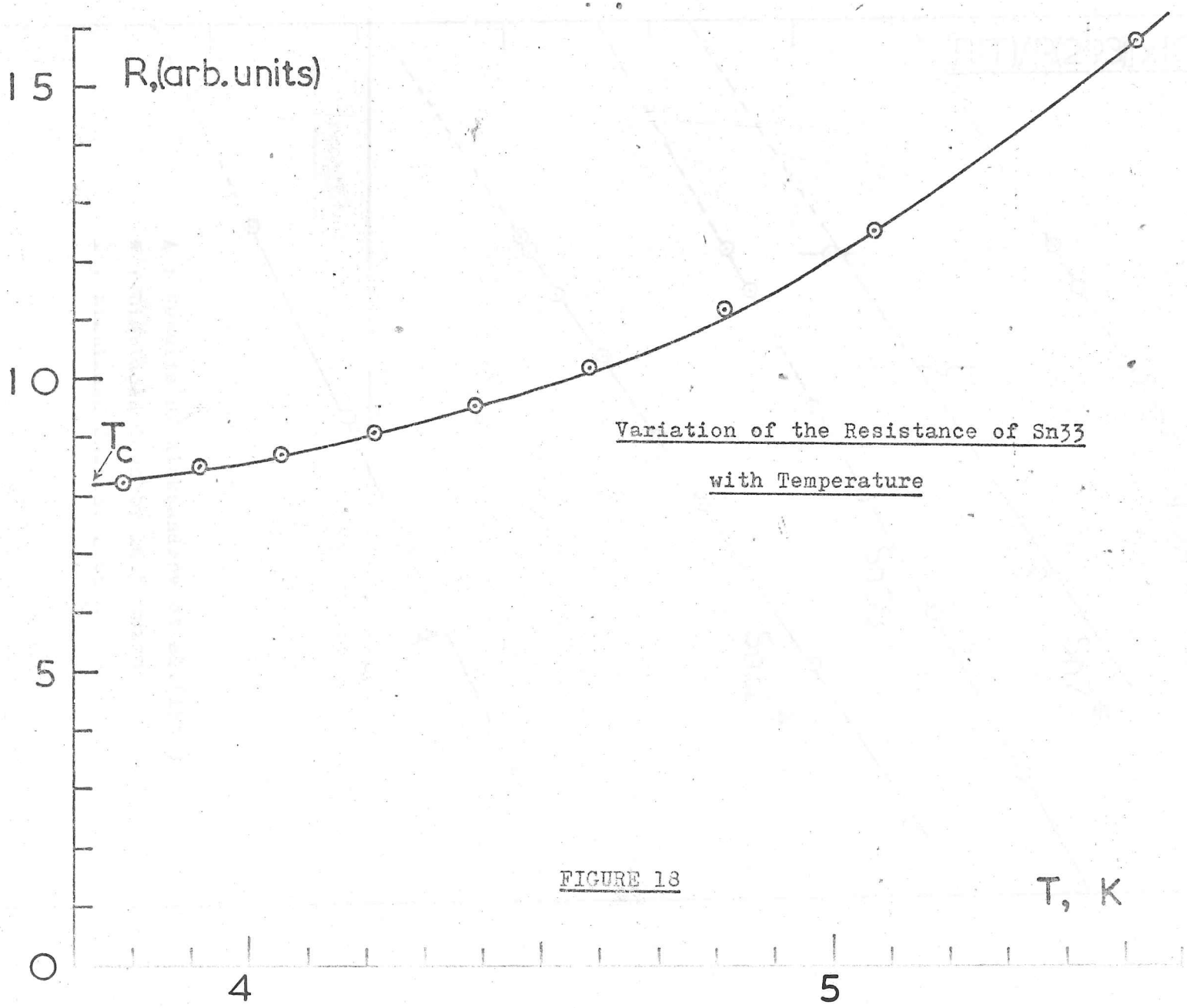

Variation of the Resistance of Sn33 with Temperature

FIGURE 18

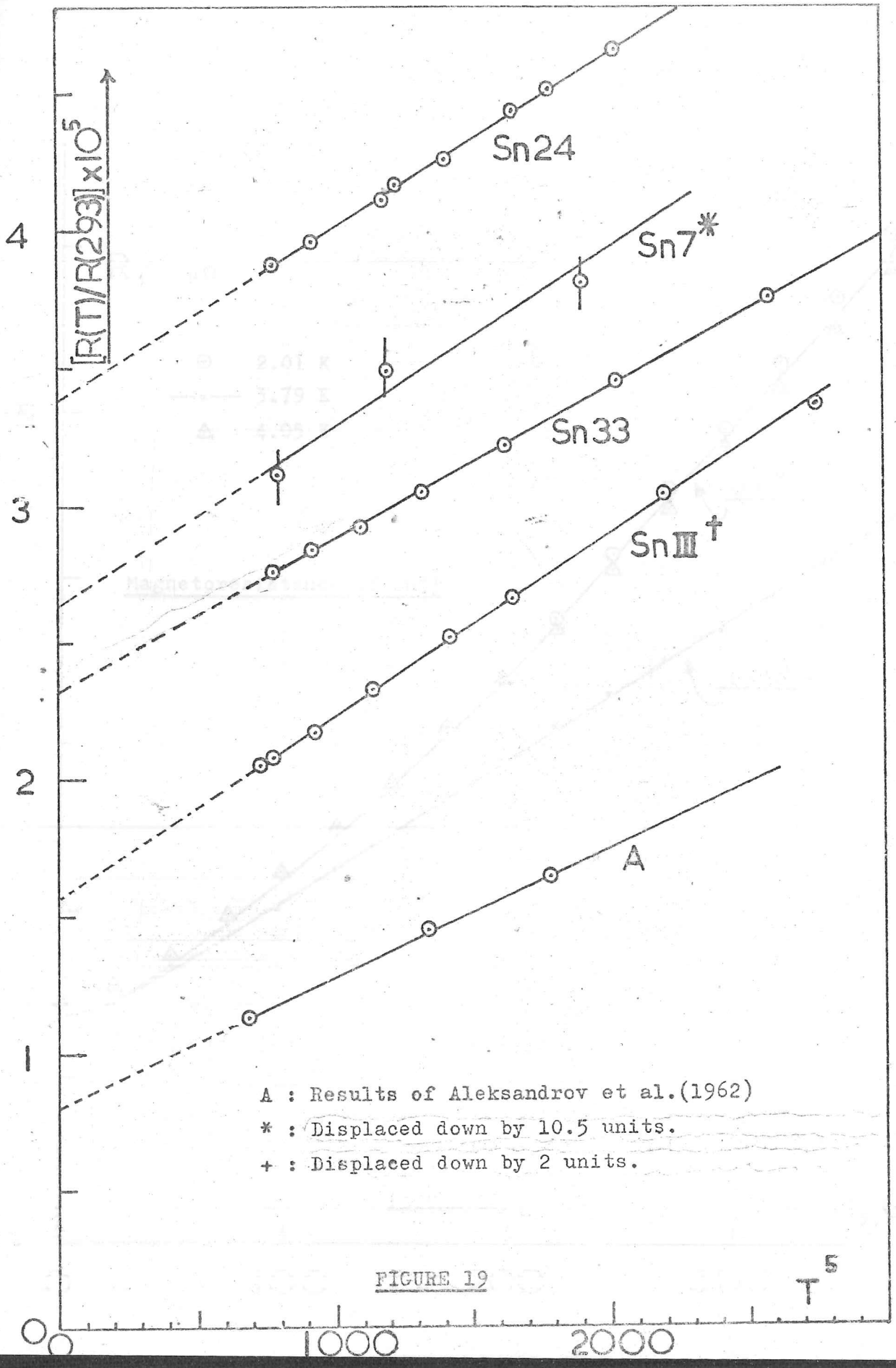

A : Results of Aleksandrov et al.(1962)

* : Displaced down by 10.5 units.

+ : Displaced down by 2 units.

FIGURE 19

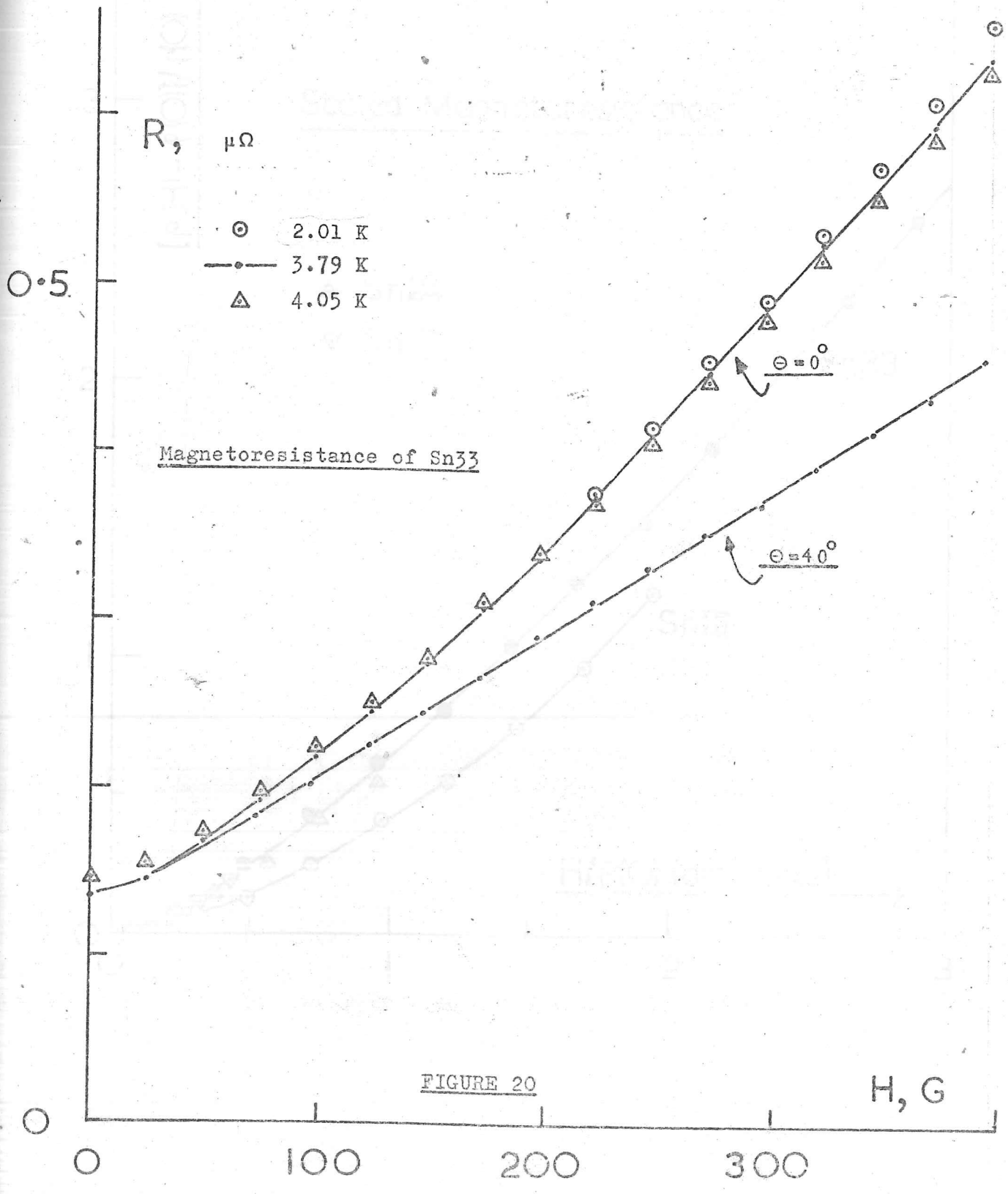
R, μΩ
2.01 K
3.79 K
4.05 K
0·5
Magnetoresistance of Sn33
Θ = 0°
Θ = 40°
0
0
100
200
300
H, G

FIGURE 20

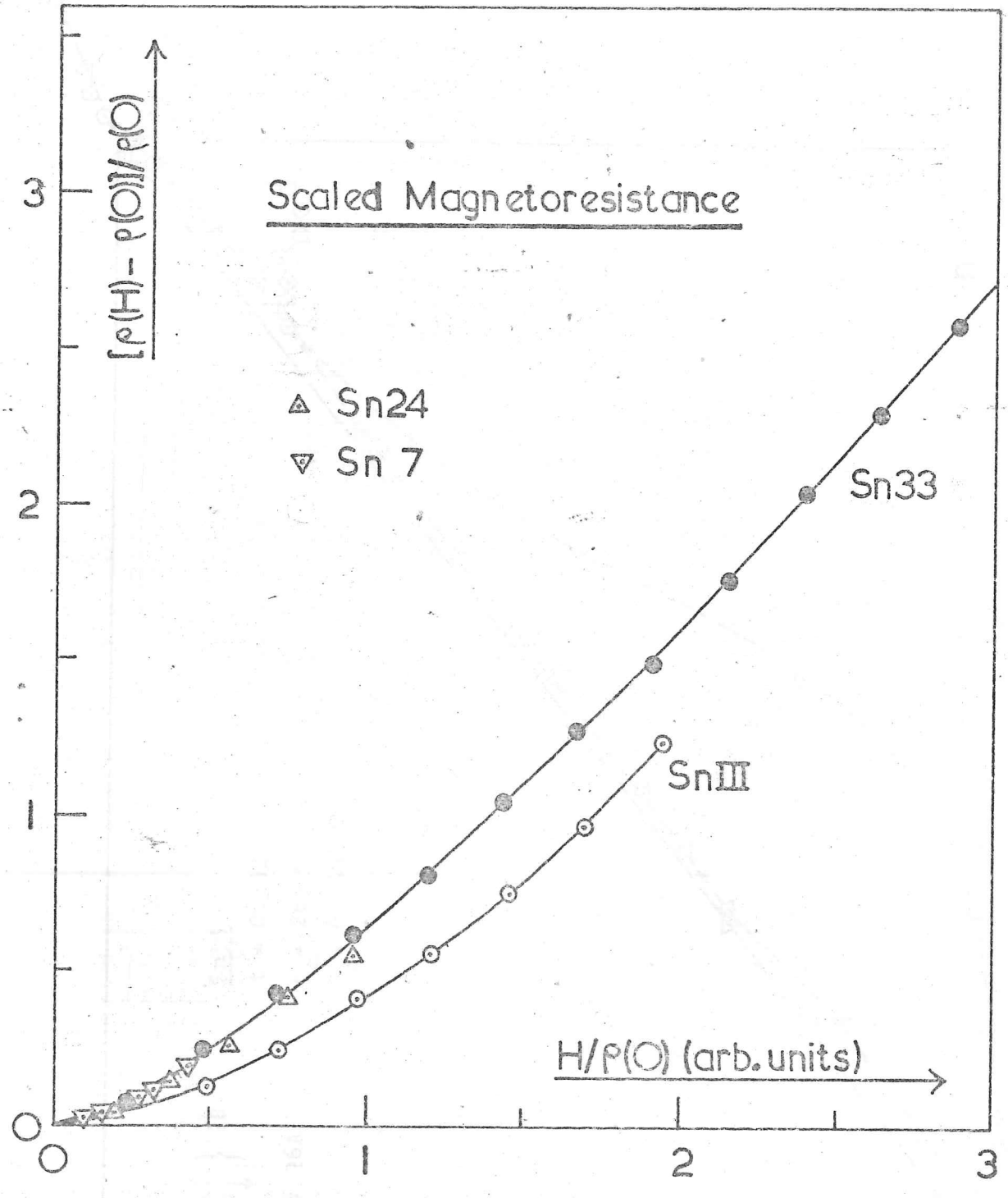
Scaled Magnetoresistance
[ρ(H) - ρ(0)]/ρ(0)
Sn24
Sn 7
Sn33
SnIII
H/ρ(0) (arb. units)
0
1
2
3

FIGURE 21

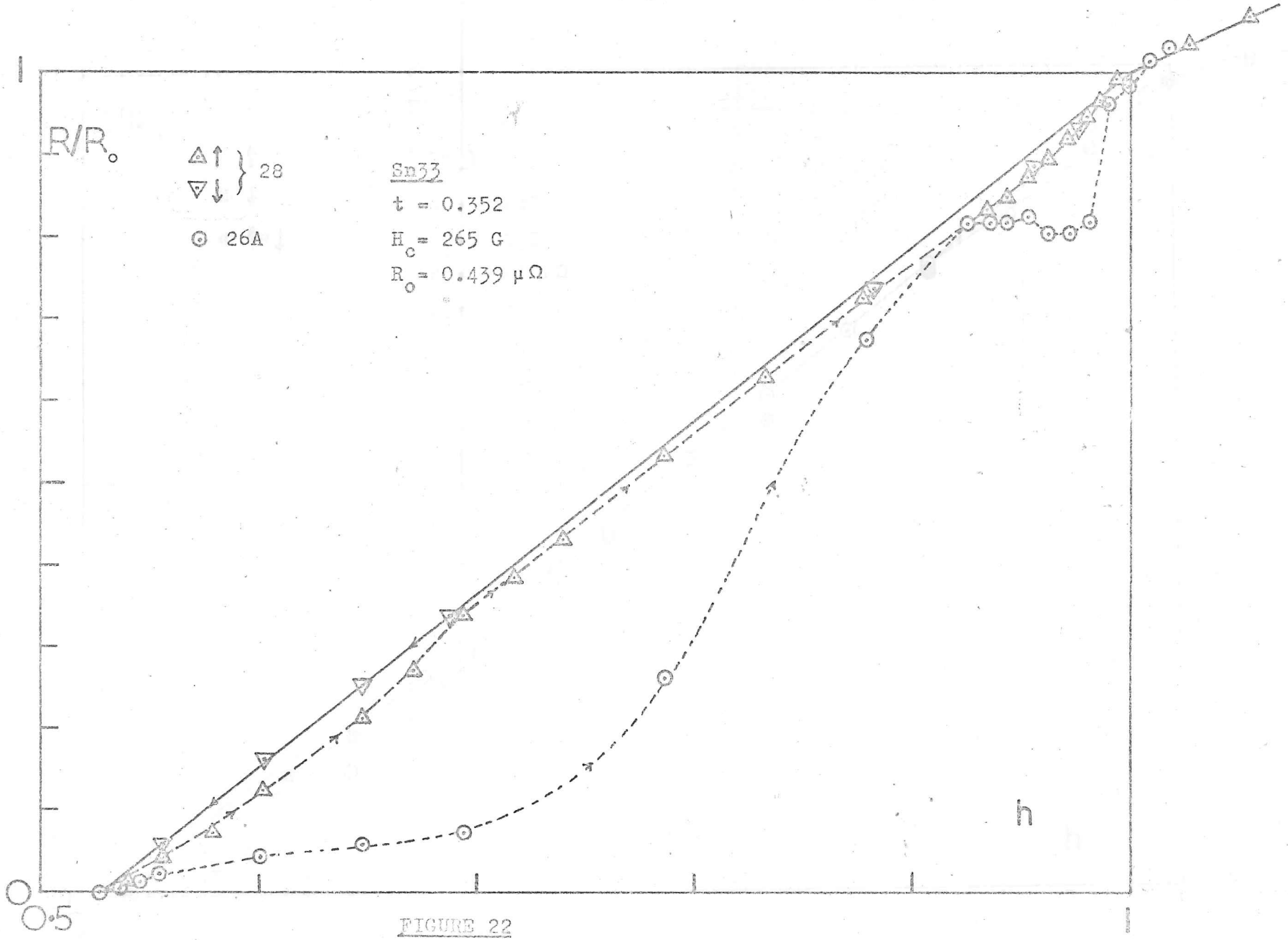

FIGURE 22

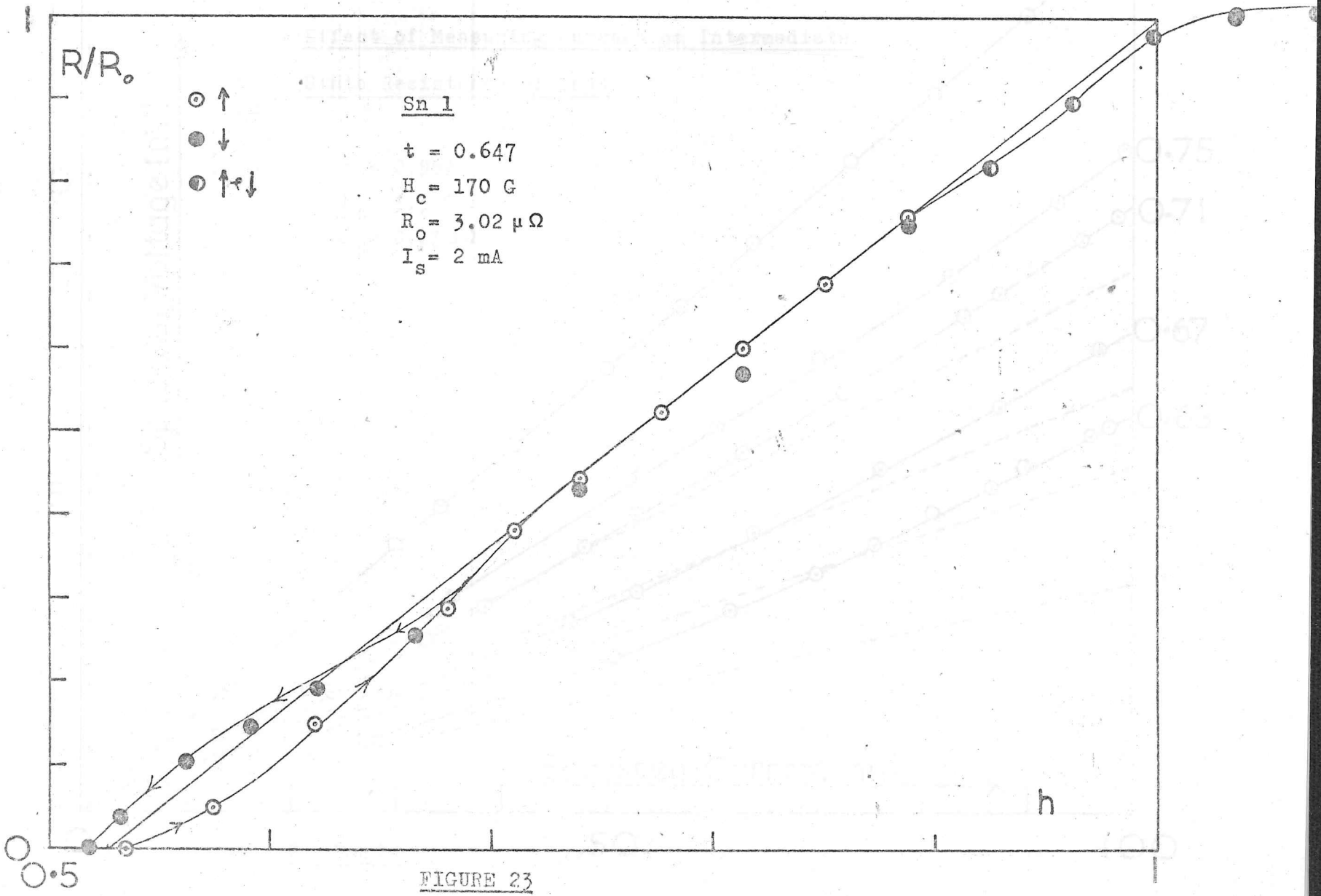

FIGURE 23

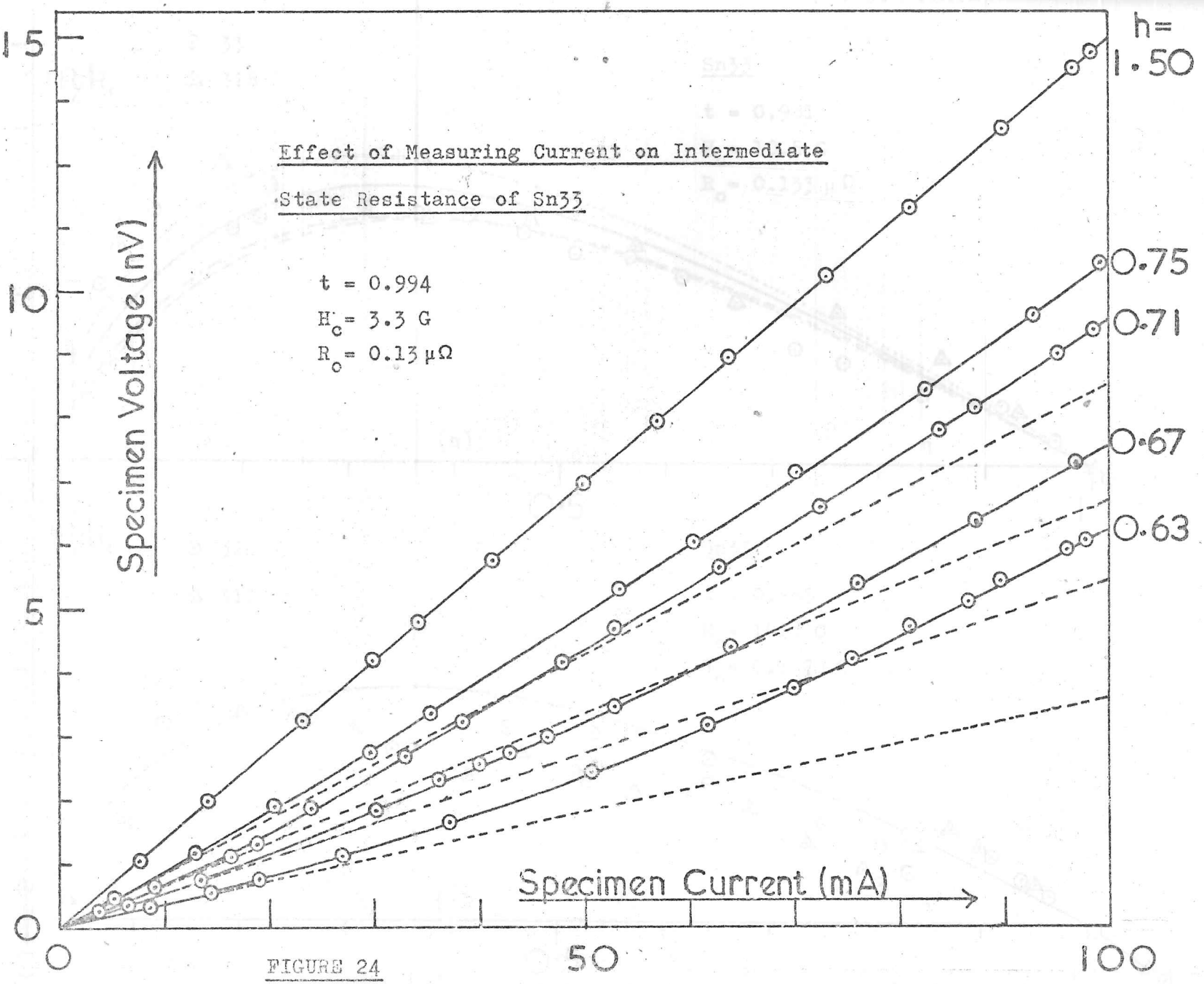
Effect of Measuring Current on Intermediate
State Resistance of Sn33
t = 0.994
H_c = 3.3 G
R_o = 0.13 μΩ
Specimen Voltage (nV)
Specimen Current (mA)
h=
1.50
0.75
0.71
0.67
0.63
15
10
5
0
0
50
100

FIGURE 24

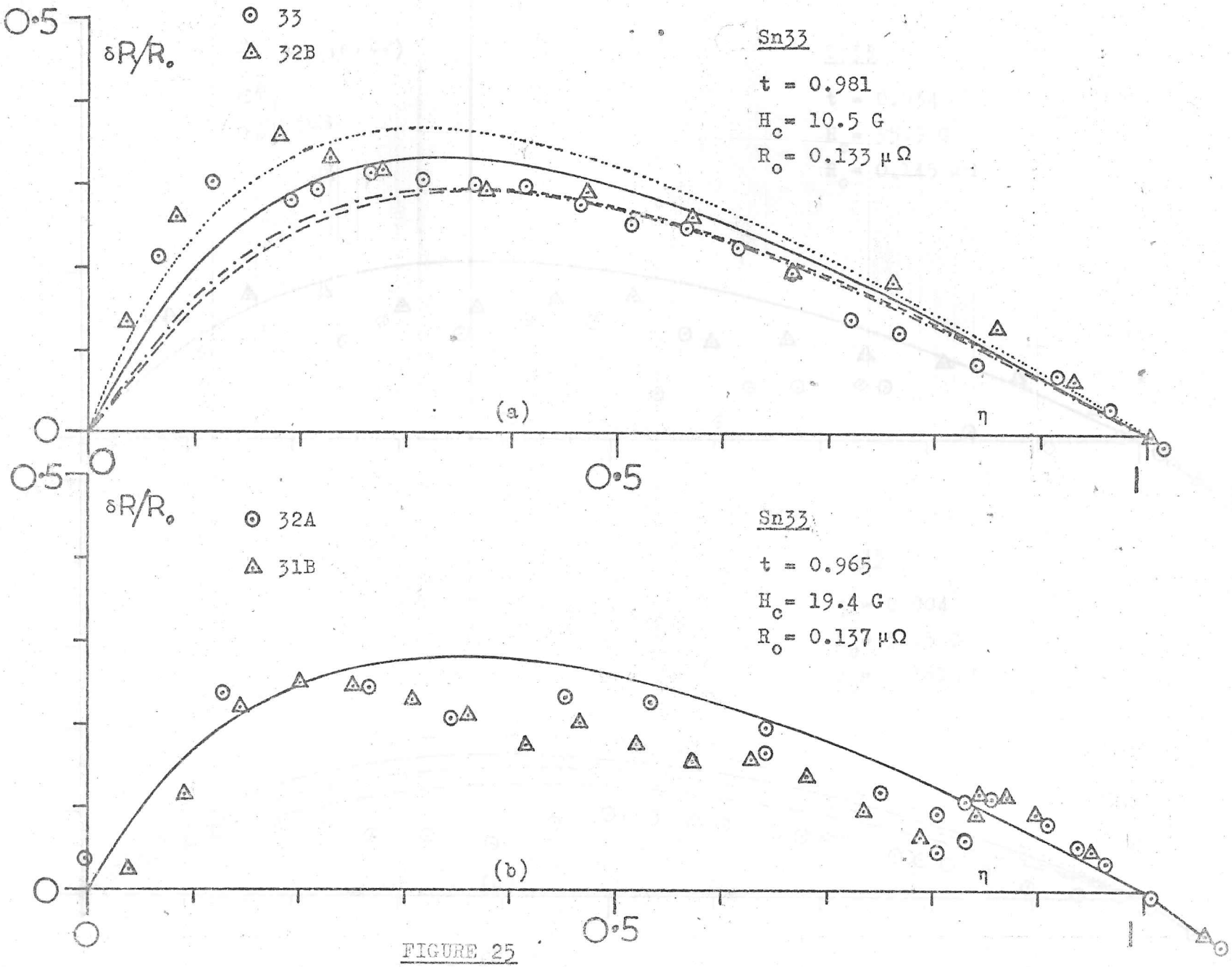
0·5
δR/R₀
33
32B
Sn33
t = 0.981
H_c = 10.5 G
R_o = 0.133 μΩ
(a)
η
0
0·5
1
0·5
δR/R₀
32A
31B
Sn33
t = 0.965
H_c = 19.4 G
R_o = 0.137 μΩ
(b)
η
0
0·5
1

FIGURE 25

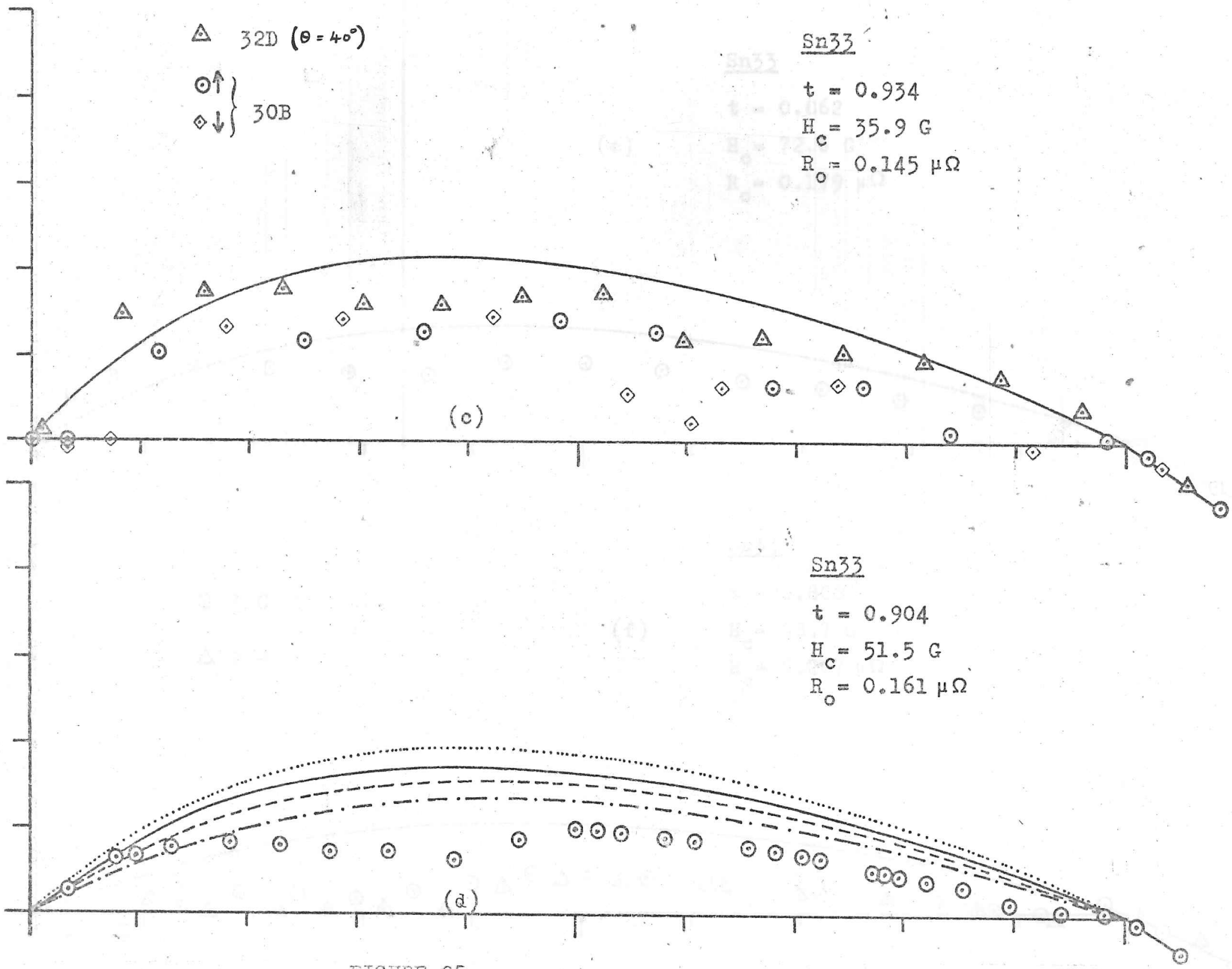
32D (θ = 40°)
30B
Sn33
t = 0.934
H_c = 35.9 G
R_o = 0.145 μΩ
(c)
Sn33
t = 0.904
H_c = 51.5 G
R_o = 0.161 μΩ
(d)

FIGURE 25

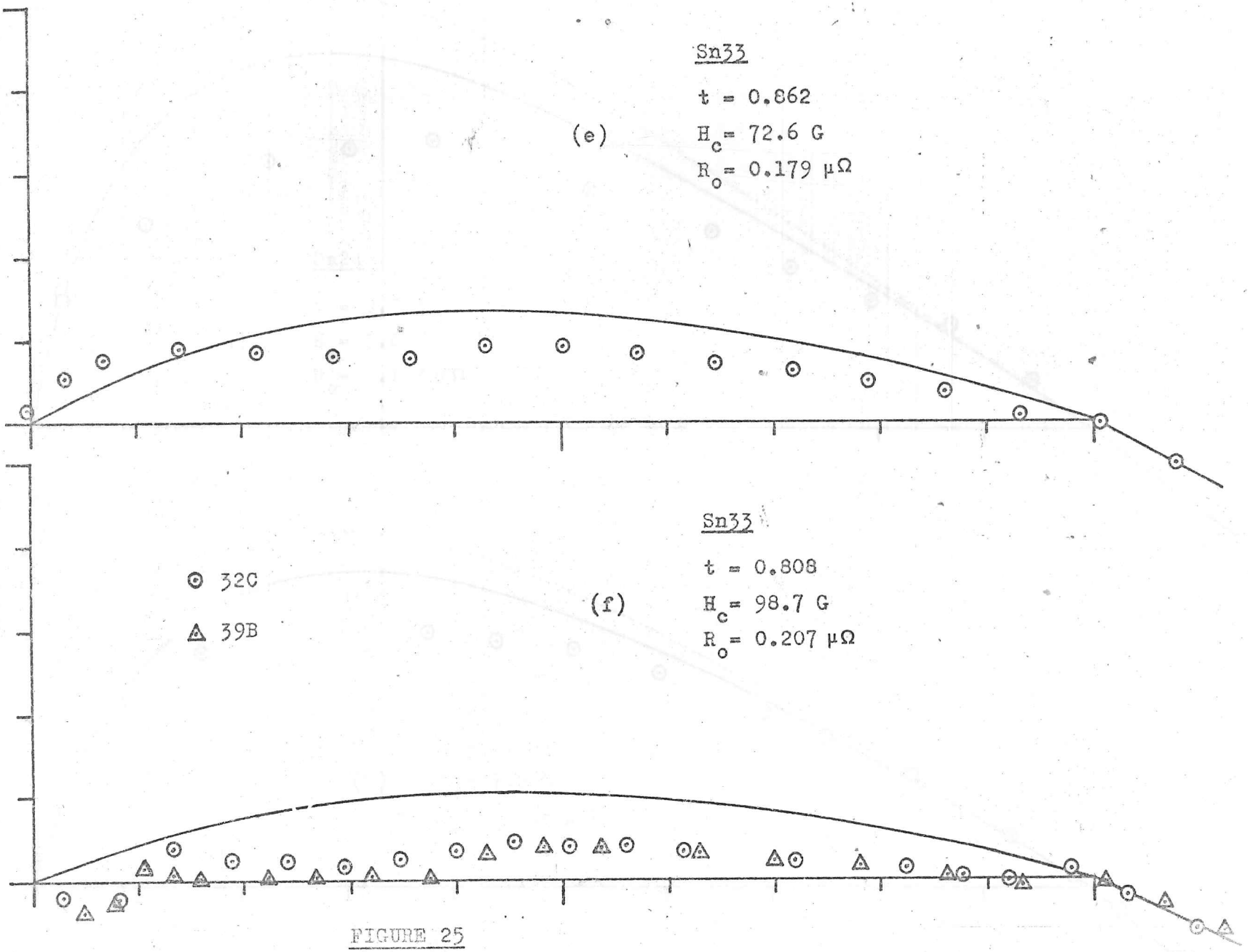
Sn33
t = 0.862
(e)
H_c = 72.6 G
R_o = 0.179 μΩ
Sn33
32C
39B
t = 0.808
(f)
H_c = 98.7 G
R_o = 0.207 μΩ

FIGURE 25

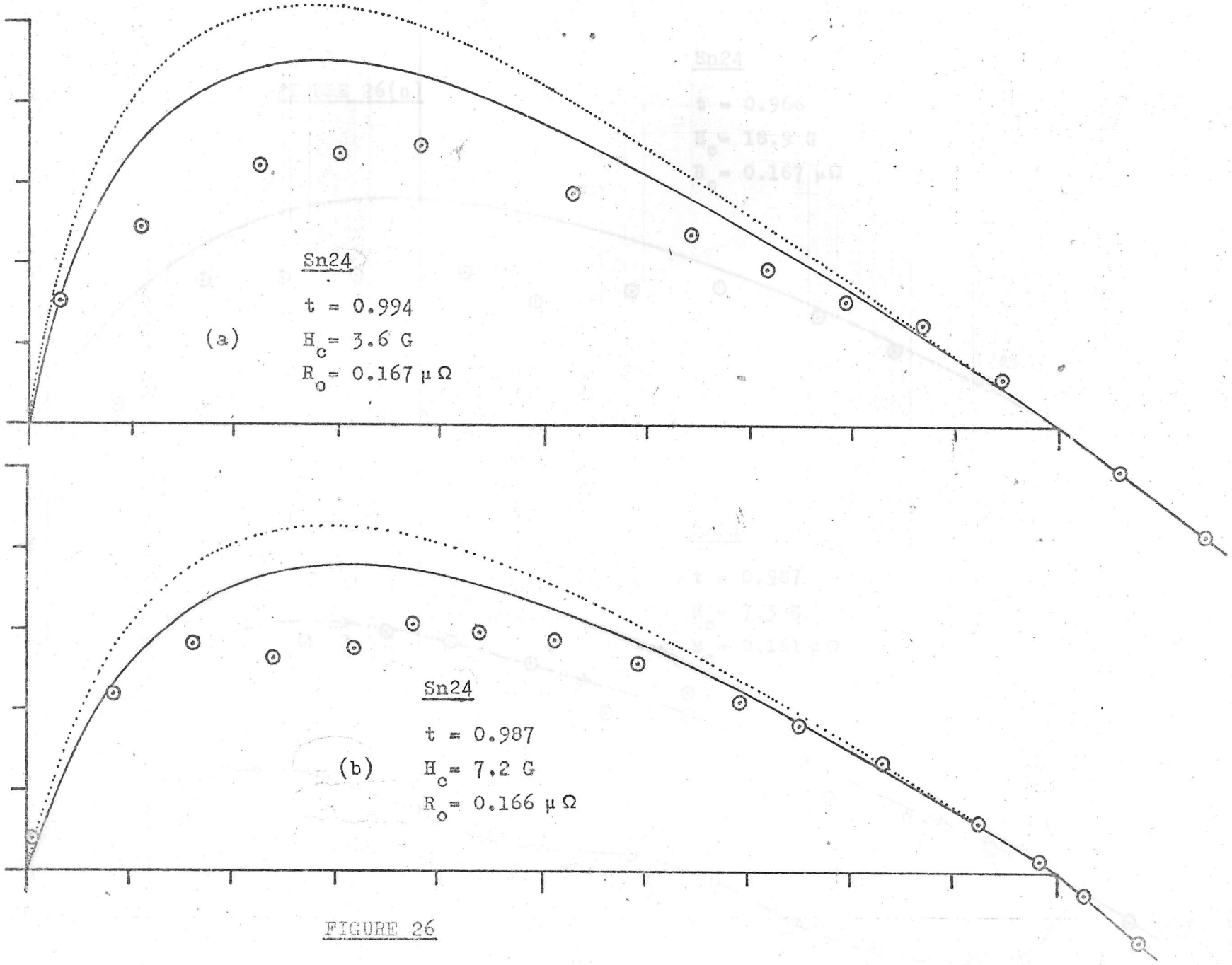

FIGURE 26

FIGURE 26(c)

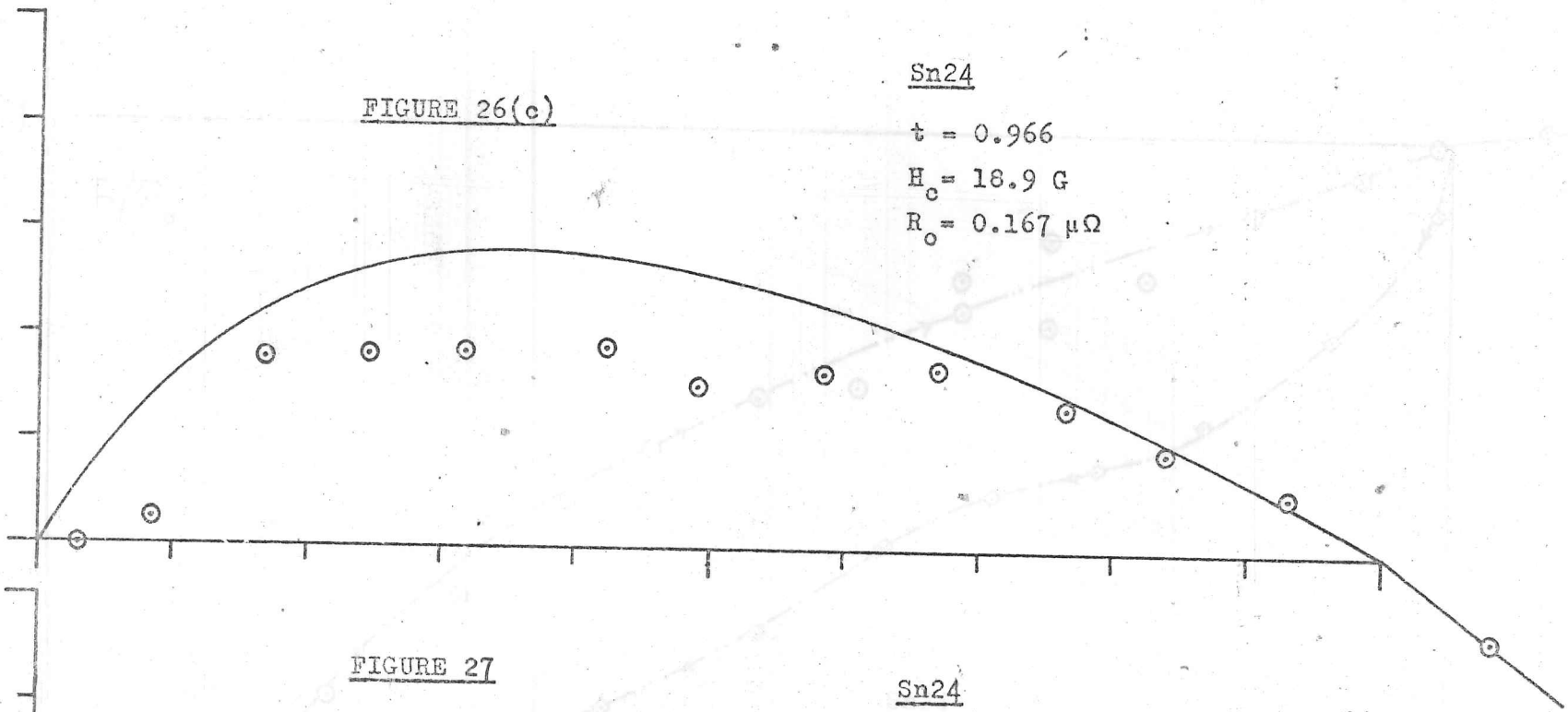

FIGURE 27

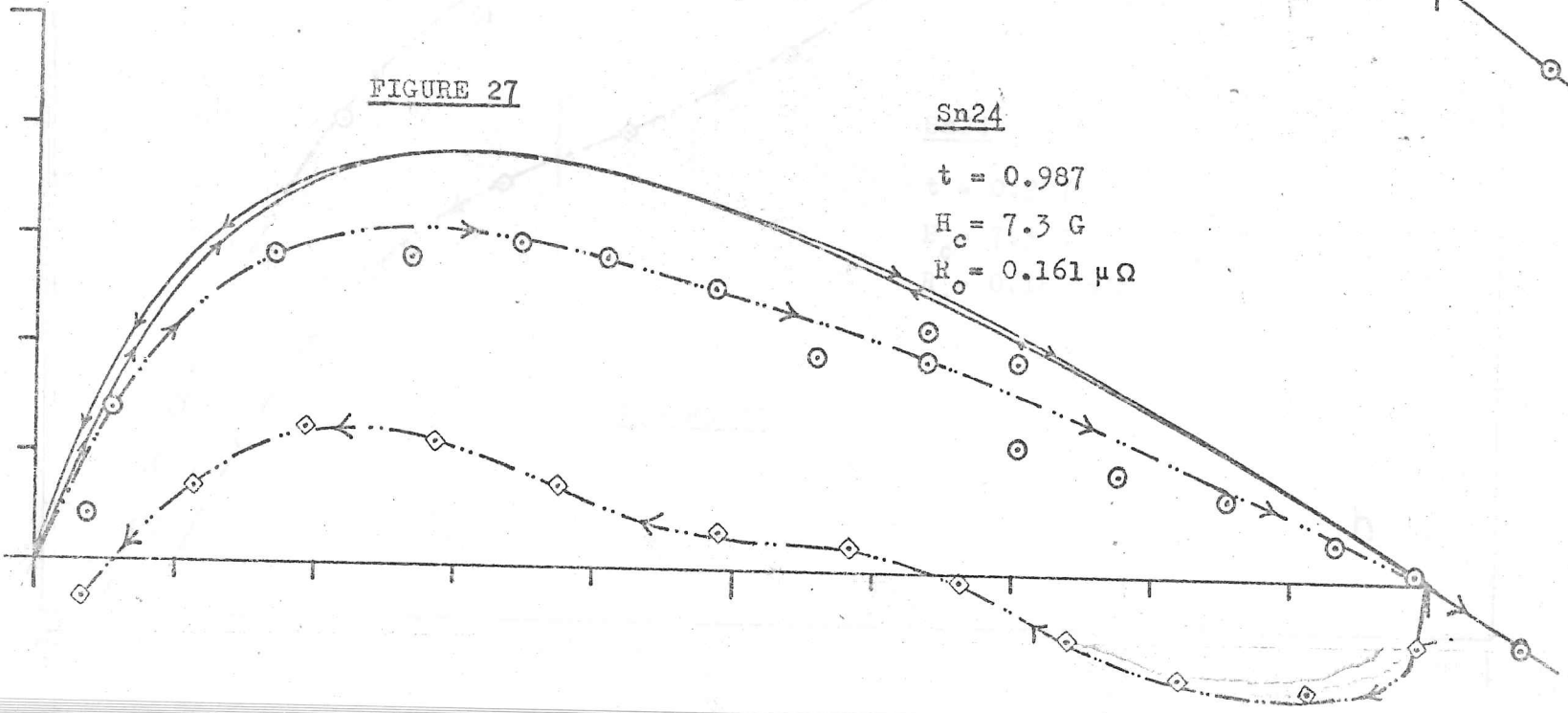

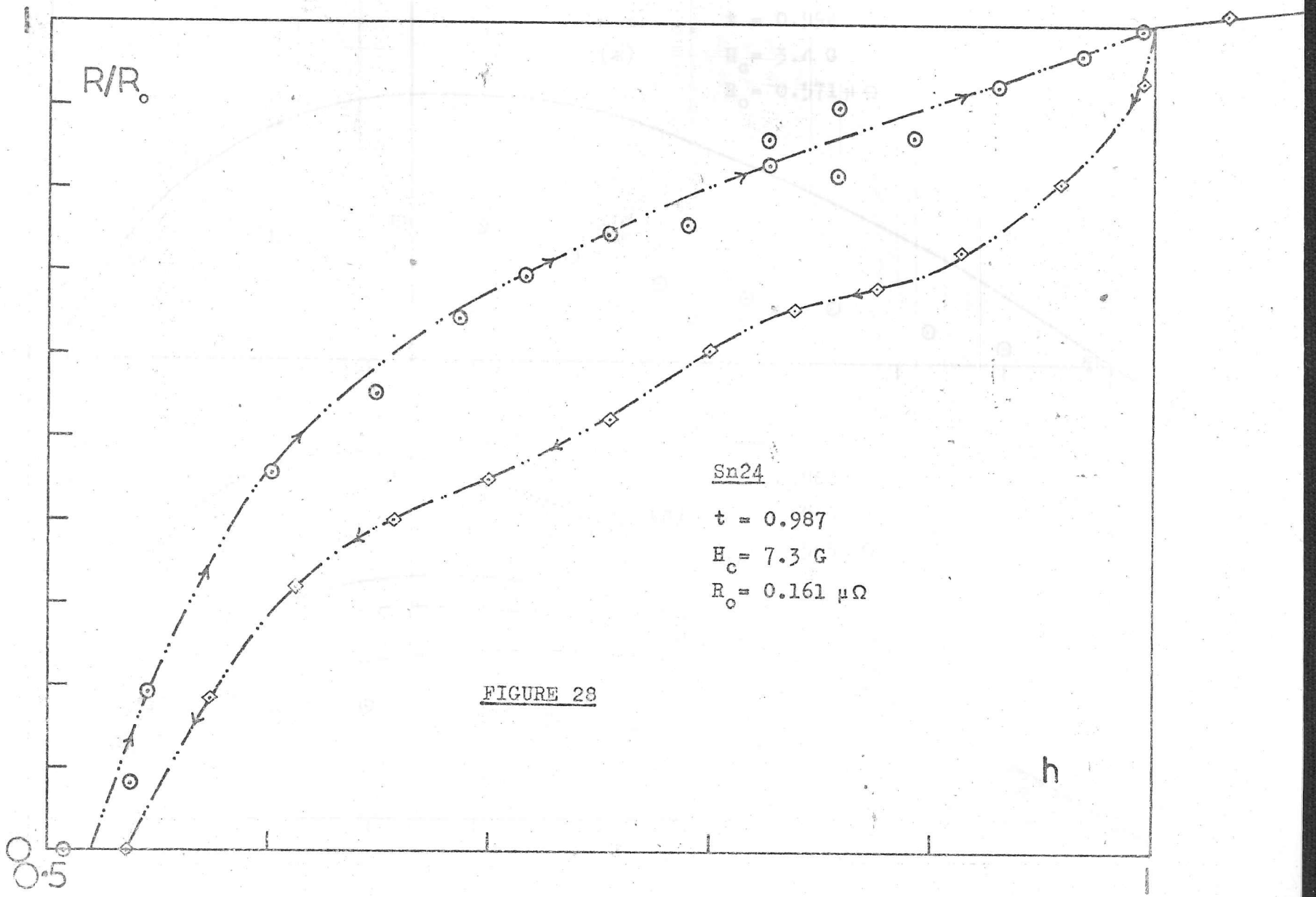

FIGURE 28

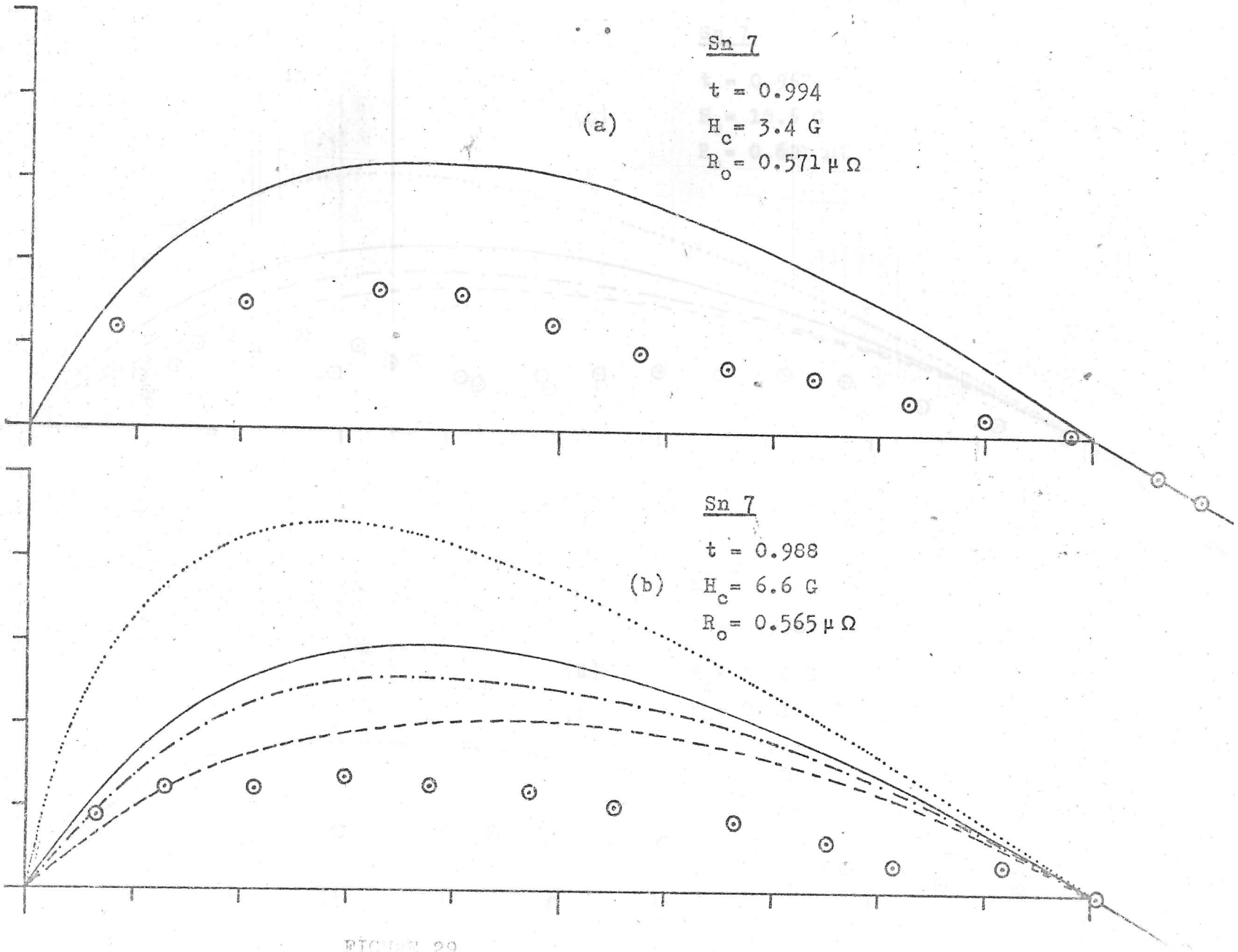

FIGURE 29

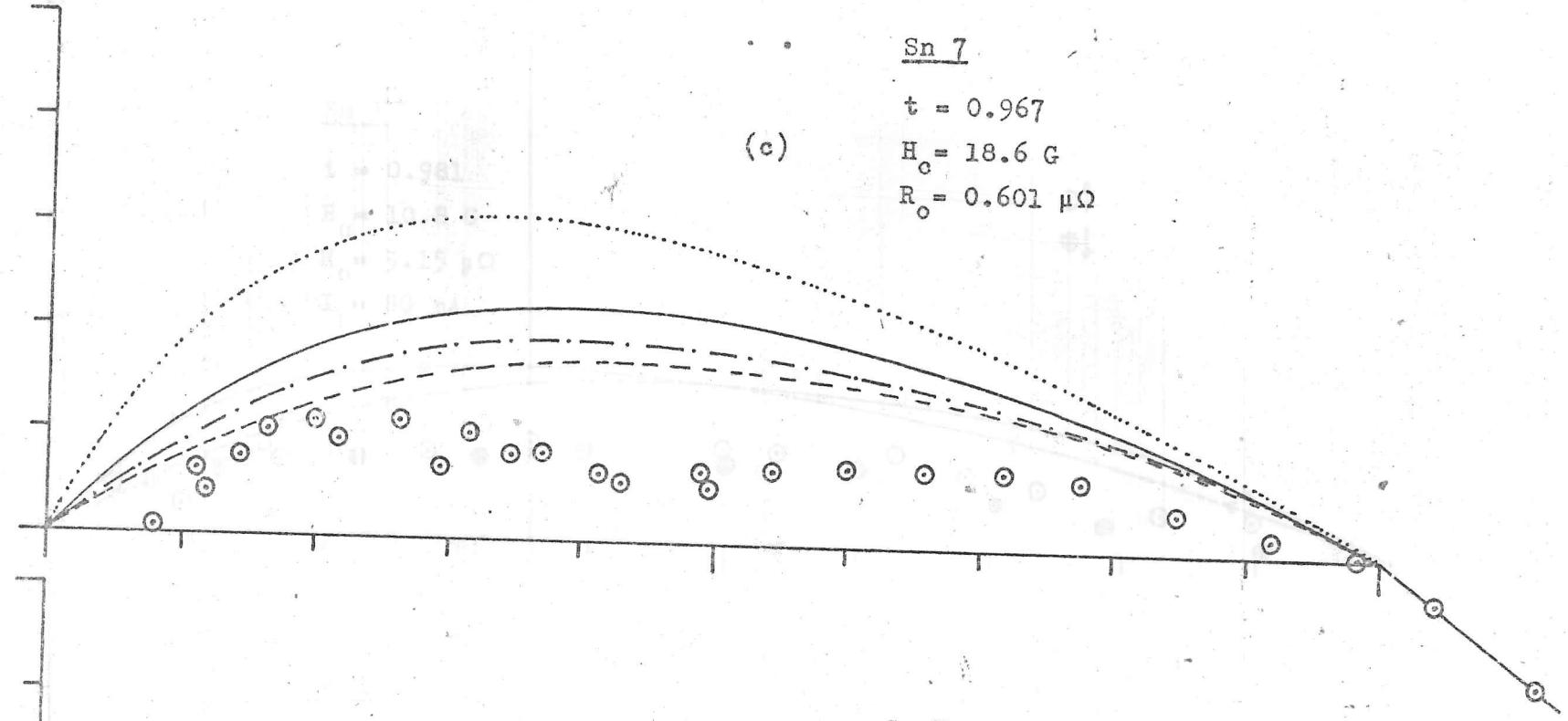

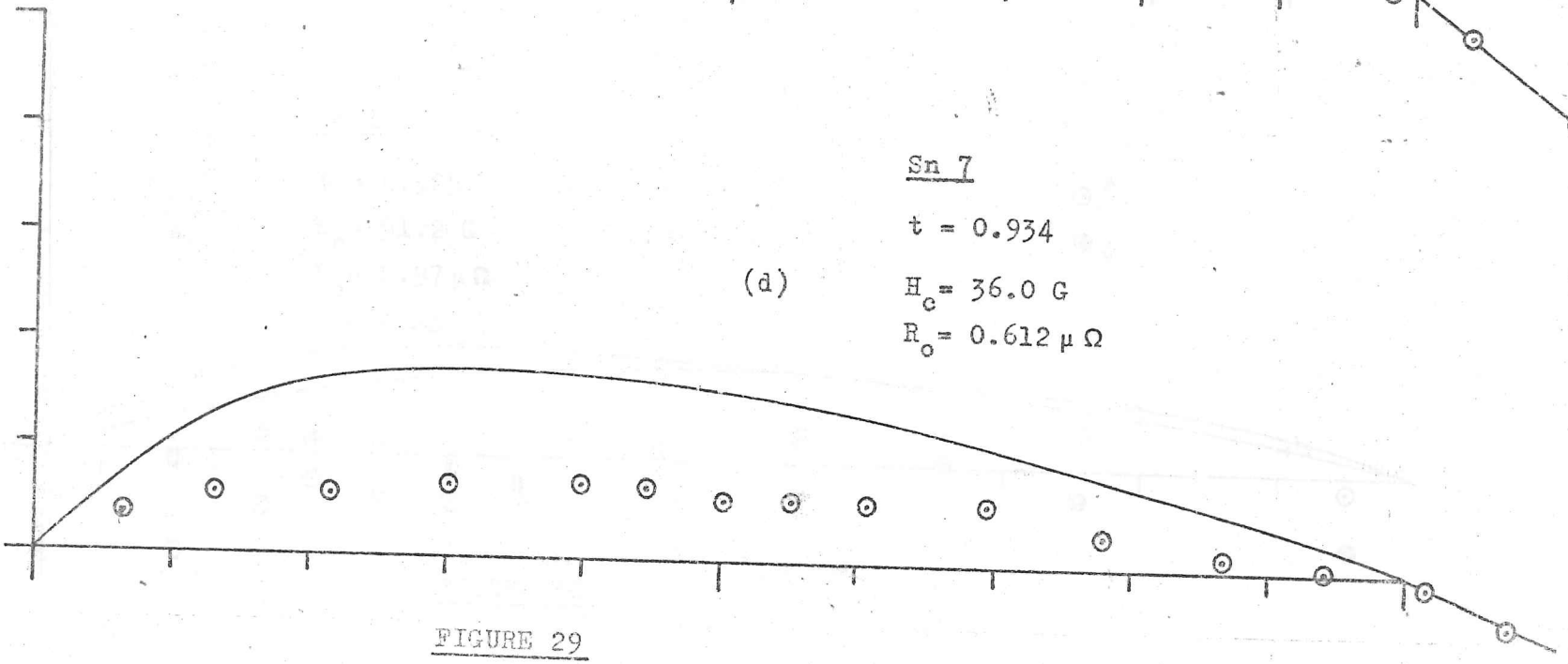

FIGURE 29

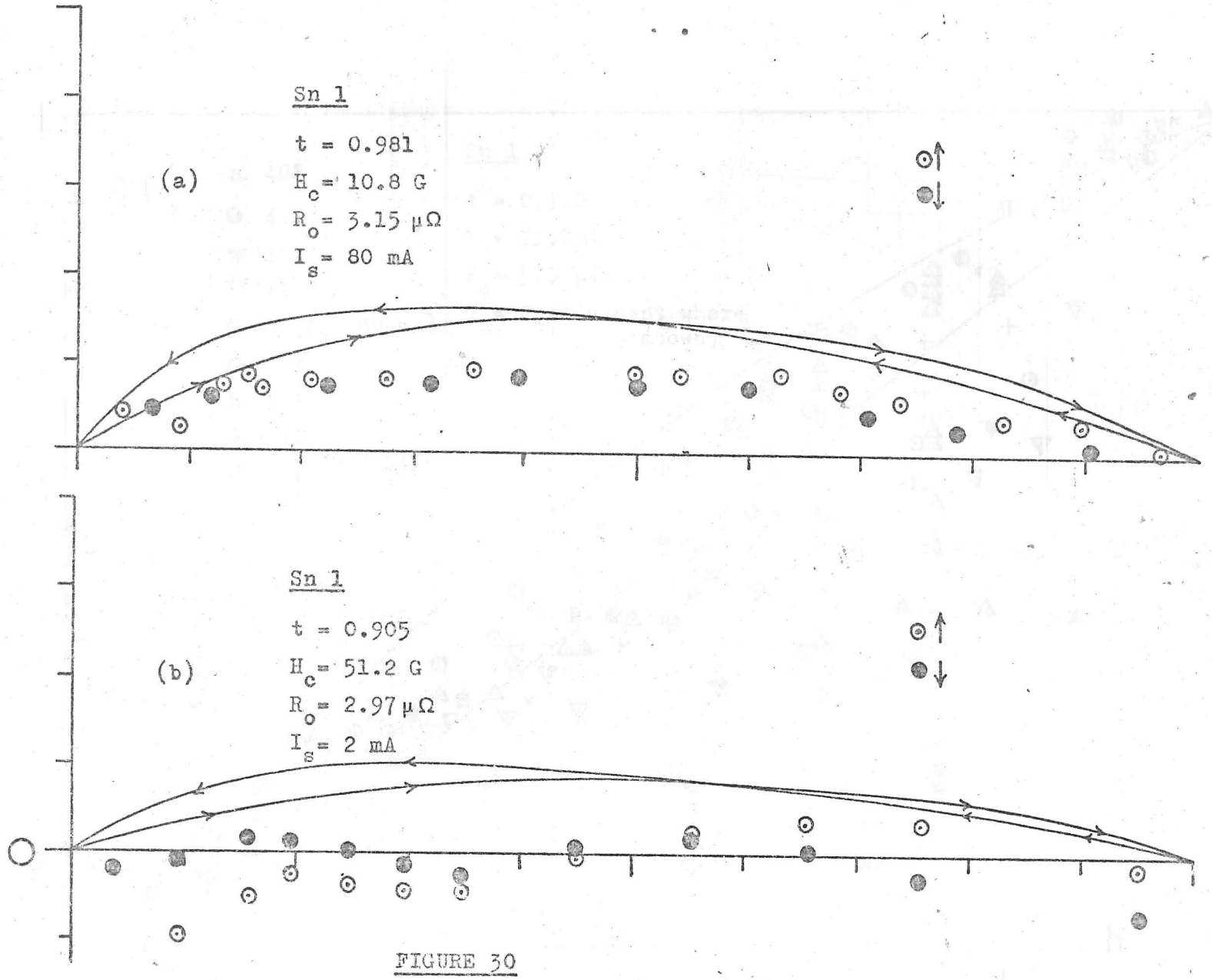
Sn 1
t = 0.981
(a)
H_c = 10.8 G
R_o = 3.15 μΩ
I_s = 80 mA
Sn 1
t = 0.905
(b)
H_c = 51.2 G
R_o = 2.97 μΩ
I_s = 2 mA

FIGURE 30

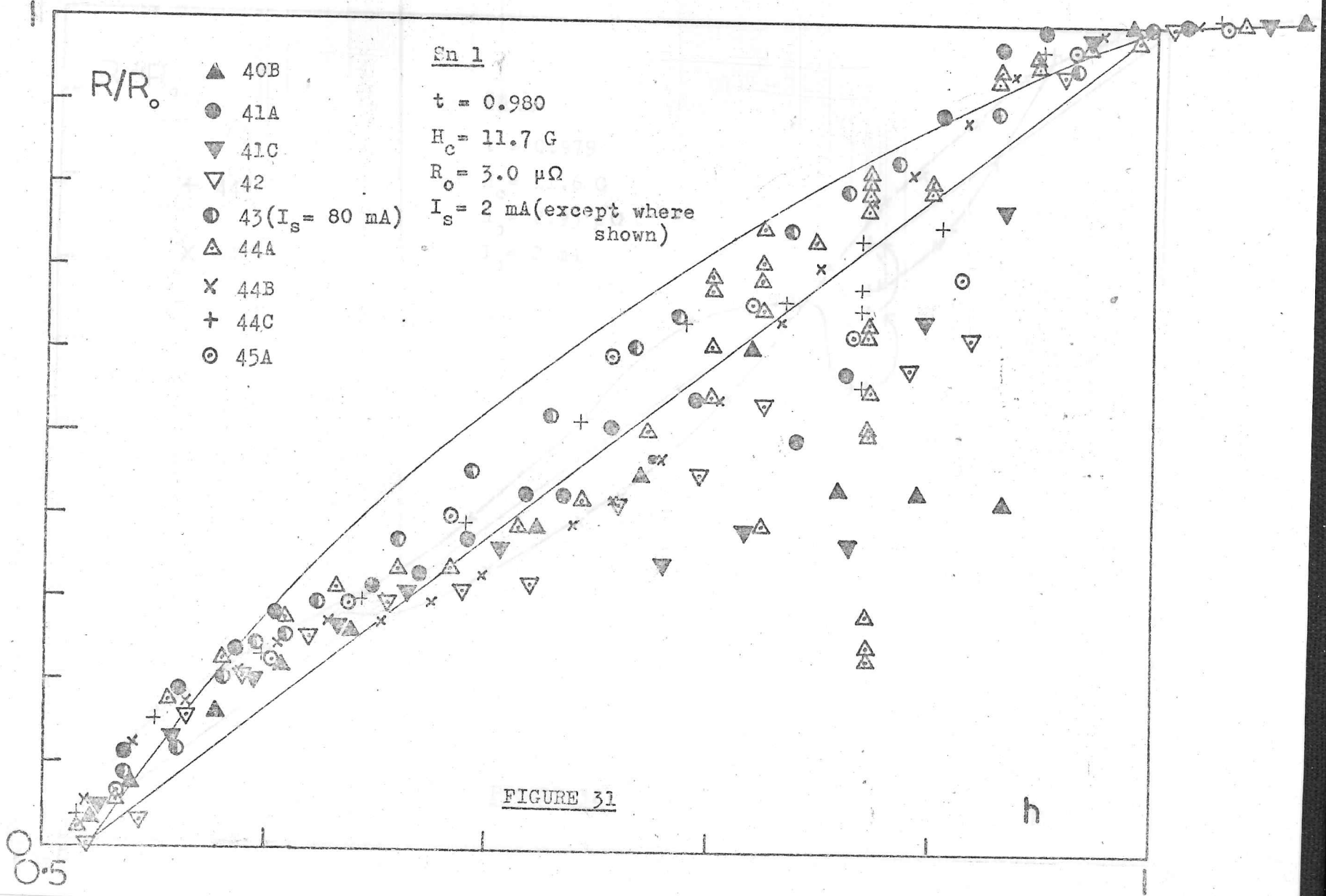
R/R$_o$
40B
41A
41C
42
43 (I_s= 80 mA)
44A
44B
44C
45A
Sn 1
t = 0.980
H_c= 11.7 G
R_o= 3.0 μΩ
I_s= 2 mA (except where shown)
h
0
0·5
1

FIGURE 31

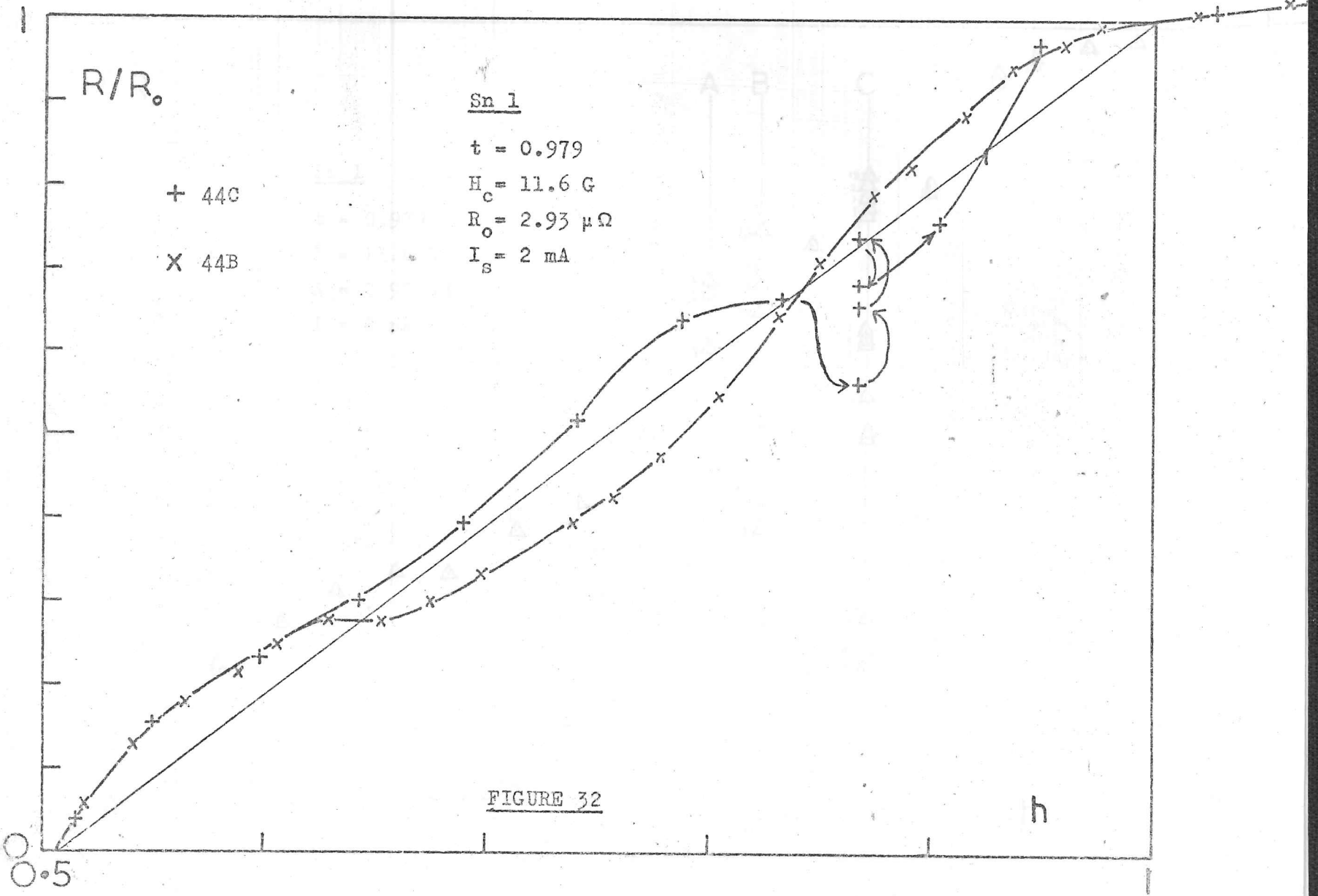

FIGURE 32

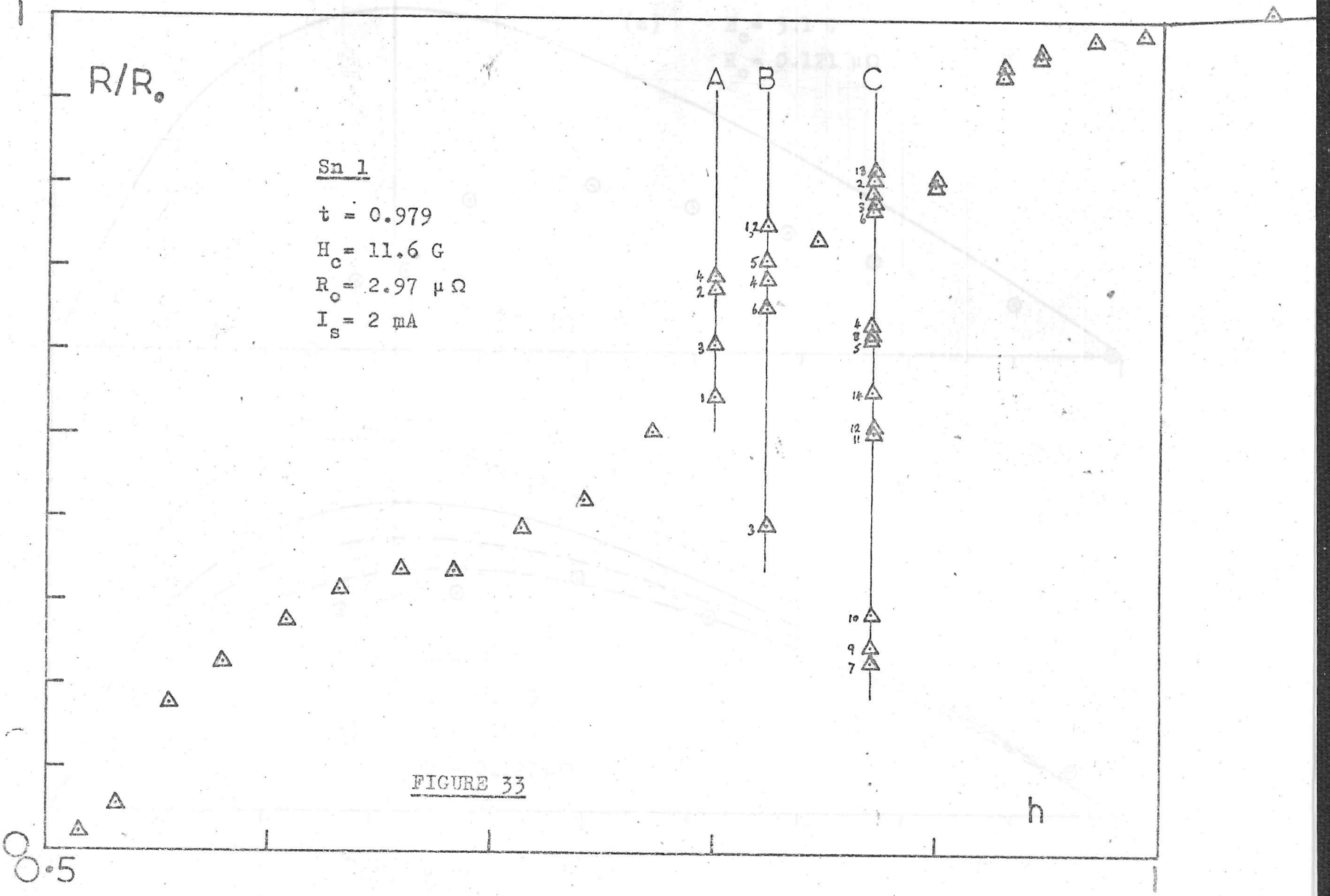

FIGURE 33

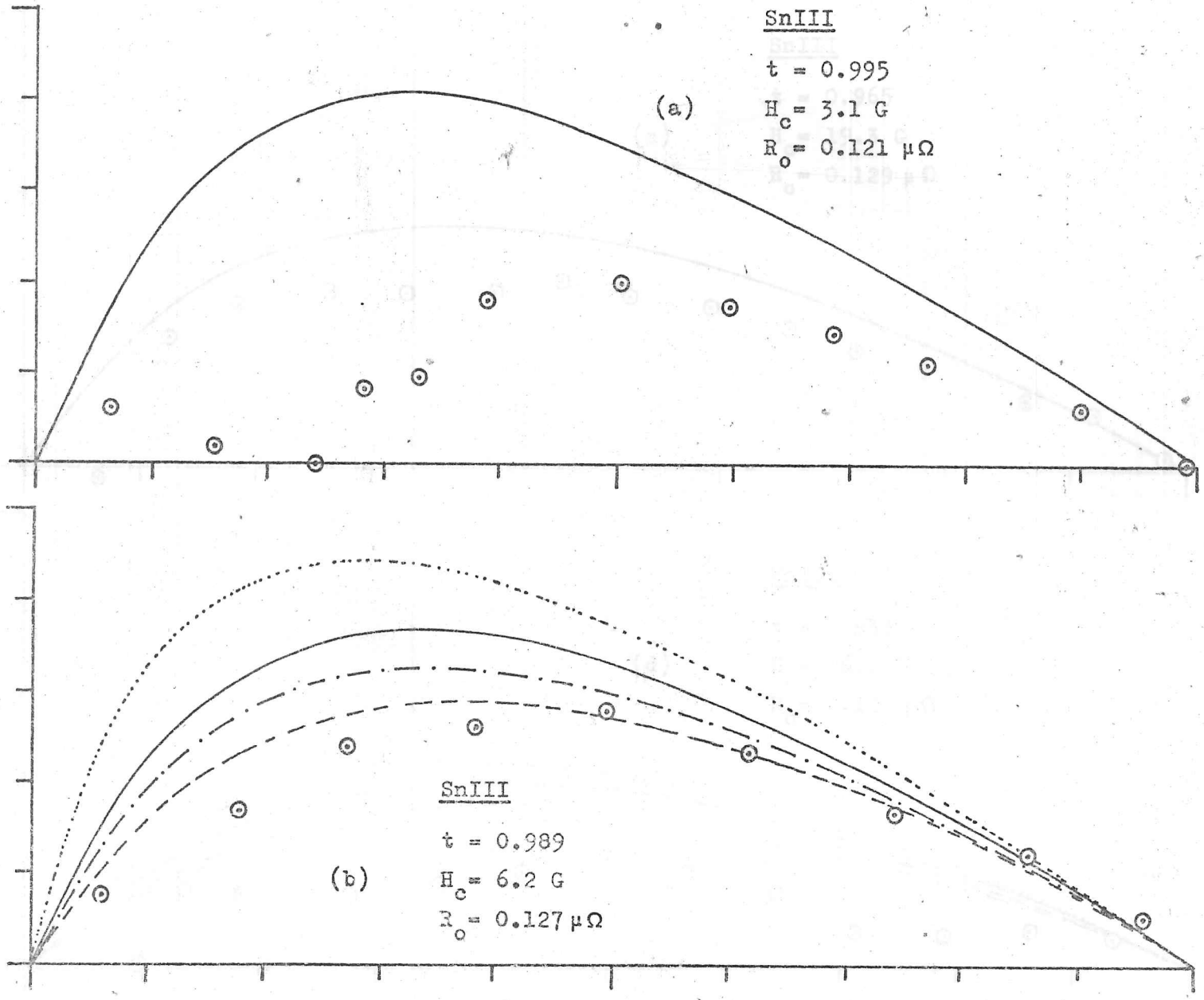

FIGURE 34

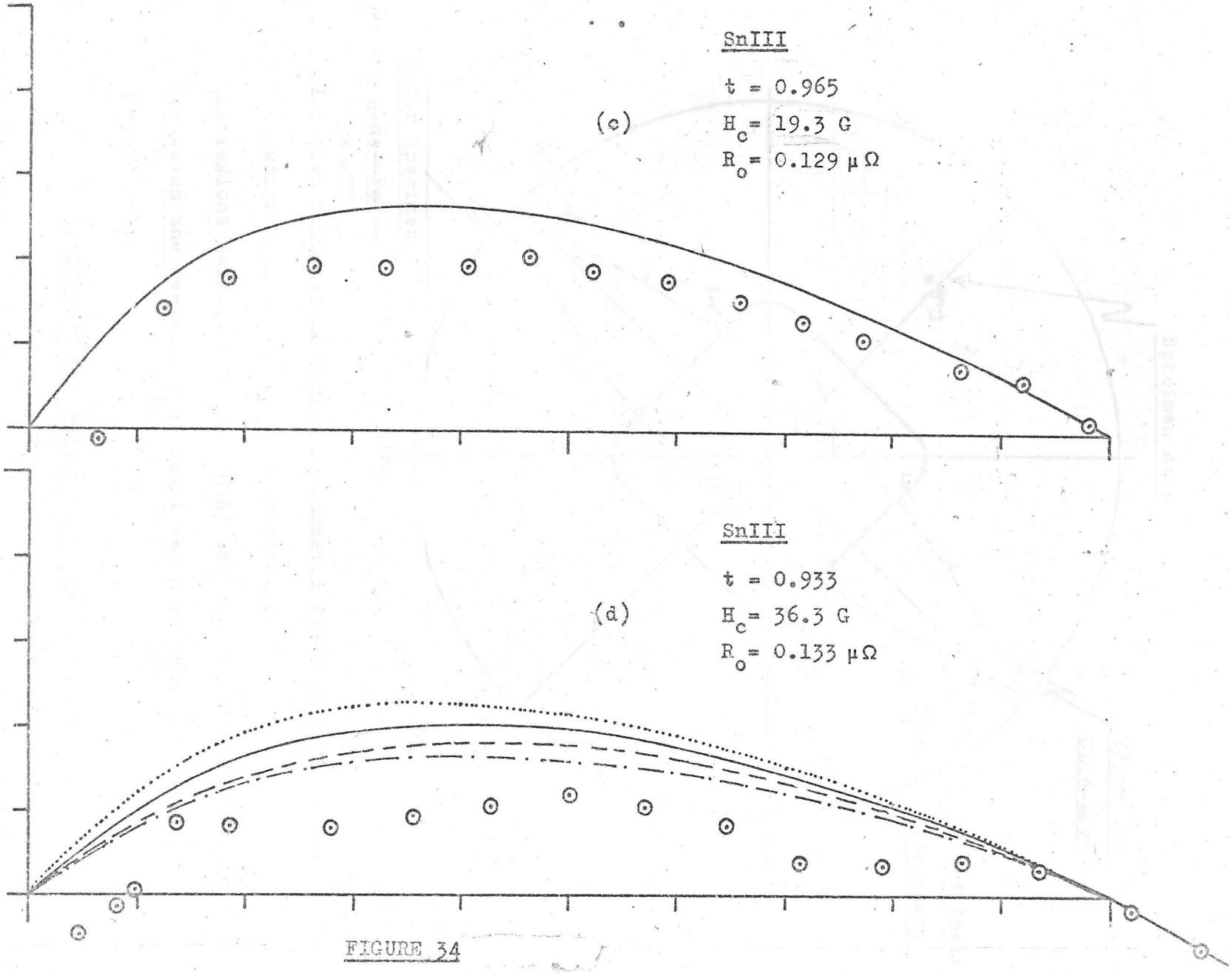
SnIII
t = 0.965
(c)
H_c = 19.3 G
R_o = 0.129 μΩ
SnIII
t = 0.933
(d)
H_c = 36.3 G
R_o = 0.133 μΩ

FIGURE 34

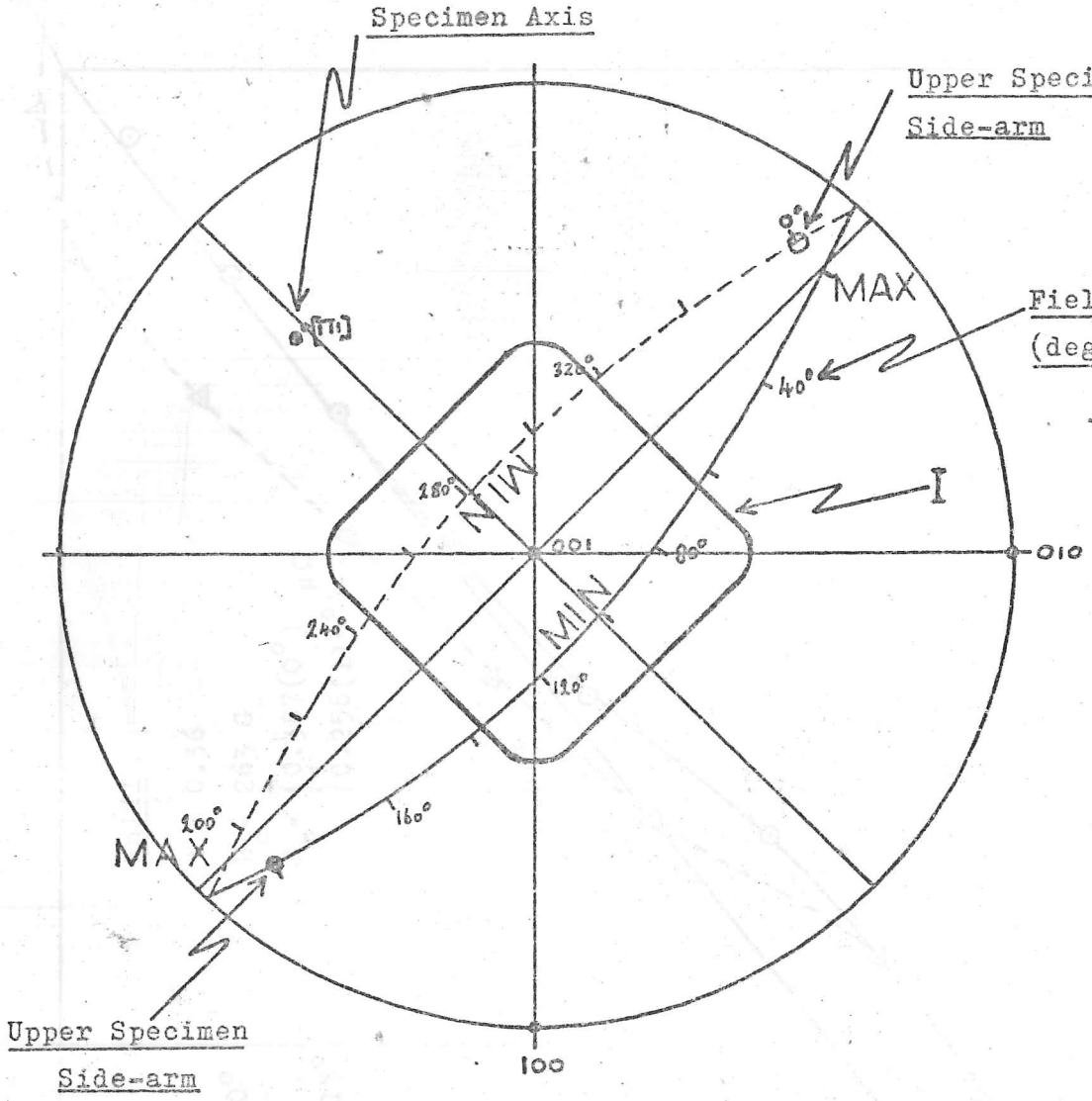

I : Two dimensional region of magnetic field directions for which open orbits exist(Alekseevskii et al.,1960)

The regions marked 'MAX' and 'MIN' are the magnetic field directions for which the resistance of SnIII was a maximum and minimum respectively.

FIGURE 35 The Orientation of Specimen SnIII

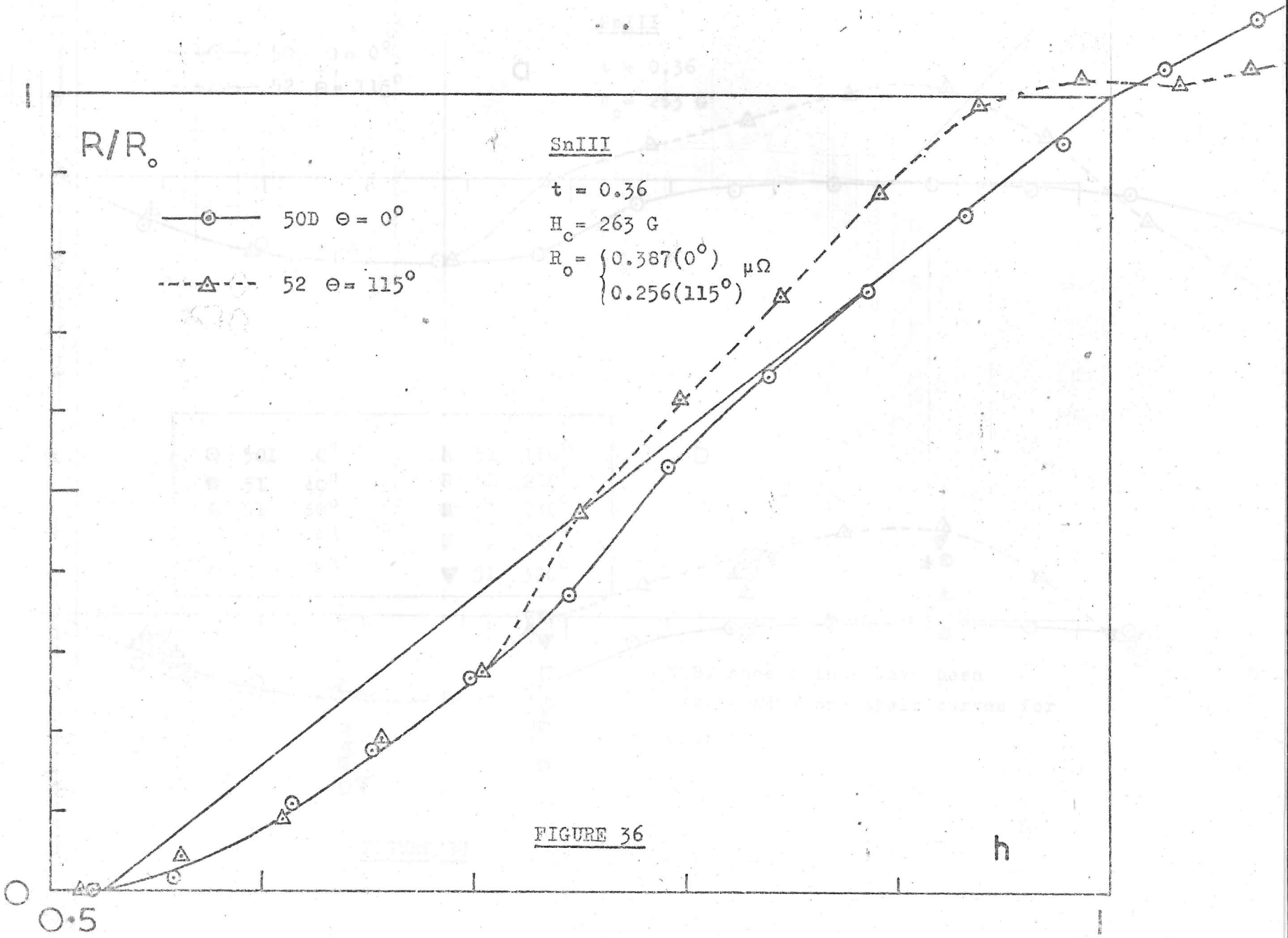
R/R₀
SnIII
t = 0.36
H_c = 263 G
R₀ = 0.387(0°) μΩ
0.256(115°)
50D Θ = 0°
52 Θ = 115°
1
0
0·5
1
h

FIGURE 36

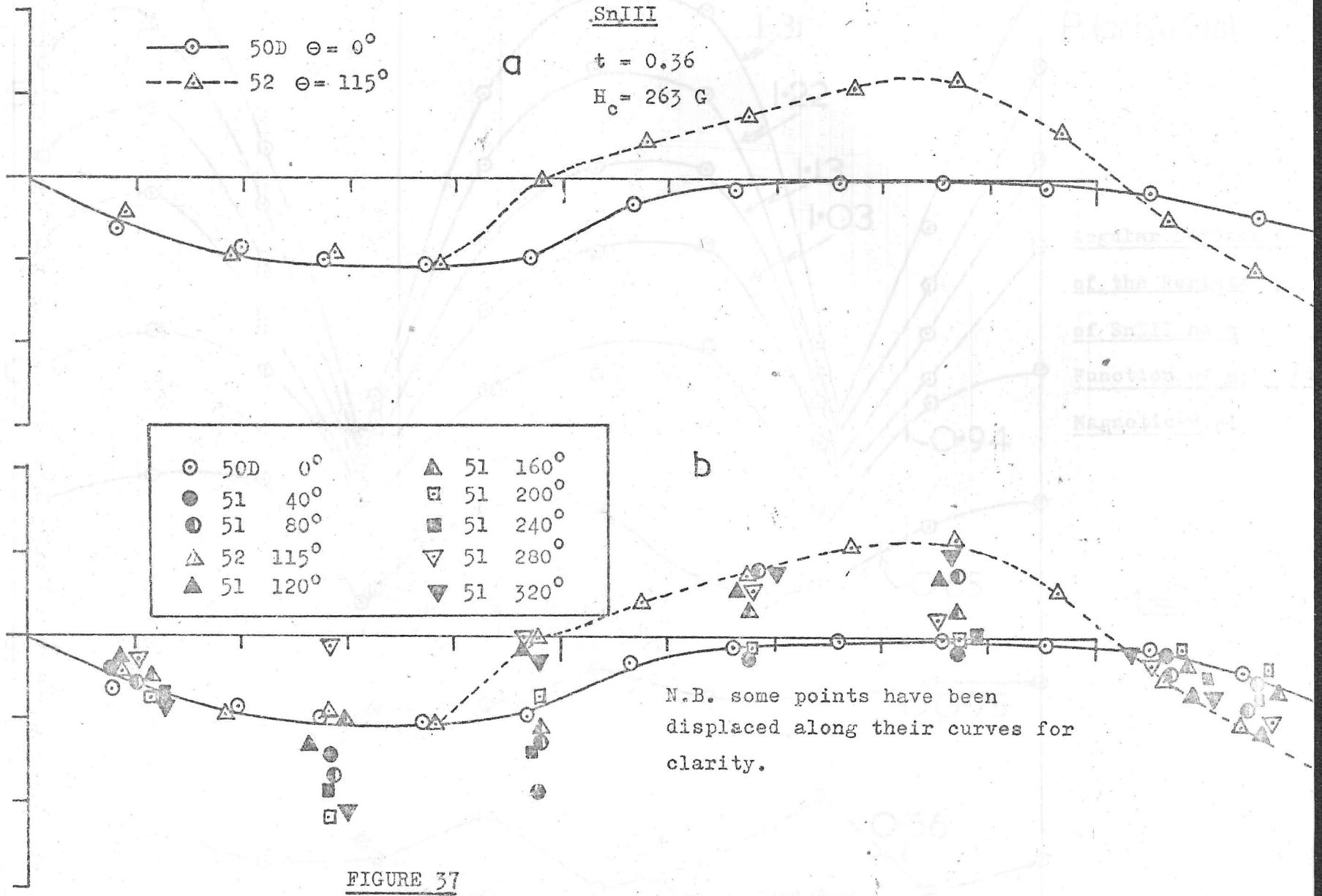

N.B. some points have been displaced along their curves for clarity.

FIGURE 37

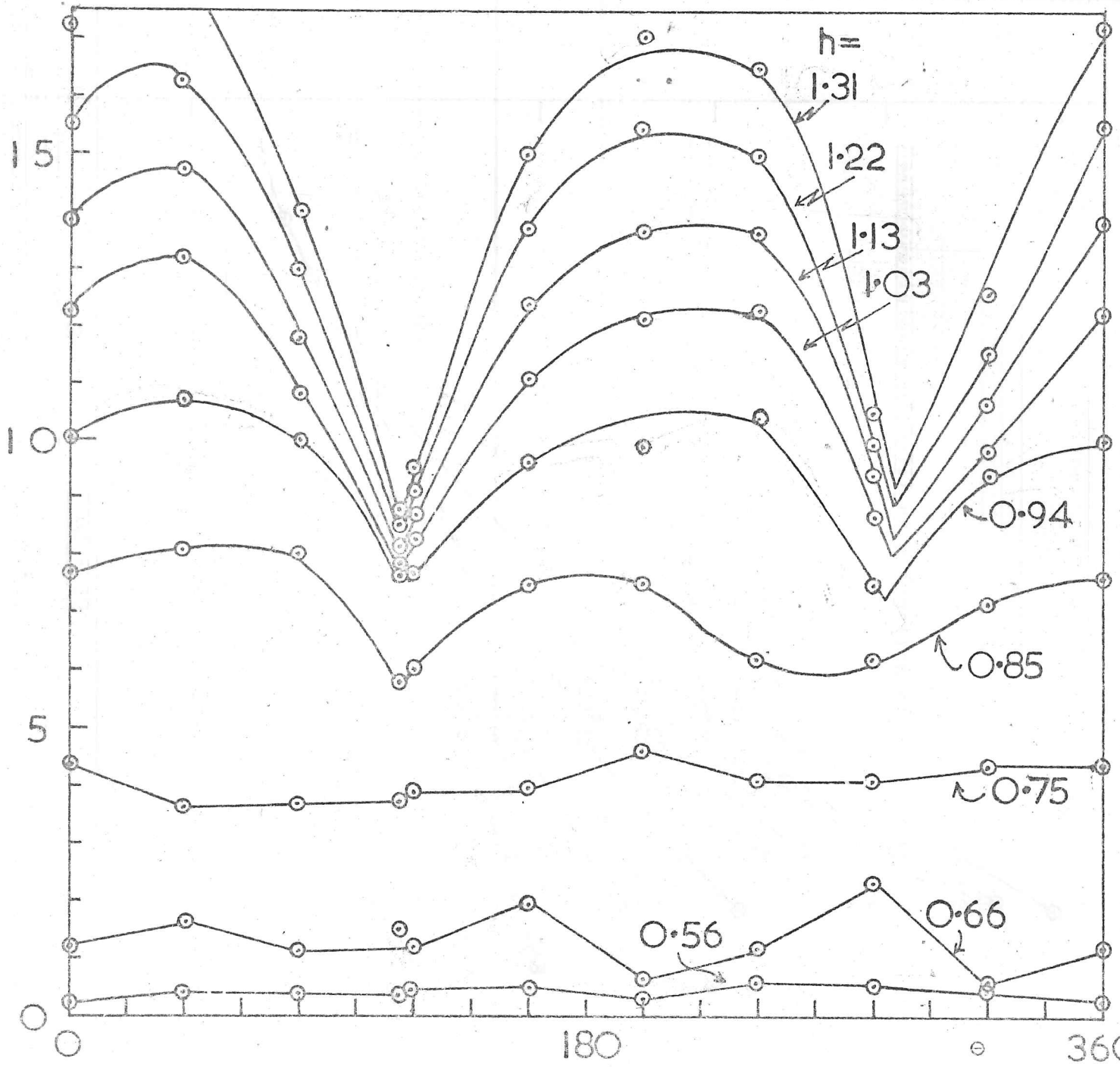

Angular Dependence of the Resistance of SnIII as a Function of Applied Magnetic Field

t=0·36

FIGURE 38

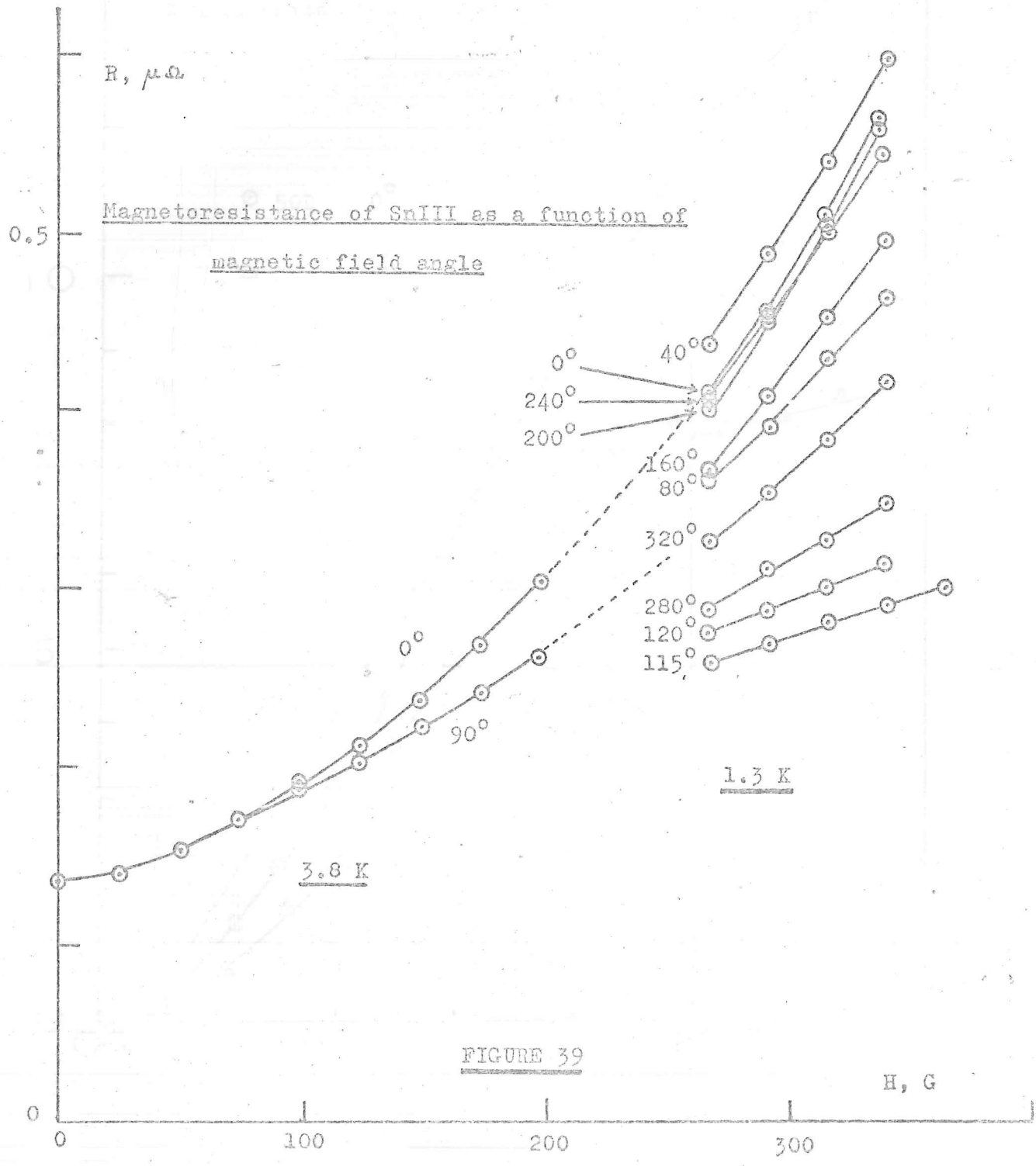
R, μΩ
Magnetoresistance of SnIII as a function of magnetic field angle
0.5
0°
40°
240°
200°
160°
80°
320°
280°
120°
115°
0°
90°
3.8 K
1.3 K
0
0
100
200
300
H, G

FIGURE 39

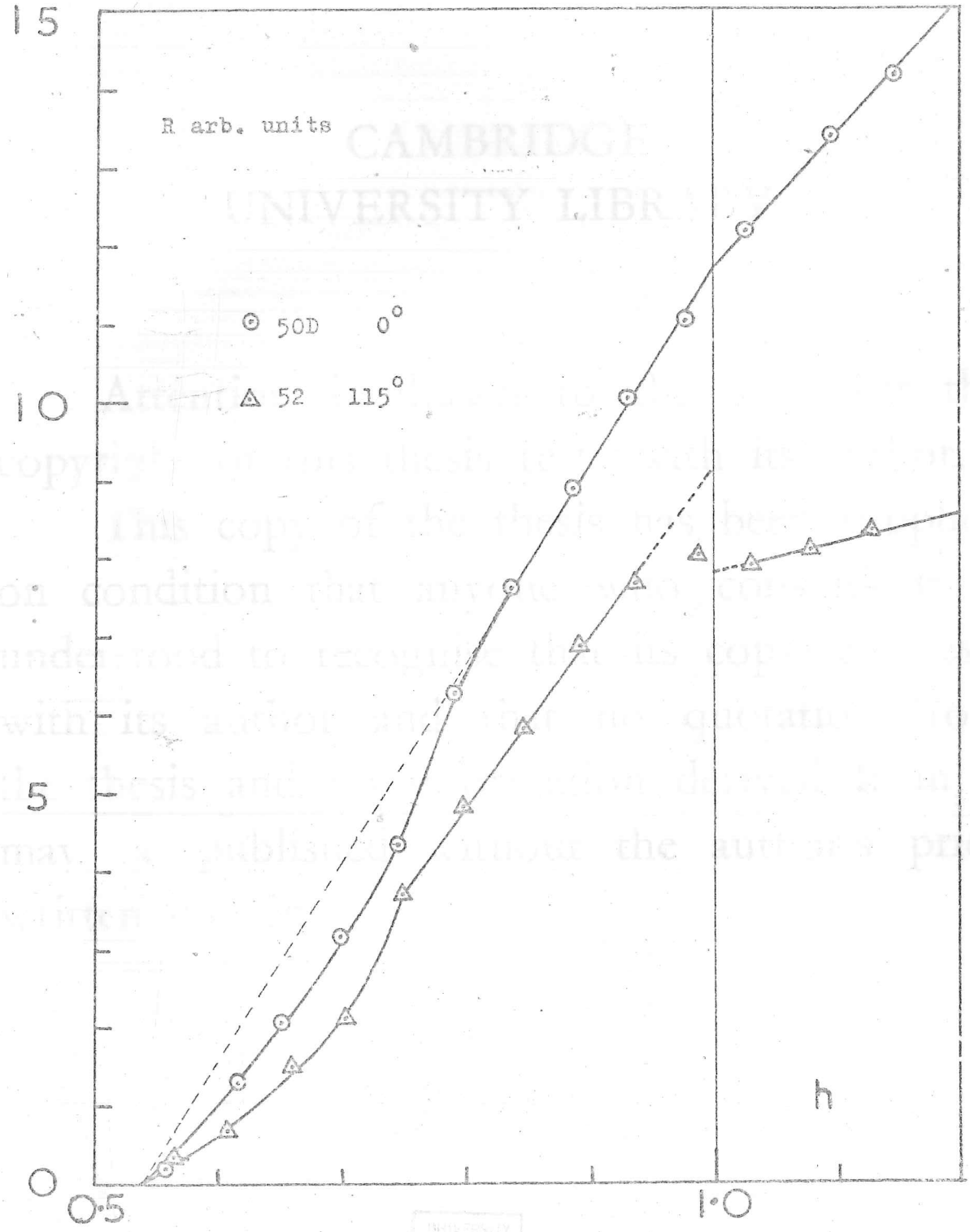

FIGURE 40